Institut Physik I - Theoretische Physik
Universität Regensburg

Semiklassik von Andreev-Billards

Diplomarbeit
von

Thomas Engl
aus
Roding

unter Anleitung von

Prof. Dr. Klaus Richter

abgegeben am
12.05.2010

Abstract

Superconductors have great influence on normal metal regions coupled to them. It has been noticed that they induce Cooper pairs into the normal region thus extending some of its anomalous properties to it. Maybe the most remarkable manifestation of this proximity effect is the formation of a minigap in the density of states which is of the order of the Thouless energy. This gap however only appears if the underlying classical dynamics of the normal region is chaotic or diffusive. Since obviously the classical dynamics play an important role it seems likely to use semiclassical methods to confirm an existing random matrix prediction. However using semiclassics based on the so-called diagonal approximation only gave an exponential damping of the density of states for low energies. This contradiction caused a great discussion and is now attributed to a new time scale: the Ehrenfest time τ_{E} separates the universal regime $\tau_{\mathrm{E}} = 0$ where random matrix theory is assumed to be valid from the Bohr-Sommerfeld regime $\tau_{\mathrm{E}} \to \infty$ where one expects to get the semiclassical result on the level of the diagonal approximation.

Other manifestations of the proximity effect have been found in the electronic transport of normal metal-superconductor interfaces, one of them being the conductance doubling indicating that the current is carried by Cooper pairs rather than electrons or holes. More surprising was the dependence of the conductance on the magnetic field. It has been found that it is non-monotonic having a local minimum at weak magnetic fields.

However up to now most investigations on the electronic transport of normal metal-superconductor hybrid structures have been made on the the effect of the interface itself but not so much work has been done on the conductance of an Andreev interferometer between two normal conducting leads. Only recently Whitney and Jacquod started considering these structures using a semiclassical method beyond the diagonal approximation to calculate the conductance in leading order in the total number of channels and in the leading order in the ratio of the number of superconducting channels and the number of normal conducting ones. Thus they considered superconducting leads small compared to the normal ones. For one specific setup where the superconductors lie on the same chemical potential as one of the two normal leads a reduction of the conductance arising from the diagonal approximation has been found. The same authors also considered the thermopower of these Andreev interferometer perturbatively in the number of superconducting channels which arises solely from the non-diagonal contributions.

In this diploma thesis we will show that a semiclassical approach beyond the diagonal approximation may be used to reproduce the random matrix theory prediction for up to two superconductors with a phase difference ϕ. With the approach presented here we are even able to calculate the level density in the intermediate regime between the universal one and the Bohr-Sommerfeld regime where a second intermediate gap appears. Moreover it is possible to calculate the density of states for the more general case that the two superconducting leads provide a different number of channels. In this case we also found a second gap.

We also extend the work of Whitney and Jacquod for the electronic transport as well as their calculation of the thermopower for three of the four setups up to all orders in the number of superconducting channels. We show that the reduction of the conductance turns into an enhancement if the number of superconducting channels becomes sufficiently large and is even doubled in the limit that it is much larger than the number of normal channels. Moreover we consider the dependence of a phase difference ϕ as well as on an magnetic field and non-zero temperature.

Contents

1 Introduction

Since the discovery of superconductivity by Kammerlingh Onnes in 1911 [1] who studied "The resistance of pure mercury at helium temperatures" much theoretical [2, 3, 4, 5] and experimental [6, 7, 8, 9, 10, 11] work has been done on superconductors. The BCS-theory [2] which predicts the formation of Cooper pairs - two electrons having opposite momentum coupled by the exchange of a virtual phonon - is accepted to be the most exhaustive theory of low temperature superconductors. The BCS-theory predicts not only the gap in the density of states of superconductors but also the isotope effect, *i.e.* that the critical temperature, above which the superconductor becomes normal again, depends on the isotopic mass, the macroscopic occupation of the BCS-ground state of the bosonic Cooper pairs, the critical magnetic field; the specific heat which jumps at the critical temperature thus indicating a thermodynamic second-order phase transition and the Meissner-Ochsenfeld effect [6]. The latter is that a superconductor expels all the flux of an applied magnetic field, namely that an applied magnetic field below the critical field forces the creation of a screening current which produces a magnetic field cancelling the applied magnetic field. Thus the magnetic flux inside the superconductor decreases exponentially and the length over which this exponential decay takes place is called the penetration depth. This penetration depth may be found using the Ginzburg-Landau theory [3] which uses thermodynamic arguments instead of a microscopic theory to describe the superconducting properties. This approach is based on an expansion of the free energy up to second order in the modulus squared of the macroscopic wave function ψ. It yields the London equations [4] describing the Meissner-Ochsenfeld effect and determining the penetration depth. Furthermore this approach provides an expression for the coherence length which is the length scale over which thermodynamic fluctuations of the superconducting phase take place.

After the superconductor itself had been quite well understood a lot of attention naturally was attracted to the interface between a superconductor and a normal metal. The first important effect in hybrid structures consisting of superconductors and normal metals has been found by Meissner [12]: He noticed that the superconductor tends to export some of its anomalous properties across the interface over a temperature dependent length scale that can be of the order of a micrometer at low temperatures. This is the so-called proximity effect which has been the focus of numerous experimental [13, 14, 15, 16, 17, 18, 19, 20, 21] and theoretical [22, 23, 24, 25] surveys. Later Bogoliubov and de Gennes derived the Bogoliubov-de Gennes equations [26] which are essentially two coupled Schrödinger equations for the quasiparticles, *i.e.* for the electrons and holes of a normal metal coupled to a superconductor. The coupling strength of the Bogoliubov-de Gennes equations is given by the superconducting pair potential Δ which is equal to the superconducting gap.

A further interesting phenomenon was noticed by Andreev [27] in 1964: He found a new scattering mechanism appearing at normal metal-superconductor (N-S) interfaces now known as Andreev reflection. This is essentially that an electron hitting the superconductor is retro-reflected as a hole as shown in figure 1.1. In particular at the interface an additional electron-hole pair is created. The two electrons then enter the superconductor forming a Cooper pair and thus the hole has to have its velocity in opposite direction as the incident electron in order to ensure conservation of momentum. This mechanism is the key concept in Andreev quantum dots - normal conducting quantum dots coupled to superconductors - also leading to the proximity effect.

With the increasing interest on mesoscopic systems, in the 1980's further features have been found. At this time transport properties of an N-S interface were mainly of interest. Thus a fairly complete theory about the current through the interface was developed by Blonder, Tinkham and Klapwijk [28] who connected the electrical current to the probabilities for transmission through the interface as well as to ordinary and Andreev reflection at the interface. This theory is now known as BTK-theory and is pretty similar to the Landauer-Büttiker formalism for normal metals [29] which also connects the

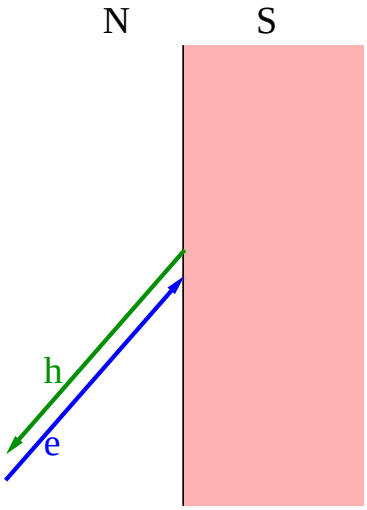

Figure 1.1: If an electron hits the N-S interface it is retro-reflected as a hole

electrical current in a lead to the transmission coefficients between the different leads. Within the BTK-theory a great variety of properties of electronic transport through N-S interfaces has been predicted. These are that for N-S junctions with sufficiently large barrier strengths between the normal conducting region and the superconductor that the differential conductance $\mathrm{d}I/\mathrm{d}V$ (where I is the current and V the applied voltage) vanishes for voltages smaller than the superconducting gap Δ/e. For these voltages the conductance is doubled compared to the conductance of the same normal conducting region with a normal conducting lead instead of the superconducting one; an indication of the proximity effect. When increasing the voltage the differential conductance has a peak at $eV \approx \Delta$ and finally approaches the conductance of the normal conducting region without the superconductor. However the total value of the current for high voltages exceeds that of a metallic junction by the so called excess current. Later experiments [30, 31] however additionally found an enhancement of the differential current at $V = 0$ later known as zero bias anomaly.

In the 1990's the density of states of Andreev quantum dots came under the focus of mainly theoretical and numerical resarch. Due to the success of the experimentalists, very clean normal regions may be created therefore exhibiting nearly completely ballistic transport, *i.e.* transport without scattering at impurity. Those systems are semiclassically very well described by billiard systems which in presence of Andreev reflections are called Andreev billiards [32]. The considerable theoretical attention raised by such a hybrid structure is related to the interesting peculiarity that by looking at the density of states of an Andreev billiard we can determine the nature of the underlying dynamics of its classical counterpart [33]. Indeed, while the density of states vanishes with a power law in energy for the integrable case, the spectrum of a chaotic billiard is expected to exhibit a true gap above E_F [33]. The width of this hard gap, also called the minigap [25], has been calculated as a purely quantum effect by using random matrix theory (RMT) and its value scales with the Thouless energy, $E_\mathrm{T} = \hbar/2\tau_\mathrm{D}$, where τ_D is the average (classical) dwell time a particle stays in the billiard between successive Andreev reflections [33].

Since the existence of this gap is expected to be related to the chaotic nature of the electronic motion, many attempts have been undertaken to explain this result in semiclassical terms [34, 35, 36, 37, 38, 39, 40], however this appeared to be rather complicated. Indeed a traditional semiclassical treatment based on the so-called Bohr-Sommerfeld (BS) approximation yields only an exponential suppression of the density of states [34, 35, 36]. This apparent contradiction of this prediction with the RMT one was resolved quite early by Lodder and Nazarov [34] who pointed out the existence of two different regimes. The characteristic time scale that governs the crossover between the two regimes is the Ehrenfest time $\tau_\mathrm{E} \sim |\ln\hbar|$, which is the time a initally localised wave packet needs to spread to a classical length scale

as (in the cases we consider here) the system size which leads to the logarithmical dependence on $\hbar$. In particular it is the ratio $\tau = \tau_E/\tau_D$, that has to be considered.

In the universal regime, $\tau = 0$, chaos sets in sufficiently rapidly and RMT is valid leading to the appearance of the aforementioned Thouless gap [33]. Although the Thouless energy E_T is related to a purely classical quantity, namely the average dwell time, we stress that the appearance of the minigap is a quantum mechanical effect, and consequently the gap closes if a symmetry breaking magnetic field is applied [41]. Similarly if two superconductors are attached to the Andreev billiard, the size of the gap will depend on the relative phase between the two superconductors, with the gap vanishing for a π-junction [41].

The deep classical limit is characterised by $\tau \to \infty$, and in this regime the suppression of the density of states is exponential and well described by the Bohr-Sommerfeld approximation. The more interesting crossover regime of finite Ehrenfest time, and the conjectured Ehrenfest time gap dependence of [34] has been investigated by various means [24, 42, 43, 44, 45, 46, 47]. Recently Kuipers, Waltner, Petitjean, Berkolaiko and Richter succeeded in calculating the density of states of an Andreev billiard with one superconducting lead in the universal regime [48]. Moreover they have been able to include the effect of non-zero Ehrenfest by simple replacements. With this breakthrough new questions arise as for example whether this approach would also be applicable to the calculation of the density of states of Andreev billiards with more than just one lead and whether *e.g.* electronic and thermal properties could be explained using the methods derived by the authors, too.

Indeed, Whitney and Jacquod [49] recently reconsidered the transport properties of Andreev billiards semiclassically using the same method. They considered a ballistic normal conducting region with a chaotic boundary and two normal conducting leads and one superconducting lead which is either isolated such that the chemical potential of the superconductor adjusts itself such that the net current through the N-S interface is zero [49] or connected to one of the two leads such that the chemical potential of the superconductor is the same as that of the lead. For the first setup with the superconducting island RMT calculations already exist [50] predicting an increase of the conductance which is doubled if the number of superconducting channels tends to infinity. Furthermore in [50] the authors considered the case of two superconductors with phase difference ϕ and found numerically that the increase of the conductance vanishes if the superconducting phase difference is equal to π.

Using a semiclassical method involving classical trajectories Whitney and Jacquod calculated the average conductance between the two normal leads of such chaotic shaped Andreev billiards up to second order in the ratio N_S/N_N where N_S is the total number of superconducting channels and $N_N = N_1 + N_2$ is the sum of the number of channels in the normal leads. If the superconducting chemical potential is the same as that of one of the two normal conducting leads they found that the correction to the classical conductance arising from the diagonal approximation is negative or positive depending on the ratio N_1/N_2 as well as on the magnetic field. The diagonal approximation is often applied to expressions depending on the action difference of several trajectories. It is to restrict oneself to trajectory sets made of pairs of trajectories with the two trajectories in each pair being the same thus having no action difference.

With the same approach they also considered the thermoelectric effect in ballistic Andreev interferometer [51], *i.e.* ballistic normal conducting regions coupled to two superconducting islands with a phase difference ϕ. They considered different setups, with three of them shown in figure 8.1, with two of them being pretty much the same as for the conductance. For the first setup they found a vanishing thermopower due to the symmetry in ϕ caused by the symmetry in exchanging the leads. For the other setups they found a thermopower antisymmetric in the phase difference

The aim of this diploma thesis is to show that trajectory based semiclassics may be used to describe several properties of chaotic Andreev billiards. For that we start with reviewing the most important facts about Andreev billiards in section 2. These are the scattering formulation which connects the density of states to the scattering matrix of the normal region and the Landauer-type formulae for electronic and thermal transport. Then the semiclassical framework will be introduced starting from the path integral approach to quantum mechanics in section 3.1. In the same section this method is then used to derive the semiclassical Greens function in which is essentially given by the action of classical trajectories and their stability. Using this Greens function one also easily finds a semiclassical expression for the

scattering matrix and therefore for the transmission coefficients. In section 4 we present the trajectory sets contributing in the semiclassical limit $\hbar \to 0$ as well as some diagrammatic rules for these sets of trajectories. Having these diagrammatic rules we are then readily prepared to calculate the density of states of chaotic Andreev billiards in section 5 where we review the results for the density of states of Andreev billiards with just one superconducting lead presented in [48] and to extend the calculations to Andreev billiards with two superconducting leads with a phase difference ϕ in section 6. Additionally we take a brief look at the effect of small superconducting gaps. The dependence on an applied magnetic field and the effect of a non-zero Ehrenfest time is also taken into account. After that in section 7 we consider the transport properties of Andreev billiards consisting of two normal and two superconducting leads having the same chemical potential but different phases. We extend the work of [49] to all orders in $N_\mathrm{S}/N_\mathrm{N}$ and show that the size of the superconductor plays an important role. Moreover we investigate the effect of a phase difference between two superconductors as well as the effect of an applied magnetic field and non-zero temperature. Finally in section 8 we apply the methods derived in section 7 to the thermopower for the first three setups of [51], *i.e.* the symmetric and asymmetric house as well as the parallelogram which consists of two dots connected by a neck and with each dot having one normal and one superconducting lead. We show that when going beyond the diagonal approximation a non-zero thermopower antisymmetric in the phase difference ϕ arises.

Please note that parts of this diploma thesis have already been submitted for publication [52] or are close to being published.

2 Theory of Andreev billiards

2.1 Scattering formulation of the density of states

2.1.1 Bogoliubov-De Gennes equation

The theory of Andreev billiards has been reviewed in detail by Beenakker in [25]. Here we will just repeat the most important facts. The electrons and holes of a closed normal metal-superconductor hybrid system are described by the Bogoliubov-de Gennes (BdG) equation [26]

$$\mathcal{H}_{\mathrm{BG}} \begin{pmatrix} u \\ v \end{pmatrix} = E \begin{pmatrix} u \\ v \end{pmatrix} \tag{2.1a}$$

$$\mathcal{H}_{\mathrm{BG}} = \begin{pmatrix} H & \Delta(\mathbf{r}) \\ \Delta^*(\mathbf{r}) & -H^* \end{pmatrix} \tag{2.1b}$$

which is the analog to the 'usual' Schrödinger equation and is in principle a Schrödinger equation with a coupling between the electrons and holes. Here $H = (\mathbf{p} + e\mathbf{A})^2/(2m) + V - E_{\mathrm{F}}$ is the Hamiltonian of an electron like quasiparticle and $-H^*$ (the negative of the complex conjugated of H) the Hamiltonian of a hole like quasiparticle. $\mathbf{p} = \partial/\partial\mathbf{r} = (\partial/\partial x, \partial/\partial y, \partial/\partial y)^T$ is the momentum operator where the superscript 'T' stands for transposed, $\mathbf{A}(\mathbf{r})$ the vector potential of an eventually applied magnetic field B, $V(\mathbf{r})$ an arbitrary potential, *e.g.* an electrostatic potential, and E_{F} is the energy. Note that with this definition the energy E is measured with respect to the Fermi energy. $u(\mathbf{r})$ and $v(\mathbf{r})$ are electron and hole wave functions, respectively. The electron and hole wave functions are coupled by the superconducting pair potential $\Delta(\mathbf{r})$. One may easily prove that if $(u, v)^T$ is an eigenvector with eigenvalue E, $(-v^*, u^*)^T$ is also an eigenfunction with eigenvalue $-E$. Thus the complete set of eigenvalues lies symmetrically around zero.

At an interface between a normal metal and a superconductor the pairing interaction drops to zero over atomic distances at the normal region. Therefore we will use the step function model

$$\Delta(\mathbf{r}) = \begin{cases} \Delta \mathrm{e}^{\mathrm{i}\phi_j} & \text{if } \mathbf{r} \in \mathrm{S}_j \,, j = 1, 2 \\ 0 & \text{if } \mathbf{r} \in \mathrm{N} \end{cases} \,, \tag{2.2}$$

where S_j stands for the j-th superconductor and N for the normal metal. This step function model is also known as the "rigid boundary condition" [53].

2.1.2 Excitation spectrum

Within the step function model the excitation spectrum of the coupled electron-hole quasiparticles can be expressed entirely in terms of the scattering matrix of the normal conducting region [54] which connects the outgoing waves to the incoming ones (see figure 2.1). Note that in order to get a well defined scattering problem the interface between the normal region to the superconductors are assumed to be provided by ideal normal leads. Nevertheless we will call these leads as well as the channels they provide 'superconducting'. Furthermore we assume that the only scattering process in the superconductor is pure Andreev reflection at the N-S interface. This also requires that the Fermi energy E_{F} is much bigger than the superconducting bulk gap Δ.

One first of all has to construct a basis for the scattering matrix which should be normalised to unit flux. This may be achieved by writing the eigenfunctions of the BdG equation in the normal lead in the

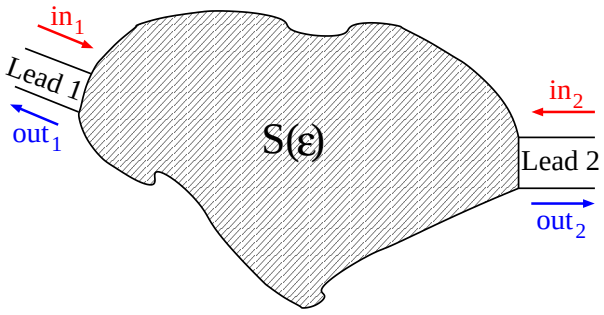

Figure 2.1: The wave outgoing wave function which is given by a linear combination of the wave functions of the given channels $i = 1, 2, \ldots$ with coefficients $\mathrm{out}_{1,i}, \mathrm{out}_{2,i}$ is connected to the incoming wave function with coefficients $\mathrm{in}_{1,i}, \mathrm{in}_{2,i}$ by the scattering matrix S via $(\mathrm{out}_1, \mathrm{out}_2)^T = S(\mathrm{in}_1, \mathrm{in}_2)^T$.

form

$$\Psi^{\pm}_{n,\mathrm{e}}(\mathrm{N}) = \begin{pmatrix} 1 \\ 0 \end{pmatrix} \frac{1}{\sqrt{k^{\mathrm{e}}_n}} \Phi_n(y,z) \mathrm{e}^{\pm \mathrm{i} k^{\mathrm{e}}_n x} \tag{2.3a}$$

$$\Psi^{\pm}_{n,\mathrm{h}}(\mathrm{N}) = \begin{pmatrix} 0 \\ 1 \end{pmatrix} \frac{1}{\sqrt{k^{\mathrm{h}}_n}} \Phi_n(y,z) \mathrm{e}^{\pm \mathrm{i} k^{\mathrm{h}}_n x}, \tag{2.3b}$$

where $k^{\mathrm{e,h}}_n = \sqrt{2m}\left(E_{\mathrm{F}} - E_n + \sigma^{\mathrm{e,h}} E\right)/\hbar$ and $\sigma^{\mathrm{e}} = 1$, $\sigma^{\mathrm{h}} = -1$. Furthermore the index n labels the modes which are equivalent to the channels, $\Phi_n(y,z)$ is the transverse wave function of the n-th mode normalised to unity and E_n is given by

$$\left[\left(p_y^2 + p_z^2\right)/(2m) + V(y,z)\right] \Phi_n(y,z) = E_n \Phi_n(y,z).$$

Note that here the local coordinate system has been chosen such that the N-S interface is at $x = 0$.

Inside the superconductor S_j the eigenfunctions are given by

$$\Psi^{\pm}_{n,\mathrm{e}}(\mathrm{S}_j) = \begin{pmatrix} \mathrm{e}^{\mathrm{i}\eta^{\mathrm{e}}_j/2} \\ \mathrm{e}^{-\mathrm{i}\eta^{\mathrm{e}}_j/2} \end{pmatrix} \frac{1}{\sqrt{2q^{\mathrm{e}}_n}} \left(E^2/\Delta^2 - 1\right)^{-1/4} \Phi_n(y,z) \mathrm{e}^{\pm \mathrm{i} q^{\mathrm{e}}_n x} \tag{2.4a}$$

$$\Psi^{\pm}_{n,\mathrm{h}}(\mathrm{S}_j) = \begin{pmatrix} \mathrm{e}^{\mathrm{i}\eta^{\mathrm{h}}_j/2} \\ \mathrm{e}^{-\mathrm{i}\eta^{\mathrm{h}}_j/2} \end{pmatrix} \frac{1}{\sqrt{2q^{\mathrm{h}}_n}} \left(E^2/\Delta^2 - 1\right)^{-1/4} \Phi_n(y,z) \mathrm{e}^{\pm \mathrm{i} q^{\mathrm{h}}_n x} \tag{2.4b}$$

with

$$q^{\mathrm{e,h}}_n = \frac{\sqrt{2m}}{\hbar} \left[E_{\mathrm{F}} - E_n + \sigma^{e,h} \left(E^2 - \Delta^2\right)^{1/2}\right]^{1/2} \tag{2.5a}$$

$$\eta^{\mathrm{e,h}} = \phi_j + \sigma^{\mathrm{e,h}} \arccos\left(\frac{E}{\Delta}\right). \tag{2.5b}$$

The wave functions (2.3a,b) and (2.4a,b) are normalised to carry the same amount of quasiparticle current. This in turn ensures the unitarity of the scattering matrix. The direction of the velocity is the same as the wave vector for the electron and opposite for the hole.

A wave incident on the Andreev billiard is described in the basis (2.3a,b) by a vector of coefficients $c^{\mathrm{in}}_{\mathrm{N}} = \left(c^+_{\mathrm{e}}, c^-_{\mathrm{h}}\right)$ while the reflected wave has a vector of coefficients $c^{\mathrm{out}}_{\mathrm{N}} = \left(c^-_{\mathrm{e}}, c^+_{\mathrm{h}}\right)$. The N here refers to the fact that the waves are in the normal lead. The mode index n has been dropped here for simplicity of notation. The scattering matrix of the normal conducting region connects these two waves to each other

via $c_{\mathrm{N}}^{\mathrm{out}} = S_{\mathrm{N}} c_{\mathrm{N}}^{in}$. Since the normal conducting region does not couple electrons and holes its scattering matrix has the block diagonal form

$$S_{\mathrm{N}}(E) = \begin{pmatrix} S(E) & 0 \\ 0 & S(-E)^* \end{pmatrix}. \tag{2.6}$$

Here $S(E)$ is the $N \times N$ unitary scattering matrix of the normal region itself corresponding to the single-electron Hamiltonian H.

For energies $0 < E < \Delta$ there are no propagating modes in the superconducting lead and the scattering matrix S_{A} of Andreev reflection at the N-S interface can be defined by $c^{\mathrm{in}} = S_{\mathrm{A}} c^{\mathrm{out}}$. Its elements can be obtained by matching the wave functions in (2.3a,b) to the corresponding ones in (2.4a,b) at $x = 0$. Note that we also assume that $E_{\mathrm{F}} \gg \Delta$ such that normal reflection at the N-S interface may be ignored and the difference in the numbers of channels for positive and negative energies may be neglected. This is known as the Andreev approximation [27]. The entries of the scattering matrix of Andreev reflection are therefore given by

$$S_{\mathrm{A}}(E) = \alpha(E) \begin{pmatrix} 0 & \mathrm{e}^{\mathrm{i}\tilde{\phi}} \\ \mathrm{e}^{-\mathrm{i}\tilde{\phi}} & 0 \end{pmatrix}, \tag{2.7}$$

where $\alpha = \mathrm{e}^{-\mathrm{i}\arccos(E/\Delta)} = E/\Delta - \mathrm{i}\sqrt{1 - E^2/\Delta^2}$ and $\tilde{\phi}$ is a diagonal matrix with its first N_{S_1} entries equal to ϕ_1, the next N_{S_2} entries equal to ϕ_2 etc. where N_{S_j}, $j \in \{1, \ldots, n\}$, is the number of channels of the j-th superconducting lead, n the number of superconducting leads and ϕ_j, $j \in \{1, \ldots, n\}$, the phase of the j-th superconductor.

As already mentioned below, Δ there are no propagating modes in the superconductor. Therefore the bound states require that $c_{\mathrm{in}} = S_{\mathrm{A}} S_{\mathrm{N}} c_{\mathrm{in}}$. Thus we have to solve an eigenvalue problem, and the bound states are given by $\det(1 - S_{\mathrm{A}} S_{\mathrm{N}}) = 0$. When inserting S_{A} and S_{N} and using

$$\det \begin{pmatrix} A & B \\ C & D \end{pmatrix} = \det\left(AD - ACA^{-1}B\right) \tag{2.8}$$

for arbitrary matrices A, B, C and D, the discrete spectrum below Δ is given by the determinental equation [54]

$$\det\left[1 - \alpha(E)^2 \mathrm{e}^{-\mathrm{i}\tilde{\phi}} S(E) \mathrm{e}^{\mathrm{i}\tilde{\phi}} S(-E)^*\right] = 0. \tag{2.9}$$

2.1.3 Density of states

In mesoscopic systems, where the density of states is big, one can no longer talk about single Andreev levels. Furthermore one has to investigate averaged quantities. An equation giving the averaged density of states directly may be found starting with (2.9) by a similar calculation as done in [55]. The scattering matrix in the secular function therein has to be replaced by the product $\bar{S}(E) = -\alpha(E)^2 \mathrm{e}^{-\mathrm{i}\tilde{\phi}} S(E) \mathrm{e}^{\mathrm{i}\tilde{\phi}} S(-E)^*$ thus giving a modified secular function

$$Z'_{sc}(E) = \det\left[1 + \bar{S}(E)\right]. \tag{2.10}$$

$\bar{S}(E)$ is obviously unitary below Δ. Therefore its eigenvalues lie on the unit circle of the complex plane and may be written as $\mathrm{e}^{\mathrm{i}\theta_n(E)}$ with $n = 0, \ldots, 2N_{\mathrm{S}}$. The phases $\theta_n(E)$ are the eigenphases of the scattering matrix. Therefore we can express the modified secular function in terms of the eigenphases $\theta_n(E)$ of $\bar{S}(E)$,

$$Z'_{\mathrm{sc}}(E) = \prod_{n=1}^{N_{\mathrm{S}}} \left(1 + \mathrm{e}^{\mathrm{i}\theta_n(E)}\right) = \exp\left(\mathrm{i} \sum_{n=1}^{N_{\mathrm{S}}} \frac{\theta_n(E)}{2}\right) 2^{N_{\mathrm{S}}} \prod_{n=1}^{N_{\mathrm{S}}} \cos\left(\frac{\theta_n(E)}{2}\right). \tag{2.11}$$

In the second step a factor $\mathrm{e}^{\mathrm{i}\theta_n(E)/2}$ has been extracted out of each term in the product such that the remaining terms are equal to $2\cos(\theta_n(E)/2)$. The real valued zeros which account for the spectrum

provide the factors $\cos(\theta_n(E)/2)$. Hence the number of eigenenergies in the interval $(0, E)$ is given by (see Appendix B for a reasoning)

$$N(E) = -\frac{1}{\pi}\lim_{\varepsilon\to 0}\operatorname{Im}\ln\prod_{n=1}^{N_\mathrm{S}}\cos\left(\frac{\theta_n(E+\mathrm{i}\varepsilon)}{2}\right) = \frac{1}{2\pi}\sum_{n=1}^{N_\mathrm{S}}\theta_n(E) - \frac{1}{\pi}\lim_{\varepsilon\to 0}\operatorname{Im}\ln\bar{S}(E+\mathrm{i}\varepsilon). \tag{2.12}$$

In the following we will drop the ε although it will always be implicitly present. The density of states is then obtained by differentiating (2.12) with respect to the energy.

$$\tilde{d}(E) = \bar{d}(E) - \frac{1}{\pi}\operatorname{Im}\frac{\partial}{\partial E}\ln\det\left[1-\alpha(E)^2\mathrm{e}^{-\mathrm{i}\tilde{\phi}}S(E)\mathrm{e}^{\mathrm{i}\tilde{\phi}}S(-E)^*\right]. \tag{2.13}$$

Here $\bar{d}(E)$ is twice the mean density of states. The logarithm of a determinant of a matrix can be written as the trace of the logarithm of the matrix defined by its Taylor series which we will use to derive the density of states in terms of traces of powers of the scattering matrix. We now divide by $\bar{d}(E) = N/(2\pi E_\mathrm{T})$ and express the energy in units of the Thouless Energy $\epsilon = E/E_T$, where $E_\mathrm{T} = 2\hbar/\tau_\mathrm{D}$ and τ_D is the mean dwell time, which is the time a quasiparticle stays on average inside the cavity between two succeeding Andreev reflections. The density of states in terms of ϵ then reads if $\phi_1, \ldots, \phi_k$ are the phases of the superconducting order parameters in the k leads

$$d(\epsilon) = 1 + 2\sum_{n=1}^{\infty}\frac{\alpha^{2n}}{n}\operatorname{Im}\frac{\partial C(\epsilon, n, \phi_1, \ldots, \phi_k)}{\partial\epsilon} \tag{2.14}$$

with the correlation functions of n scattering matrices multiplied by a diagonal matrix containing the phases of the superconductors.

$$C(\epsilon, n, \phi_1, \ldots, \phi_k) = \frac{1}{N}\operatorname{Tr}\left[\mathrm{e}^{-\mathrm{i}\tilde{\phi}}S^*\left(-\frac{\epsilon\hbar}{2\tau_\mathrm{D}}\right)\mathrm{e}^{\mathrm{i}\tilde{\phi}}S\left(\frac{\epsilon\hbar}{2\tau_\mathrm{D}}\right)\right]^n. \tag{2.15}$$

From now on we will restrict ourselves to Andreev billiards with two superconductors with phases ϕ_1 and ϕ_2, respectively. Then the correlation function and the density of states of course will only depend on the difference $\phi = \phi_1 - \phi_2$ such that we will call the correlation function in this case $C(\epsilon, n, \phi)$ and in the case that there is just one superconductor the phase should not play any role so that we will write $C(\epsilon, n)$.

2.2 Random matrices versus diagonal approximation

2.2.1 Random matrix theory

Equation (2.9) is the starting equation for the calculation of the density of states when using Random matrix theory (RMT). In RMT the Hamiltonian of the system is replaced by matrices with randomly chosen entries following a certain distribution. In the end one averages over many of these randomly chosen matrices. It is believed that a quantum system which underlying classical dynamic is chaotic is well described by RMT [56]. This is the Bohigas-Gianonni-Schmidt- (BGS-) conjecture.

The RMT approach to the density of states of an chaotic Andreev billiard was initially considered in [33, 41] where the actual setup treated is depicted in figure 2.2. It consists of a normal metal (N) connected to two superconductors (S_1, S_2) by narrow leads carrying N_{S_1} and N_{S_2} channels. The superconductors' order parameters are considered to have phases $\pm\phi/2$, with a total phase difference ϕ. Moreover a perpendicular magnetic field B was applied to the normal part. We note that although this figure have spatial symmetry the treatment is actually for the case without such symmetry.

As above, the limit $\Delta \ll E_\mathrm{F}$ was taken so that normal reflection at the N-S interface can be neglected and the symmetric case where both leads contain the same number, $N_\mathrm{S}/2$, of channels was considered

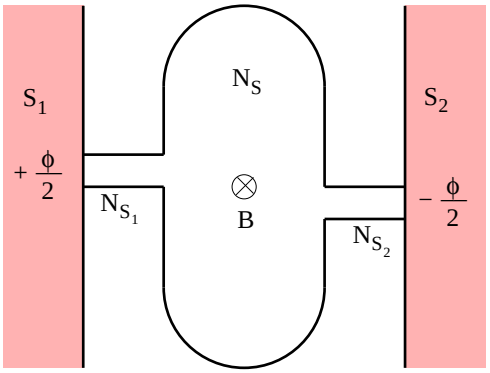

Figure 2.2: An Andreev billiard connected to two superconductors (S_1, S_2) at phases $\pm\phi/2$ via leads carrying N_{S_1} and N_{S_2} channels, all threaded by a perpendicular magnetic field B.

[33, 41]. Finally it was also assumed that $\alpha \approx -\mathrm{i}$, valid in the limit $E, E_\mathrm{T} \ll \Delta \ll E_\mathrm{F}$. For such a setup, the determinantal equation (2.9) becomes

$$\det\left[1 + S(E)\mathrm{e}^{\mathrm{i}\tilde{\phi}}S^*(-E)\mathrm{e}^{-\mathrm{i}\tilde{\phi}}\right] = 0, \tag{2.16}$$

where $\tilde{\phi}$ is a diagonal matrix whose first $N_\mathrm{S}/2$ elements are $\phi/2$ and the remaining $N_\mathrm{S}/2$ elements $-\phi/2$. We note that though we stick to the case of perfect coupling here, the effect of tunnel barriers was also included in [33].

The first step is to rewrite the scattering problem in terms of a low energy effective Hamiltonian $\mathcal{H}$

$$\mathcal{H} = \begin{pmatrix} \hat{H} & \pi XX^T \\ -\pi XX^T & -\hat{H}^* \end{pmatrix}, \tag{2.17}$$

where $\hat{H}$ is the $M \times M$ Hamiltonian of the isolated billiard and X an $M \times N$ coupling matrix. Eventually the limit $M \to \infty$ is taken and to mimic a chaotic system the matrix $\hat{H}$ is replaced by a random matrix following the Pandey-Mehta distribution [57]

$$P(H) \propto \exp\left(-\frac{N_\mathrm{S}^2\left(1+a^2\right)}{64ME_\mathrm{T}^2}\sum_{i,j=1}^{M}\left[\left(\mathrm{Re}\hat{H}_{ij}\right)^2 + a^{-2}\left(\mathrm{Im}\hat{H}_{ij}\right)^2\right]\right). \tag{2.18}$$

The parameter a measures the strength of the time-reversal symmetry breaking so we can investigate the crossover from the ensemble with time reversal symmetry (GOE) to that without (GUE). It is related to the magnetic flux Φ through the two-dimensional billiard of area A and with Fermi velocity v_F by

$$Ma^2 = c\left(\frac{e\Phi}{h}\right)^2 \hbar v_\mathrm{F}\frac{N}{2\pi E_\mathrm{T}\sqrt{A}}. \tag{2.19}$$

Here c is a numerical constant of order unity depending only on the shape of the billiard. The critical flux is then defined via

$$Ma^2 = \frac{N}{8}\left(\frac{\Phi}{\Phi_\mathrm{c}}\right)^2 \qquad \Leftrightarrow \qquad \Phi_\mathrm{c} \approx \frac{h}{e}\left(\frac{2\pi E_\mathrm{T}}{\hbar v_\mathrm{F}}\right)^{\frac{1}{2}} A^{\frac{1}{4}}. \tag{2.20}$$

The density of states, divided for convenience by twice the mean density of states of the isolated billiard, can be written as

$$d(\epsilon) = -\mathrm{Im}W(\epsilon), \tag{2.21}$$

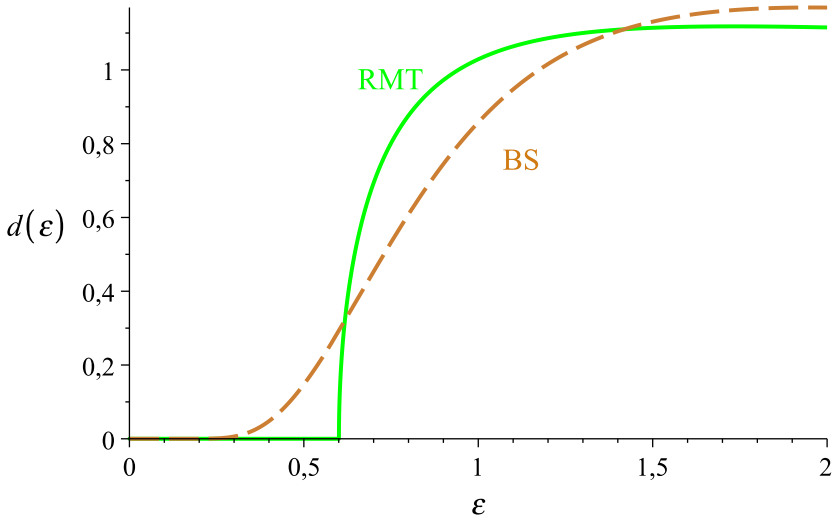

Figure 2.3: The density of states obtained using RMT (solid) and the diagonal approximation (dashed). While RMT predicts an hard gap up to $\approx 0.6E_{\mathrm{T}}$ the Bohr-Sommerfeld result is just exponentially suppressed.

where $W(\epsilon)$ is the trace of a block of the Green function of the effective Hamiltonian of the scattering system and for simplicity here we express the energy in units of the Thouless energy $\epsilon = E/E_{\mathrm{T}}$. This is averaged by integrating over (2.18) using diagrammatic methods [58], which to leading order in inverse channel number $1/N_{\mathrm{S}}$ leads to the expression [41]

$$W(\epsilon) = \left(\frac{b}{2}W(\epsilon) - \frac{\epsilon}{2}\right)\left(1 + W^2(\epsilon) + \frac{\sqrt{1+W^2(\epsilon)}}{\beta}\right), \tag{2.22}$$

where $\beta = \cos(\phi/2)$ and $b = (\Phi/\Phi_{\mathrm{c}})^2$ with the critical magnetic flux Φ_{c} for which the gap in the density of states closes (at $\phi = 0$). Equation (2.22) may also be rewritten as a sixth order polynomial and when substituting into (2.21), we should take the solution that tends to 1 for large energies. In particular, when there is no phase difference between the two leads ($\phi = 0$, or equivalently when we consider a single lead carrying N_{S} channels) and no magnetic field in the cavity ($\Phi/\Phi_{\mathrm{c}} = 0$) the density of states is given by a solution of the cubic equation

$$\epsilon^2 W^3(\epsilon) + 4\epsilon W^2(\epsilon) + (4+\epsilon^2)W(\epsilon) + 4\epsilon = 0. \tag{2.23}$$

2.2.2 Diagonal approximation

The diagonal approximation will be introduced in section 4.1 but we anticipate the result obtained previously when using the diagonal approximation for the density of states of Andreev billiards without going into the details at this stage. In [36] the authors found a density of states of an Andreev billiard with just one superconducting lead given by

$$d_{\mathrm{BS}}(\epsilon) = \left(\frac{\pi}{\epsilon}\right)^2 \frac{\cosh(\pi/\epsilon)}{\sinh^2(\pi/\epsilon)}. \tag{2.24}$$

The results of the RMT prediction given by the solution of (2.23) and the Bohr-Sommerfeld result (2.24) are compared to each other in figure 2.3. The density of states predicted by RMT for one superconducting lead and zero magnetic field is compared to the prediction of the semiclassical calculation based on the

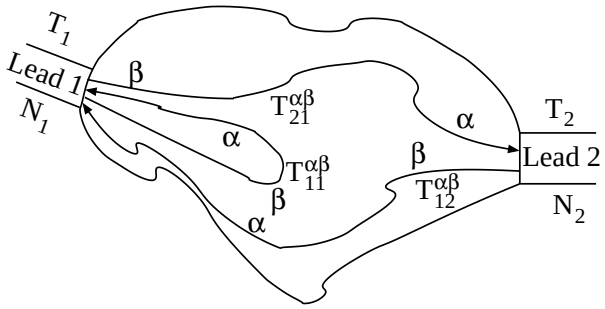

Figure 2.4: Three examples for paths contributing to the transmission from lead 1 to lead 2 $T_{21}^{\alpha\beta}$, from lead 1 back to lead 1 $T_{11}^{\alpha\beta}$ and from lead 2 to lead 1 $T_{12}^{\alpha\beta}$ while being converted from a β-type quasiparticle to an α-type one. The leads provide N_1 and N_2 channels respectively and have temperatures T_1 and T_2.

diagonal approximation. While the density of states has a hard gap of the order of the Thouless energy, *i.e* that it is zero up to an energy $\epsilon \approx 0.6E_{\mathrm{T}}$, the Bohr-Sommerfeld result is only exponentially suppressed for low energies. We will see in section 5 how this discrepancy may be resolved.

2.3 Transport theory

Another problem often considered in condensed matter physics, but also closely related to the scattering matrix is electrical transport. For this we attach additional normal leads to the normal region. The transport through N-S junctions as well as the theory of the transport through a phase coherent superconductor-normal metal hybrid systems has been reviewed in [59]. Originally the theory we will use here was developed by Lambert [60] for a two terminal system and was later generalised to multi-probe systems [61]. It yields a variety of transport coefficients including electrical transport and was derived under the condition that the condensate chemical potentials μ of all superconducting leads are identical. This condition allows one to consider time independent order parameter phases and a time independent scattering approach is applicable. Lambert's derivation of the fundamental current-voltage relation is fairly similar to the multi-channel scattering theory developed by Landauer and Büttiker [29] for non-superconducting mesoscopic structures. In this approach which is now well known as the Landauer-Büttiker formalism, the electrical conductance G_{ij} for a current from lead j to lead i of a two terminal device is related to the transmission coefficient T_{ij}^{ee} of an electron entering the scattering region at lead j and leaving it at lead i as an electron as shown in figure 2.4 with choosing $\alpha = \beta = e$,

$$G_{ij} = \frac{\mathrm{e}^2}{\pi\hbar} T_{ij}^{ee}, \tag{2.25}$$

where $\hbar$ is Planck's constant and the superscript ee here denotes that the incoming and outgoing quasiparticle are both electrons. We will always make use of $\hbar$ rather than of $h = 2\pi\hbar$, although usually in the literature h is used, in order to avoid mixing it up with the 'h' used for labeling holes. This however is not valid in the presence of Andreev scattering since for example this process separates charge and energy: If a quasiparticle hits the interface and is Andreev reflected the energy of the excitation is reflected back into the superconductor while a charge of 2e is injected into the superconductor (c.f. [59]).

2.3.1 Conductance of a multi-probe structure

It is no longer enough to consider the scattering matrix of the normal conducting region as done for the density of states. Instead one has to make use of a more general scattering matrix which also allows conversions from an electron-like to hole-like quasi particle or vice versa. This generalised scattering

matrix $\tilde{S}(E)$ may be written in four blocks

$$\tilde{S}(E) = \begin{pmatrix} S^{ee}(E) & S^{eh}(E) \\ S^{he}(E) & S^{hh}(E) \end{pmatrix}, \tag{2.26}$$

where $S^{\alpha\beta}(E)$ is the scattering matrix which connects the coefficients of the outgoing wave functions of a β type quasiparticle to the coefficients of the incoming wave functions of an α type quasiparticle. Note that this is just one possibility to write this generalised scattering matrix. The block form used here holds if the vector of incoming and outgoing wave coefficients is filled by the coefficients of the electron wave functions before the first coefficient of a hole wave function is entered. A different form has been used in [59, 60] where the authors used the two component wave function such that the wave functions have two components. The generalised scattering matrix has all the known properties of the scattering matrix of the normal metal with all their consequences: It is unitary ensuring current conservation and if an applied magnetic field is reversed this is equivalent to transposing the generalised scattering matrix. Moreover, if the energy E is measured with respect to the condensate chemical potential μ, it satisfies the electron hole symmetry relation $S^{\alpha\beta}(E) = -(-1)^{\delta_{\alpha\beta}}[S^{\bar{\alpha}\bar{\beta}}(-E)]^*$, where $\bar{\alpha}$ denotes a hole if α denotes an electron and vice versa.

The coefficients $T_{kl}^{\alpha\beta}(E)$ for the transmission of a β type quasiparticle in lead l to an α type quasiparticle in lead k as those depicted in figure 2.4 is given by the entries of $S^{\alpha\beta}(E)$ via

$$T_{kl}^{\alpha\beta}(E) = \sum_{o,i} \left| S_{oi}^{\alpha\beta}(E) \right|^2, \tag{2.27}$$

where the sum runs over all channels o in lead k (we will refer to it as an 'outgoing' channel) and all channels i in lead l (we will refer to it as an 'incoming' channel). The properties of the generalised scattering matrix imply some important properties of the transmission coefficients. These are

$$\sum_{\beta,l} T_{kl}^{\alpha\beta}(E) = \sum_{\alpha,l} T_{kl}^{\alpha\beta}(E) = N_k \tag{2.28}$$

due to the unitarity of $\tilde{S}(E)$, particle-hole symmetry

$$T_{kl}^{\alpha\beta}(E) = T_{kl}^{\bar{\alpha}\bar{\beta}}(-E) \tag{2.29}$$

and the time reversibility saying that when reversing an applied field this is equivalent to exchanging k and l as well as α and β. Note that for simplicity of notation we have assumed that the number of open channels in each lead is equal for electrons and holes.

Analogously to the Landauer-Büttiker formalism [29] the current in lead k is given by

$$I_k = \frac{\mathrm{e}}{\pi\hbar} \sum_{j=1}^{N_\mathrm{N}} \sum_{\alpha=e,h} \sigma^\alpha \int_0^\infty \mathrm{d}E \left[\delta_{kl} N_k f_k^\alpha(E) - \sum_{\beta=e,h} T_{kl}^{\alpha\beta}(E) f_l^\beta(E) \right], \tag{2.30}$$

where $f_l^\alpha(E) = \exp\left\{-\left[E - \sigma^\alpha\left(eV_l - \mu\right)\right] / \left(k_\mathrm{B}T\right)\right\}$ is the Fermi function for an α type quasiparticle, V_l is the voltage applied to the l-th lead and N_N is the total number of channels of all the normal leads together. The typical Landauer-Büttiker formula is derived in the linear response regime. This is that the voltage differences are small such that the occurring Fermi functions can be expanded around the chemical potential of the superconductors up to first order in the voltage differences. If we do so apart from different signs the Fermi functions for electrons and holes will be the same and the entries of the conductance matrix which entries connect the current in the k-th lead to the voltages in the different leads via $I_k = \sum_l G_{kl}\left(V_l - V_\mathrm{S}\right)$ with $V_\mathrm{S} = \mu/\mathrm{e}$ are

$$G_{kl} = \frac{\mathrm{e}^2}{\pi\hbar} \int_0^\infty \mathrm{d}\epsilon \left[2\delta_{kl} N_k - T_{kl}^{ee}(\epsilon) + T_{kl}^{eh}(\epsilon) - T_{kl}^{hh}(\epsilon) + T_{kl}^{he}(\epsilon) \right] \left(-\frac{\partial f(\epsilon)}{\partial \epsilon} \right), \tag{2.31}$$

where the energy is again measured in units of the Thouless energy E_T. If one applies the electron-hole symmetry (2.29) one could remove for example $T^{hh}_{kl}(\epsilon)$ and $T^{he}_{kl}(\epsilon)$ in (2.31) by extending the integral over the energy to $-\infty$.

2.3.2 Two-probe formulae

In the case of two normal leads the current-voltage relation may be written in matrix form

$$\begin{pmatrix} I_1 \\ I_2 \end{pmatrix} = \begin{pmatrix} G_{11} & G_{12} \\ G_{21} & G_{22} \end{pmatrix} \begin{pmatrix} V_1 - V_\mathrm{S} \\ V_2 - V_\mathrm{S} \end{pmatrix}. \tag{2.32}$$

The conductance matrix connecting the current to the applied voltages is then given by

$$\begin{pmatrix} G_{11} & G_{12} \\ G_{21} & G_{22} \end{pmatrix} = \frac{\mathrm{e}^2}{\pi\hbar} \int_{-\infty}^{\infty} \mathrm{d}\epsilon \begin{pmatrix} N_1 - T^{ee}_{11}(\epsilon) + T^{he}_{11}(\epsilon) & T^{he}_{12}(\epsilon) - T^{ee}_{12}(\epsilon) \\ T^{he}_{21}(\epsilon) - T^{ee}_{21}(\epsilon) & N_2 - T^{ee}_{22}(\epsilon) + T^{he}_{22}(\epsilon) \end{pmatrix} \left(-\frac{\partial f}{\partial \epsilon}\right). \tag{2.33}$$

Note that we have used the electron hole symmetry to extend the integral to $-\infty$.

If the superconducting condensate chemical potential is not controlled externally it adjusts itself so that the net current through the N-S interfaces are zero and therefore the current in lead 2 has to be the opposite of that in lead 1, *i.e.* $I_1 = -I_2 = I$. The conductance G of the system may then be calculated by $G = I/(V_1 - V_2)$. For this we first have to eliminate the chemical potential of the superconductors. Thus one first has to invert (2.32) giving

$$\begin{pmatrix} V_1 - V_\mathrm{S} \\ V_2 - V_\mathrm{S} \end{pmatrix} = \frac{1}{d} \begin{pmatrix} G_{22} & -G_{12} \\ -G_{21} & G_{11} \end{pmatrix} \begin{pmatrix} I \\ -I \end{pmatrix} \tag{2.34}$$

with the determinant of the conductance matrix $d = G_{11}G_{22} - G_{12}G_{21}$. At zero temperature the derivative of the Fermi function becomes a δ-function and all the transmission and reflection coefficient have to be evaluated at $\epsilon = 0$ and the dimensionless conductance $g = G\pi\hbar/\mathrm{e}^2$ which measures the conductance in units of the conductance quantum $\mathrm{e}^2/\pi\hbar$ therefore reads [61]

$$g = T^{ee}_{21} + T^{he}_{21} + \frac{2\left(T^{he}_{11}T^{he}_{22} - T^{he}_{21}T^{he}_{12}\right)}{T^{he}_{11} + T^{he}_{22} + T^{he}_{21} + T^{he}_{12}}. \tag{2.35}$$

In this equation the number of channels N_i has been replaced by transmission coefficients by using (2.28). For a symmetric scatterer, where $T^{\alpha\beta}_{12} = T^{\alpha\beta}_{21}$ and $T^{\alpha\beta}_{22} = T^{\alpha\beta}_{11}$ this reduces to $g = T^{ee}_{21} + T^{he}_{11}$ whereas in absence of transmission between the two leads the resistance g^{-1} reduces to a sum of two resistances $g^{-1} = (2T^{he}_{11})^{-1} + (2T^{he}_{22})^{-1}$. When combining the particle hole symmetry with the unitarity of the scattering matrix one finds that $T^{ee}_{21} + T^{he}_{21} = T^{ee}_{12} + T^{he}_{12}$ and thus (2.35) is symmetric under exchanging primed and unprimed coefficients.

2.4 Thermopower

If the different leads have, additional to the different voltages V_j, different temperatures T_j then equation (2.30) has to be slightly modified. Each transmission (and reflection) coefficient T_{kl} is multiplied with the Fermi function of the incoming lead l [62] and hence depends on the temperature T_l of this lead, *i.e.* the Fermi functions in (2.30) are now given by $f^\alpha_l(E) = \exp\left\{-\left[E - \alpha\left(eV_l - \mu\right)\right]/\left(k_\mathrm{B}T_l\right)\right\}$, where T_l is the temperature in the l-th lead. With this replacement (2.30) also describes the thermoelectrical effect, *i.e.* that a temperature difference causes a voltage difference.

If one again linearises (2.30) with the Fermi functions with different temperatures not only in the voltage but also in the temperatures one finds for a two terminal setup with isolated superconducting leads, where the net electrical current and heat current in the superconducting leads are zero [63]

$$\begin{pmatrix} I_1 \\ I_2 \end{pmatrix} = G \begin{pmatrix} V_1 - V_\mathrm{S} \\ V_2 - V_\mathrm{S} \end{pmatrix} + B \begin{pmatrix} T_1 - T \\ T_2 - T \end{pmatrix}, \tag{2.36}$$

where T is the base temperature of the cavity and the superconductors and B is a 2×2 matrix with entries

$$B_{ij} = -\frac{\mathrm{e}}{\pi\hbar T} \int_0^\infty \mathrm{d}\epsilon\, \epsilon \frac{\partial f}{\partial \epsilon} \left(T_{ij}^{ee} - T_{ij}^{he} + T_{ij}^{eh} - T_{ij}^{hh} \right). \tag{2.37}$$

Additionally one may consider the heat current $\mathbf{Q}$ which is given by [51]

$$\begin{pmatrix} Q_1 \\ Q_2 \end{pmatrix} = \Gamma \begin{pmatrix} V_1 - V_\mathrm{S} \\ V_2 - V_\mathrm{S} \end{pmatrix} + \Xi \begin{pmatrix} T_1 - T \\ T_2 - T \end{pmatrix} \tag{2.38}$$

with

$$\Gamma_{ij} = -\frac{\mathrm{e}}{\pi\hbar} \int_0^\infty \mathrm{d}\epsilon\, \epsilon \frac{\partial f}{\partial \epsilon} \left(T_{ij}^{ee} + T_{ij}^{he} - T_{ij}^{eh} - T_{ij}^{hh} \right) \tag{2.39a}$$

$$\Xi_{ij} = \frac{1}{\pi\hbar T} \int_0^\infty \mathrm{d}\epsilon\, \epsilon^2 \frac{\partial f}{\partial \epsilon} \left(2N_i\delta_{ij} - T_{ij}^{ee} - T_{ij}^{he} - T_{ij}^{eh} - T_{ij}^{hh} \right). \tag{2.39b}$$

Thus when combining (2.36) and (2.38) one gets a four-dimensional linear equation.
If the superconductors are isolated so that the net currents in the superconducting leads are zero the currents in the leads 1 and 2 have to be opposite, *i.e.* they have to satisfy $I_1 = -I_2 = I$ and $Q_1 = -Q_2 = Q$. By inverting the four matrices above one may again eliminate V_S and T in the same way as in section 2.3.2 and finds that the currents only depend on $\Delta V = V_1 - V_2$ and $\Delta T = T_1 - T_2$. Thus (2.36) and (2.38) may be rewritten as a 2×2 system of linear equations [63]

$$\begin{pmatrix} I \\ Q \end{pmatrix} = \begin{pmatrix} \tilde{G} & \tilde{B} \\ \tilde{\Gamma} & \tilde{\Xi} \end{pmatrix} \begin{pmatrix} \Delta V \\ \Delta T \end{pmatrix} \tag{2.40}$$

with

$$\tilde{G} = \frac{2\mathrm{e}^2}{\mathrm{h}} \left(\hat{T}_{21}^{ee} + \hat{T}_{21}^{he} + 2\frac{\hat{T}_{11}^{he}\hat{T}_{22}^{he} - \hat{T}_{21}^{he}\hat{T}_{12}^{he}}{\hat{T}_{11}^{he} + \hat{T}_{22}^{he} + \hat{T}_{21}^{he} + \hat{T}_{12}^{he}} \right) \tag{2.41a}$$

$$\tilde{B} = \frac{2\mathrm{e}}{\mathrm{h}T} \left(\bar{T}_{12}^{ee} - \bar{T}_{12}^{he} - 2\frac{\left(\bar{T}_{11}^{he} + \bar{T}_{21}^{he}\right)\left(\hat{T}_{11}^{he} + \hat{T}_{12}^{he}\right)}{\hat{T}_{11}^{he} + \hat{T}_{22}^{he} + \hat{T}_{21}^{he} + \hat{T}_{12}^{he}} \right) \tag{2.41b}$$

$$\tilde{\Gamma} = -\frac{2\mathrm{e}}{\mathrm{h}} \left(\bar{T}_{21}^{ee} + \bar{T}_{21}^{he} + 2\frac{\left(\tilde{T}_{11}^{he} + \tilde{T}_{21}^{he}\right)\left(\bar{T}_{11}^{he} + \bar{T}_{12}^{he}\right)}{\hat{T}_{11}^{he} + \hat{T}_{22}^{he} + \hat{T}_{21}^{he} + \hat{T}_{12}^{he}} \right) \tag{2.41c}$$

$$\tilde{\Xi} = -\frac{2}{\mathrm{h}T} \left(\hat{T}_{21}^{ee} + \hat{T}_{21}^{he} + 2\frac{\left(\bar{T}_{11}^{he} + \bar{T}_{21}^{he}\right)\left(\bar{T}_{11}^{he} + \bar{T}_{12}^{he}\right)}{\hat{T}_{11}^{he} + \hat{T}_{22}^{he} + \hat{T}_{21}^{he} + \hat{T}_{12}^{he}} \right) \tag{2.41d}$$

where $\hat{T}_{ij}^{\alpha\beta} = -\int_{-\infty}^{\infty} \mathrm{d}\epsilon\, (\partial f/\partial\epsilon)\, T_{ij}^{\alpha\beta}$ and $\bar{T}_{ij}^{\alpha\beta} = -\int_{-\infty}^{\infty} \mathrm{d}\epsilon\, \epsilon\, (\partial f/\partial\epsilon)\, T_{ij}^{\alpha\beta}$. Note that in [63] these coefficients have been written down only for low temperatures using Sommerfeld expansion.
The strength of the coupling of electrical and thermal properties may for example be measured by the thermopower [64]

$$S = -\left.\frac{\Delta V}{\Delta T}\right|_{I=0} \tag{2.42}$$

also known as the Seebeck coefficient where $\Delta V = V_1 - V_2$ is the voltage drop between the two leads and $\Delta T = T_1 - T_2$ the temperature difference between them. It has to be evaluated at zero current since

if a temperature gradient is present the voltage adjusts itself such that - as long as there is no external voltage applied - the net current is zero. Using (2.42) and (2.40) one immediately finds

$$S = -\frac{\tilde{B}}{\tilde{G}}. \tag{2.43}$$

What we have discussed in this chapter, namely the scattering approach to the density of states of Andreev billiards and the relation between the transmission coefficients and the conductance and the thermopower will be used in sections 5, 6, 7 and 8 where we use semiclassical methods to derive the density of states, the electrical conductance and the thermopower of Andreev billiards.

3 Basic Semiclassics

3.1 Path integrals

In [33] it has been noticed that the shape of the density of states depends on whether the underlying classical dynamics is chaotic or integrable. A framework which naturally connects quantum mechanical properties to the classical dynamics is semiclassics expressing the quantum mechanical properties of a system by properties of the classical trajectories of the system. The starting point to derive the semiclassical framework including scattering matrices is often the path integral approach to quantum mechanics.

3.1.1 Feynman's introduction of the path integral

In 1948 Richard Phillips Feynman introduced his now famous (quantum mechanical) path integral method [65]. It provides a very powerful method not only in quantum mechanics but also in quantum electrodynamics [66] as well as in quantum field theory. Moreover it provides an intuitive way to obtain the classical motion from quantum mechanics [65, 67].

When Feynman introduced his path integral he started with considering an imaginary experiment with three arbitrary measurements showing one of the paradigms of quantum mechanics: first a quantity A should be measured then a quantity B and finally a quantity C. He considered the probabilities P_{abc} for the measurements B and C giving the results b and c, respectively, provided that in A a was measured as well as the probability P_{ab} that when measurement A gives a measurement B gives b and the corresponding probabilities P_{ac} and P_{bc}. If the events are independent $P_{abc} = P_{ab}P_{bc}$ which is true in quantum mechanics if B fully specifies the state, *i.e.* the states are not degenerate with respect to B. Moreover classically $P_{ac} = \sum_b P_{abc}$ yielding $P_{ac} = \sum_b P_{ab}P_{bc}$. Quantum mechanically however this depends on whether measurement B has been done or not: The probabilities P_{ab}, P_{bc}, P_{ac} are replaced by the squared modulus of complex numbers $\phi_{ab}, \phi_{bc}, \phi_{ac}$ which satisfy $\phi_{ac} = \sum_b \phi_{ab}\phi_{bc}$. If measurement B did not take place this gives a probability P_{ac} differing from the classical one. However if the measurement takes place the resulting probabilities are the same in both cases. The next step was to generalise it to k measurements Feynman denoted by $A, \ldots, K$ at times $t_1, t_1+\kappa, t_1+2\kappa \ldots, t_1+k\kappa$. Again the probabilities that an arbitrary series out of the k measurements (with fixed order, *i.e* A should always be measured at first, B before C, C before D etc.) gives the corresponding results out of $a, b \ldots, k$ is given by the squared modulus of a complex number, for example $P_{ack} = |\sum_{b,d,\ldots} \phi_{abc\ldots k}|^2$. If all the measurements are the measurement of the location $\mathbf{r}$ of a quantum mechanical particle. From a classical point of view the measured coordinates $\mathbf{r}_1, \ldots \mathbf{r}_k$ then define a path $\mathbf{r}(t)$ with the measured locations $\mathbf{r}_i = \mathbf{r}(t_i)$. Of course the coordinates are continuous variables rather than discrete ones such that the previous sums over $a, b, c, \ldots$ have to be replaced by integrals over the coordinates $\mathbf{r}_i$. If additionally the limit $\kappa \to 0$ and $k \to \infty$ with $k\kappa$ fixed is taken this already provides the definition of the path integral of the ϕ's. The probability that x_i, $i \in \{1, \ldots, k\}$ lies between a_i and b_i is

$$\lim_{\kappa\to 0} \int_{a_1}^{b_1} \mathrm{d}x_1 \ldots \int_{a_k}^{b_k} \mathrm{d}\mathbf{r}_k F(\mathbf{r}_1, \ldots \mathbf{r}_k) = \int_R \mathcal{D}\mathbf{r}(t)\phi[\mathbf{r}(t)], \tag{3.1}$$

where we used the notation $\mathrm{d}\mathbf{r} = \mathrm{d}x\mathrm{d}y\mathrm{d}z$ for the measure and $k = \Delta t/\kappa$ with Δt the time over which the (imaginary) measurements take place. R denotes the region in which the paths $\mathbf{r}(t)$ shall be. Whether an integral is a path integral or not can be seen on the symbol denoting the measure. While for 'normal' integration a roman d is used for the path integral we will use a calligraphic $\mathcal{D}$.

3.1.2 Path integrals in quantum mechanics

The next step is to apply the above derived path integral method to quantum mechanics. Schrödinger's quantum mechanics is based on the Schrödinger equation in configuration space

$$\mathrm{i}\hbar\frac{\partial\psi}{\partial t} = H\psi \tag{3.2}$$

with the Hamilton operator $H = \frac{\mathbf{p}^2}{2m} + V(\mathbf{r})$, where $\mathbf{p} = -\mathrm{i}\hbar\nabla$ with $\nabla = \partial/\partial\mathbf{r} = (\partial/\partial x, \partial/\partial y, \partial/\partial z)^T$ and m the mass of the particle described by the wave function $\psi(\mathbf{r}, t)$ which depends on the location $\mathbf{r} = (x, y, z)^T$, where the superscript T stands for transposing.

The solution of a differential equation may be found by using a Greens function which in this case is also called 'propagator'. The propagator in coordinate space $K(\mathbf{r}, \mathbf{r}'; t, t')$ depends on the spatial coordinates $\mathbf{r}$ and $\mathbf{r}'$ as well as on the times t and t' and has to be a solution of

$$\left(H_{\mathbf{r}} - \mathrm{i}\hbar\frac{\partial}{\partial t}\right) K(\mathbf{r}, \mathbf{r}'; t, t') = -\mathrm{i}\hbar\delta(\mathbf{r} - \mathbf{r}')\,\delta(t - t'), \tag{3.3}$$

where the index $\mathbf{r}$ of the Hamiltonian $H_{\mathbf{r}}$ indicates that it depends on $\mathbf{r}$. Due to the definition of the propagator by (3.3) the wave functions $\psi(\mathbf{r}, t)$ solving the Schrödinger equation (3.2) can then be found using that when multiplying the propagator with the wave function at the point $\mathbf{r}'$ and time t' this product is equal to the wave function at the point $\mathbf{r}$ and time t, hence the propagator propagates the wave function from the space time point $(\mathbf{r}', t')$ to the space time point $(\mathbf{r}, t)$. That is where the name propagator comes from. Therefore if one knows the wave function at an initial space time point $(\mathbf{r}_0, t_0)$ and the Greens function one can calculate the wave function at any space time point,

$$\psi(\mathbf{r}, t) = K(\mathbf{r}, \mathbf{r}_0; t, t_0)\psi(\mathbf{r}_0, t_0). \tag{3.4}$$

For a time independent Hamiltonian H the propagator depends solely on the difference $t - t'$ such that in the following we set $t' = 0$. The propagator is then given by

$$K(\mathbf{r}, \mathbf{r}'; t) = \left\langle \mathbf{r} \left| \mathrm{e}^{-\mathrm{i}Ht/\hbar} \right| \mathbf{r}' \right\rangle. \tag{3.5}$$

A path integral description of the propagator is obtained as follows: First one decomposes the exponential factor in N equal factors and writes the Hamiltonian as the sum of the kinetic energy $T = \mathbf{p}^2/(2m)$ and the potential V. When decomposing each exponential factor into $\mathrm{e}^{-\mathrm{i}Tt/(N\hbar)}\mathrm{e}^{-\mathrm{i}Vt/(N\hbar)}$ the Zassenhaus-formula [68]

$$\mathrm{e}^{X+Y} = \mathrm{e}^X + \mathrm{e}^Y + \mathrm{e}^{\frac{1}{2!}[X,Y]}\mathrm{e}^{\frac{1}{3!}(2[Y,[X,Y]]+[X,[X,Y]])}\cdots,$$

where X and Y are two arbitrary operators and $[X, Y] = XY - YX$ is the commutator, implies thatthe error is of the order of $1/N^2$. Therefore in the limit $N \to \infty$ the propagator may therefore be written as

$$K(\mathbf{r}, \mathbf{r}'; t) = \lim_{N\to\infty} = \left\langle \mathbf{r} \left| \left(\mathrm{e}^{-\mathrm{i}Tt/(\hbar N)}\mathrm{e}^{-\mathrm{i}Vt/(\hbar N)}\right)^N \right| \mathbf{r}' \right\rangle. \tag{3.6}$$

This equality is provided by the so called Trotter product formula. More details about this formula and its proof may be found in [67, 69], a rigorous mathematical can be found in [70]. After inserting the identity operator $1 = \int \mathrm{d}\mathbf{r}_j |\mathbf{r}_j\rangle\langle\mathbf{r}_j|$ between each term of the product one gets

$$K(\mathbf{r}, \mathbf{r}'; t) = \lim_{N\to\infty} \int \mathrm{d}\mathbf{r}_1 \cdots \mathrm{d}\mathbf{r}_{N-1} \prod_{j=0}^{N-1} \left\langle \mathbf{r}_{j+1} \left| \mathrm{e}^{-\mathrm{i}Tt/(\hbar N)}\mathrm{e}^{-\mathrm{i}Vt/(\hbar N)} \right| \mathbf{r}_j \right\rangle, \tag{3.7}$$

we have defined $\mathbf{r}_0 = \mathbf{r}'$ and $\mathbf{r}_N = \mathbf{r}$. One may then use the diagonality of V in configuration space to pull the second exponential factor out of the scalar product. In order to be able to also pull out

the exponential factor containing the kinetic energy we insert a complete set of momentum eigenstates $|\mathbf{p}\rangle$ which satisfy $\langle\mathbf{p}|\mathbf{x}\rangle = (2\pi\hbar)^{-d/2}\mathrm{e}^{-\mathrm{i}\mathbf{p}\cdot\mathbf{x}/\hbar}$, where d is the dimension. Finally this leads to a Gaussian integral and after its evaluation the propagator becomes [65]

$$K(\mathbf{r},\mathbf{r}';t)\lim_{N\to\infty}\int \mathrm{d}\mathbf{r}_1\cdots\mathrm{d}\mathbf{r}_{N-1}\left(\frac{mN}{2\pi\mathrm{i}\hbar t}\right)^{\frac{Nd}{2}}\prod_{j=0}^{N-1}\exp\left[-\frac{m\left(\mathbf{r}_{j+1}-\mathbf{r}_j\right)^2 N}{2\mathrm{i}\hbar t}-\frac{\mathrm{i}tV(\mathbf{r}_j)}{\hbar N}\right]. \tag{3.8}$$

When performing the limit $N\to\infty$ the sum over the times has to be replaced by an integral and the differences of the coordinates become derivatives with respect to the time yielding the velocity. Thus the path integral representation of the propagator is

$$K(\mathbf{r},\mathbf{r}';t)=\int \mathcal{D}q\mathrm{e}^{\frac{\mathrm{i}}{\hbar}\int_0^t \mathrm{d}t' L(\mathbf{q},\dot{\mathbf{q}})}, \tag{3.9}$$

where $L(\mathbf{q},\dot{\mathbf{q}})=\dot{\mathbf{q}}^2/(2m)-V(\mathbf{q})$ is the Lagrangian of the classical system and the paths $\mathbf{q}(t)$ satisfy $q(0)=\mathbf{r}'$ and $\mathbf{q}(t)=\mathbf{r}$. The exponent therefore is given by Hamilton's principal function $W=\int_0^t \mathrm{d}t' L(\mathbf{q},\dot{\mathbf{q}})$ of the path $q(t)$ measured in units of $\hbar$.

3.2 Semiclassical Greens function

Equation (3.9) is the starting point for the derivation of the semiclassical propagator. However we will give only a qualitative explanation for the functional form of the semiclassical propagator rather than an exact derivation. For a more detailed description of how to get from (3.9) to the semiclassical propagator see for example [71].

In order to get the semiclassical propagator out of (3.9) we need the method of stationary phase approximation. This is to expand the (imaginary) exponent in a stationary point (where the exponent is extremal) up to second order in the integration variable. This leads to Fresnel integrals $\int_{-\infty}^{\infty}\mathrm{d}x\mathrm{e}^{\mathrm{i}x^2}=\sqrt{\mathrm{i}\pi}$. In our case we have a functional rather than a function that has to be stationary. Thus for the expansion we have to use variations instead of derivatives. The condition for the stationarity of the exponent in this case is that the action has to be extremal. If one performs the variation of W with respect to the path $\mathbf{q}(t)$ with fixed starting and end points $\mathbf{q}(0)$ and $\mathbf{q}(t)$ one arrives at the Euler-Lagrange equations $\partial L/\partial\mathbf{q}-\mathrm{d}/\mathrm{d}t(\partial L/\partial\dot{\mathbf{q}})=0$ which are equivalent to Newton's law $\mathbf{F}=m\mathbf{a}$, where $\mathbf{F}$ is a force and $\mathbf{a}$ the acceleration. Hence the paths contributing in the semiclassical limit $\hbar\to 0$ are the classical trajectories ζ starting at $t=0$ at $\mathbf{x}'$ and reaching $\mathbf{x}$ after a time t. A more precise derivation of the semiclassical propagator gives[71]

$$K^{\mathrm{sc}}(\mathbf{r},\mathbf{r}';t)=(2\pi\mathrm{i}\hbar)^{-d/2}\sum_{\zeta}C_\zeta^{1/2}\mathrm{e}^{\mathrm{i}W_\zeta(t)/\hbar-\mathrm{i}\nu_\zeta\pi/2} \tag{3.10}$$

with C_ζ being the modulus of the determinant of the matrix $-\partial^2 W_\zeta/(\partial\mathbf{x}'\partial\mathbf{x})$ with the derivative of W towards x_i and x_j in the j-th column of the i-th row. ν_ζ is the number of conjugated points including their multiplicativity. Conjugated points of a trajectory are the points where all trajectories arising from a small perturbation of ζ cross each other in configuration space.

In most systems however the time is not available but instead the energy E may be measured or even controlled. Therefore in most cases the Greens function $G(\mathbf{r},\mathbf{r}',E)$ which is derived out of the propagator by a Fourier transform is of interest:

$$G(\mathbf{r},\mathbf{r}';E)=-\frac{\mathrm{i}}{\hbar}\int_0^\infty \mathrm{d}t\mathrm{e}^{\mathrm{i}Et/\hbar}K(\mathbf{r},\mathbf{r}';t). \tag{3.11}$$

Using the semiclassical approximation of the propagator (3.10) and applying the stationary phase approximation yields the condition $\partial W_\zeta/\partial t|_{t=0}=-E$. Therefore the constant term in the exponent (without

the phases arising from the conjugated points) is given by $\mathrm{i}(W_\zeta(t_0)+Et_0)/\hbar = \mathrm{i}S_\zeta(E)/\hbar$ with the classical action $S_\zeta(E)$ of the trajectory ζ at energy E. In particular the semiclassical Greens function after expressing all the appearing principal functions by the action is given by

$$G^{\mathrm{sc}}(\mathbf{r},\mathbf{r}';E) = \frac{1}{\mathrm{i}\hbar}(2\pi\mathrm{i}\hbar)^{-d/2}\sum_\zeta D_\zeta^{\frac{1}{2}}\,\mathrm{e}^{\mathrm{i}S_\zeta(E)/\hbar-\mathrm{i}\eta_\zeta\pi/2} \tag{3.12}$$

with

$$D_\zeta = \left|\det\begin{pmatrix} -\frac{\partial^2 S}{\partial\mathbf{x}'\partial\mathbf{x}} & -\frac{\partial^2 S}{\partial\mathbf{x}'\partial E} \\ -\frac{\partial^2 S}{\partial\mathbf{x}\partial E} & -\frac{\partial^2 S}{\partial E^2}\end{pmatrix}\right| \tag{3.13}$$

and η is the number of conjugated points plus the number of changes of the sign of $\partial^2 W_\zeta/\partial t^2\big|_{t=0}$.

3.3 Semiclassical scattering matrix and transmission coefficients

3.3.1 Scattering matrix

The connection between Greens functions and the scattering matrix has been established by Fisher and Lee [72]. The Fisher Lee relations express the transmission and reflection amplitudes S_{oi} (if i and o are in the same lead this is a reflection amplitude and it is a transmission amplitude otherwise) between incoming channels i and outgoing channels o in terms of the projection of the Greens function of the scattering region onto the transverse modes $\phi_i(y)$ and $\phi_o(y')$ of the incoming and outgoing channel:

$$S_{oi}(E) = \delta_{oi} - \mathrm{i}\hbar\,(v_o v_i)^{1/2}\int \mathrm{d}y'\int \mathrm{d}y\phi_o^*(y')\phi_i(y)G\,(x',y',x,y;E)\,. \tag{3.14}$$

x and x' denote the directions along the incoming and outgoing leads, respectively and v_i and v_o denote the corresponding longitudinal velocities. The integrals with respect to y and y' are taken over the cross section of the leads.

To derive a semiclassical expression for the entries of the scattering matrix [73] one replaces the Greens function $G(x',y',x,y;E)$ in (3.14) by the semiclassical Greens function (3.12).

One then has to evaluate the projection integrals in (3.14) for appropriate transversal wave functions ϕ_i and ϕ_o. Since we are considering ideal (impurity free) leads with hard boundaries the wave function in the incoming lead is given by $\phi_i(y) = \sqrt{2/W_i}\sin(i\pi y/W_i)$ and in the outgoing one $\phi_o(y) = \sqrt{2/W_o}\sin(o\pi y/W_o)$, where W_i and W_o are the widths of the incoming and outgoing lead, respectively. Using these wave functions the integrals with respect to y and y' may be evaluated using stationary phase approximation. In order to be able to use stationary phase approximation one first uses $\sin(x) = \left(\mathrm{e}^{\mathrm{i}x}-\mathrm{e}^{-\mathrm{i}x}\right)/(2\mathrm{i})$. After that stationary phase approximation is applicable leading to the condition [74, 75] $(\partial S/\partial y)_{y'} = -\bar{i}\hbar\pi/W_i$ for the y integral with $\bar{i} = \pm i$ and the same for the y' integral but with y and y' exchanged and i replaced by o and W_i replaced by W_o. Remember also that in general $\partial S/\partial y = -p_y$, where p_y is the momentum of the trajectory in y direction. Thus the modulus of the momentum in y direction of the classical trajectory has to the same as the one of the (expectation value of the) momentum in y-direction of the transversal wave function $\langle\hat{p}_y\rangle = \hbar k\sin(\theta)$ in the incoming lead, where $k = \sqrt{2mE}/\hbar$ and θ is the angle under which the particle enters the scattering region with respect to the direction of the lead. Therefore only those paths which enter the cavity at (x,y) with a fixed angle $\sin\theta = \pm i\pi/(kW_i)$ and exit the cavity at (x',y') with an angle $\sin\theta' = \pm o\pi/kW_o$ contribute to the entries of the scattering matrix.

The entries of the scattering matrix in terms of classical trajectories are then given by [74, 76]

$$S_{oi} = \delta_{o,i} - \sqrt{\frac{\pi\mathrm{i}\hbar}{2W_iW_o}}\sum_{\zeta(\bar{o},\bar{i})}\mathrm{sign}(\bar{o})\mathrm{sign}(\bar{i})\sqrt{A_\zeta}\mathrm{e}^{\mathrm{i}\tilde{S}_\zeta(\bar{o},\bar{i};E)/\hbar-\mathrm{i}\pi\tilde{\mu}_\zeta/2} \tag{3.15}$$

with the reduced action $\tilde{S}(\bar{o},\bar{i};E) = S_\zeta(E) + \hbar k_y(E)\sin\theta - \hbar k'_y(E)\sin\theta'$. The phases $\tilde{\mu_\zeta}$ contain not only the number of conjugate points but also an additional phase arising from the integrations over y and y' and the prefactors are $A_\zeta = |(\partial y/\partial\theta')_\theta| \,/\, (\hbar k\,|\cos\theta'|)$. The classical trajectories ζ enter the scattering region at the incoming channel i and leave it at channel o.

Note that the entries of the scattering matrix are typically written in a slightly different form,

$$S_{oi}(E) = \frac{1}{\sqrt{T_\mathrm{H}}} \sum_{\zeta(i\to o)} A_\zeta \mathrm{e}^{\mathrm{i}S_\zeta(E)/\hbar}, \tag{3.16}$$

where T_H is the so called Heisenberg time which is the time corresponding to the mean level spacing and is related to the mean dwell time τ_D via $T_\mathrm{H} = N\tau_\mathrm{D}$. The dwell time is the time a particle typically stays inside the cavity. Here the amplitude A_ζ has been redefined to include the signs as well as the additional phases. If $i = o$ the trajectories are periodic orbits including the trajectories of length zero thus including the additional term given by the Kronecker delta in (3.15)

3.3.2 Semiclassical transmission coefficients

The transmission coefficients for transmission from lead l to lead k needed for example in the Landauer Büttiker formalism [29] are related to the entries of the scattering matrix as

$$T_{kl}(E) = \sum_{o\in k}\sum_{i\in l} |s_{oi}|^2 . \tag{3.17}$$

After inserting (3.16) for the elements of the scattering matrix in (3.17) the transmission coefficients read in the semiclassical approximation [74, 75, 77]

$$T_{kl}(E) = \frac{1}{T_\mathrm{H}} \sum_{o\in k}\sum_{i\in l}\sum_{\zeta(i\to o)}\sum_{\zeta'(i\to o)} A_\zeta A^*_{\zeta'} \mathrm{e}^{\mathrm{i}\left(S_\zeta(E) - S_{\zeta'}(E)\right)/\hbar}. \tag{3.18}$$

Thus in the semiclassical approximation the scattering matrix and the transmission coefficients are given by the properties of the classical trajectories. In what follows we will have to evaluate a set of an even number of trajectories. This is for example that for the density of states we have to evaluate the correlation function C (2.15) of $2n$ scattering matrices, $n \in \mathbb{N}$. Since the entries of each scattering matrix are given by the sum over all classical trajectories connecting the corresponding channels to each other this will lead to $2n$ classical trajectories where due to the complex conjugation of n of the scattering matrices the phase of the correlation function is given by the difference of the classical actions. Due to the average in the semiclassical limit $\hbar \to 0$ only those trajectory sets contribute which cause a total action difference small enough not to be cancelled due to oscillations on averaging. The next task is therefore to find and evaluate those trajectory sets causing a small action difference and therefore contributing in the semiclassical limit.

4 Correlated trajectories in semiclassics

4.1 Trajectory sets

When we insert the expressions for the scattering matrix into the correlation function $C(\epsilon, n)$ of $2n$ scattering matrices this leads to expressions of the type

$$\frac{1}{T_{\mathrm{H}}^n}\left\langle \sum_{i_1,\ldots,i_n}\sum_{o_1,\ldots,o_n}\sum_{\zeta_1,\ldots,\zeta_n}\sum_{\zeta'_1,\ldots,\zeta'_n}\left(\prod_{j=1}^{n} A_{\zeta_j}A^*_{\zeta'_j}\exp\left(\frac{\mathrm{i}}{\hbar}\left(S_{\zeta_j}(E_j)-S_{\zeta'_j}(E'_j)\right)\right)\right)\right\rangle, \tag{4.1}$$

where n is the number of path pairs in the cavity and $\langle\ldots\rangle$ denotes an average over the billiard shape or over the Fermi energy E_{F} within an classically small energy range but large enough quantum mechanically to smooth out fluctuations. This average will be left out in the following equations although always implicitly present. Moreover ζ_j and ζ'_j are classical trajectories, where ζ_j starts at channel i_j (incoming channel) and ends at channel o_j (outgoing channel), $j \in \{1,\ldots,n\}$. The primed trajectories may in general connect arbitrary channels to each other but they have to connect an incoming to an outgoing channel or vice versa. When we will treat the density of states for example ζ'_j will start at channel o_j and end at channel i_{j+1}, where $i_{n+1} = i_1$. This implies, that each channel is hit by two different trajectories. A_ζ is the stability amplitude of the trajectory and $S_\zeta(E)$ is the classical action of the trajectory ζ at energy E which is measured with respect to some given reference energy E_0 which will later be for example the Fermi energy. However for the moment we will restrict ourselves to the case $E \equiv 0$ since including the energy dependence will be done later by expanding the classical actions in the energy around E_0.

In the semiclassical limit $\hbar \to 0$ the phase factors containing the action differences oscillate widely and therefore cancel on averaging unless the action difference becomes of the order of $\hbar$. The first attempt often done is the so-called diagonal approximation [78] where one pairs identical trajectories to each other, *i.e.* $\zeta_i = \zeta_j$ for $i \neq j$. These pairs obviously have the same action such that the difference between their actions vanishes and the paths contribute in the semiclassical limit. However as already mentioned in the introduction this contribution does not give the whole truth. A better approximation is achieved by collapsing trajectories onto each other, as shown schematically for the simple case $n = 3$ in figure 4.1, leading to a structure consisting of path pairs where a trajectory is retraced by another one (the partner trajectory) and small regions where in general an arbitrary number, say l, of trajectories 'cross' each other and the same number of trajectories 'avoid' crossing each other in configuration space. In phase space they of course do not cross since trajectories coinciding in one phase-space point are identical, but they come close to each other (which is necessary to ensure a small action difference). Such a region with in total $2l$ trajectory stretches will be called an l-encounter. Moreover we will call l the degree of the encounter. The diagonal contributions may then be treated as arising from trajectories with at least one encounter but all the encounters moved into the leads as indicated in figure 4.1. Encounters have been considered for the first time for the case $l = 2$ by Sieber and Richter [79, 80]. In these considerations the encounters have been built by only two trajectories which form loops and thus are self-encounters and were created due to small differences in the initial conditions of the trajectories. In our case however an l-encounter will be created by the encounter of $2l$ different trajectories connecting different channels. The reason for the creation of encounters will not only be the difference in the incidence of the trajectories (at the normal conducting leads) but also the imperfectness of Andreev reflection, *i.e.* the fact that the retro-reflected hole (or electron) does not retrace the original electron- (hole-) path exactly but differs a little bit.

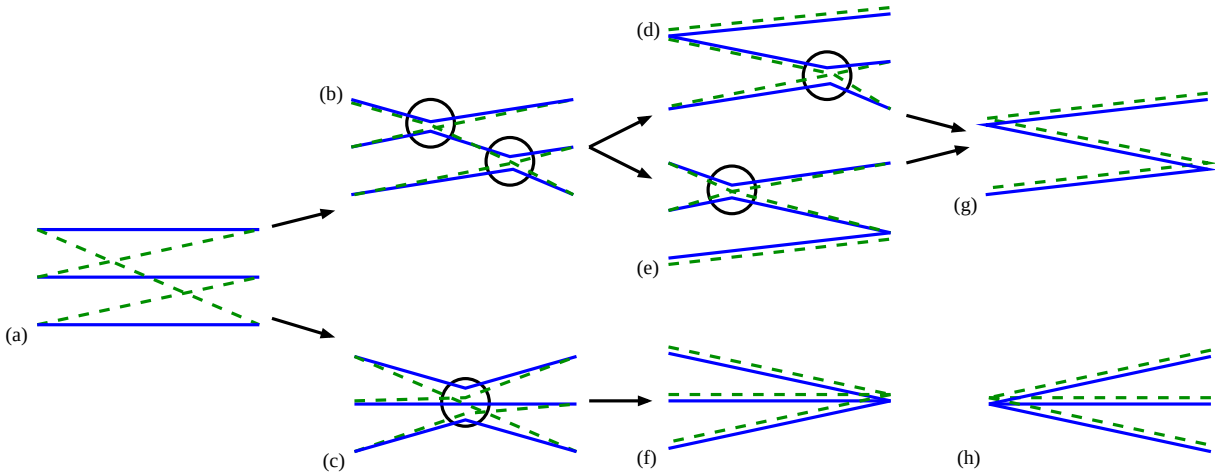

Figure 4.1: Collapsing trajectories onto each other creates encounters. The encounters are marked with circles. When all the encounters are slided into the superconductor one reproduces diagonal-type trajectory sets.

4.2 Diagrammatic rules without magnetic field

4.2.1 Action difference of trajectories

When Sieber and Richter considered an encounter for the first time their calculation of its contribution was based on the the expansion of the action difference of two trajectories ΔS in the small angle between the two crossing trajectory stretches. An arbitrary trajectory set however will in general not lead to just one 2-encounter but to an arbitrary number of encounters with different degrees. In this case and also in the extention to 3 dimensions the approach introduced by Sieber and Richter is not such simple any more. A better approach to find the contribution of the encounters and path pairs connected to them turned out to be the phase space approach [81, 82, 83, 84, 84] which will be reviewed here in detail. For this we will assume that the original trajectories ζ_j, $j \in \{1, \ldots, n\}$ do not cross while their partner trajectories ζ'_j do since the final result will not depend on which trajectories cross.

One first puts a Poincaré surface of section $\mathcal{P}_\sigma$ across the σ-th encounter [85, 81, 82] ($\sigma \in \{1, \ldots, V\}$ with V the total number of encounters) as depicted in figure 4.2 for the case of two trajectories forming one 2-encounter with its centre at one of the l original stretches which will be arbitrarily chosen to be the first encounter stretch. The centre of $\mathcal{P}_\sigma$ is denoted by the phase space vector $\xi_{\sigma,1}$. We choose the time in such a way that this trajectory pierces through $\mathcal{P}_\sigma$ at $t = 0$. The remaining $l - 1$ original stretches pierce through $\mathcal{P}_\sigma$ at points $\xi_{\sigma,2}, \ldots, \xi_{\sigma,l}$. For simplicity in the following we will drop the 'σ'. For each of the remaining $l - 1$ encounter stretches we will define the phase space point $\chi_j = \xi_j$ if the jth encounter stretch is traversed in the same direction as the first one and $\chi_j = \mathcal{T}\xi_j$ if it is traversed in opposite direction. Here $\mathcal{T}$ is the time reversal operator. With this definition the difference between ξ_1 and χ_j is very small. The best way to find the contribution of the set of trajectories is to express the differences $\chi_j - \xi_1$ ($j = 2, \ldots, l$) in terms of the stable and unstable directions in the Poincaré surface of section $\mathbf{e}^s_m$, $\mathbf{e}^u_m$, where $m \in \{1, \ldots, f-1\}$ where f is the number of degrees of freedom. The difference between two encounter stretches in phase space may then be written as [86, 81, 82]

$$\chi_j - \xi_1 = \sum_{m=1}^{f-1} \left[s_{j,m} \mathbf{e}^s_m(\xi_1) + u_{j,m} \mathbf{e}^u_m(\xi_1) \right], \tag{4.2}$$

where $s_{j,m}$ and $u_{j,m}$ denote the stable and unstable components (in direction $\mathbf{e}^s_m$ and $\mathbf{e}^u_m$ respectively) which depend on time. In the limit of long time T the stable component decreases exponentially with

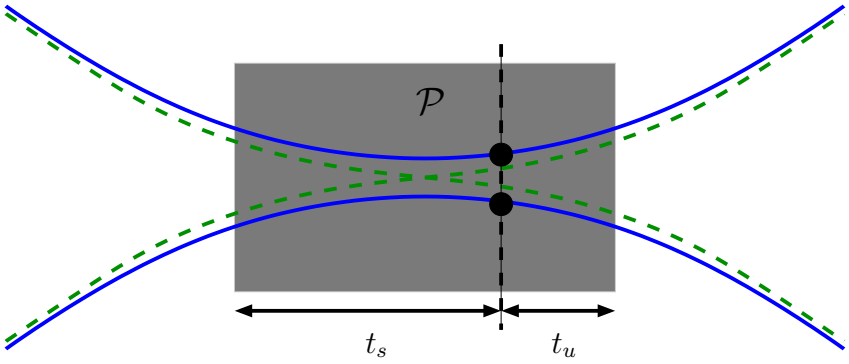

Figure 4.2: We put a Poincaré surface of section at an arbitrary phase space point inside the encounter. The encounter duration is given by t_u and t_s. The trajectory pair falls into several parts. The upper dot marks the centre of the Poincaré surface of section and the lower one the point at which the second stretch pierces through $\mathcal{P}$.

a decay rate given by the Lyapunov exponent λ while the unstable one increases exponentially with the same rate. Note that we will assume that for a given trajectory the Lyapunov exponent is (apart from its sign) the same for all stable and unstable directions. Therefore the names 'stable' and 'unstable' refer to the following: If the initial point of a given trajectory is slightly moved along a stable direction this perturbed trajectory always stays in the vicinity of the original one and will coincide with it after long times. However if the perturbation happens in one of the unstable direction the distance between the original unperturbed and the perturbed trajectory will increase exponentially with time and therefore the perturbed trajectory will drift away from the original one.

The stable and unstable coordinates of the partner trajectories may be determined by the condition that it shall follow some part of one of the previously considered trajectories. Within our choice of time for positive times (in general this would be "for times larger than the one at which the arbitrarily chosen first trajectory crosses ξ_1") the j-th partner trajectory shall follow say the j-th trajectory. If the unstable coordinates would be different those two trajectories would differ from each other by a quite large amount. Therefore the unstable coordinates have to be the same. For negative times the role of the stable and unstable coordinates are exchanged due to the exponential time dependence. Therefore if the j-th partner trajectory follows the k-th trajectory (with $k \neq j$) for negative times their stable coordinates have to be the same.

The duration of the encounter t_{enc} is determined by the condition that the stable and unstable coordinates have to be smaller than an arbitrary value c which exact value will not matter in the final result [81, 83, 84]. We denote t_u the time that the trajectory needs from $\mathcal{P}$ till the point where the first unstable component reaches c and t_s the time the trajectory needs from $\mathcal{P}$ till the point where the last stable coordinate falls below c. As shown in figure 4.2 the encounter duration is then given by $t_s + t_u$. Due to the asymptotic behaviour of the stable and unstable components the duration of the encounter is given by [83]

$$t_{enc} = t_s + t_u = \frac{1}{\lambda} \ln \left(\frac{c^2}{\max_i\{|s_i|\} \max_j\{|u_j|\}} \right) \tag{4.3}$$

The next step is to evaluate the classical action difference which arises from the encounters. Using $S_\gamma = \int_{\mathbf{q}_0}^{\mathbf{q}_1} \mathbf{p} \cdot \mathrm{d}\mathbf{q}$, where $\mathbf{q}_0$ and $\mathbf{q}_1$ are the starting and end points of the trajectory and $\mathbf{p}$ is the momentum one finds after expanding the action differences in the stable and unstable coordinates [84] that the action difference of the $2n$ trajectories within the encounter is given by [81, 84]

$$\Delta S = \sum_{j=1}^{l-1} s_j u_j = \mathbf{s} \cdot \mathbf{u}, \tag{4.4}$$

where we additionally defined the vectors of the stable and unstable components $\mathbf{s} = (s_1, \ldots, s_{l-1})^T$ and $\mathbf{u} = (u_1, \ldots, n' u_{l-1})^T$. Note that the differences s_j and u_j in general depend on the ordering of the stretches but the total action difference stays the same [87]. This also implies that the duration of the encounter also depends logarithmically on the action difference. Note that the action difference however has to be of the order of $\hbar$ in order to survive the averaging. Thus the duration of the encounter is of the order of the Ehrenfest time τ_{E} which is the time scale after which the motion of an initial wave package differs from its classical motion.

4.2.2 Diagrammatic rules

Since the position of the Poincaré surface of section is arbitrary we have to average over all possible stable and unstable components. Since the possibility to put $\mathcal{P}$ at a certain point inside the encounter is given by the duration of the encounter itself and the possibility to put the encounter to a certain phase space point of the trajectory. In an ergodic system, *i.e.* in a system where each trajectory 'uniformly' explores the energy shell $\Omega(E_0)$ being the set of all phase space points having energy E_0, the probability to put it to a certain point ξ inside the encounter is given by $1/\Omega t_{enc}$. Here 'uniformly' means that a time average of a quantity f is the same as a phase average:

$$\lim_{T\to\infty} \int_{-T}^{T} \mathrm{d}t f\big(\mathbf{p}(t), \mathbf{q}(t)\big) = \int \mathrm{d}\mathbf{p} \int \mathrm{d}\mathbf{q} f(\mathbf{p}, \mathbf{q}) \delta\big(E - H(\mathbf{p}, \mathbf{q})\big),$$

where H is the Hamiltonian of the classical system. Moreover since the trajectories are close to each other their stability amplitudes are approximately the same. Thus the total amplitude of the summands in (4.1) is $\prod_{j=1}^{n} |A_j|^2$. For these stability amplitudes system Richter and Sieber established the sum rule [80]

$$\sum_{\zeta: i\to o} |A_\zeta| \ldots = \int_0^\infty \mathrm{d}T \exp\left(-\frac{T}{\tau_{\mathrm{D}}}\right) \ldots . \tag{4.5}$$

This sum rule however requires an ergodic and hyperbolic system. A system is hyperbolic, if all fixed points are hyperbolic, *i.e.* all fixed points are unstable. The exponential factor $\exp(-T/\tau_{\mathrm{D}})$ plays the role of a classical survival probability of a classical trajectory, *i.e* the probability that a trajectory stays inside the cavity for a time T, which is the dwell time of the trajectory. On average the trajectory stays for the mean dwell time τ_{D} in the cavity.

However in general a set of several trajectories will have more than just one encounter. We will characterise the set of trajectories by the vector $\mathbf{v}$ which we will call the characteristic of a trajectory set where the l-th entry v_l of $\mathbf{v}$ is the number of l-encounters. With this we may write the total number of encounters $V(\mathbf{v}) = \sum_l v_l$ and the total number of stretches entering encounters will be defined by $L(\mathbf{v}) = \sum_l l v_l$ [88, 84]. For example the trajectories schematically drawn in figures 4.1b,c have $\mathbf{v} = (2, 0, 0, \ldots)$ and $\mathbf{v} = (0, 1, 0, \ldots)$. Therefore the trajectory set in figure 4.1b has in total $V(\mathbf{v}) = 2$ encounters with $L = 2 \cdot 2 = 4$ while the one in figure 4.1c has just one encounter ($V(\mathbf{v}) = 1$) and $L = 3$. Since we will consider the set of all encounters characterised by $\mathbf{v}$ in the following we use the index σ labelling the encounters again. For a characteristic $\mathbf{v}$ in the exponent the time has to be replaced by the 'exposure' time [83] $T_{\mathrm{exp}} = \sum_{i=1}^{L+n} t_i + \sum_{\sigma=1}^{V} t_\sigma$, where t_i is the duration of the i-th path pair connecting two encounters, two channels or one channel and one encounter to each other. In the following such a path pair will be called a 'link'. t_σ is the duration of the σ-th encounter. n depends on the actual problem and is given by the difference between the total number of links and L. If the encounters are formed by loops of two trajectories, which are no periodic orbits, such as in [82, 80, 79] $n = 1$. If however each encounter stretch belongs to a different trajectory (again no periodic orbits) n is the number of unprimed trajectories. For example if in figure 4.1b all the stretches belong to different trajectories we have 3 unprimed trajectories. Thus there are in total $7 = 4 + 3$ links. Note that we will use roman letters for path pairs and Greek letters for the encounters. Thus the exposure time is smaller by an amount of $\sum_\sigma (l-1) t_\sigma$ than the

sum of the durations of each single trajectory and therefore the survival probability is increased by the presence of an encounter [82]. This is due to the fact that a trajectory traversing an encounter has to stay at least for the duration of the encounter inside the cavity.

Hence if we do the averaging over the position of the Poincaré surface of section and apply the sum rule with the mentioned modification (4.1) decomposes into a product over the links and a product over the encounters [82].

However up to now we considered trajectories with the same energy. Especially for the calculation of the density of states of an Andreev billiard it will be necessary to consider trajectories at different energies, too. To do this we expand the action of the trajectory ζ around the reference energy E_0. For this we use that $\partial S/\partial E|_{E=E_0} = T$. Moreover we consider energy differences small enough that the stability amplitudes are approximately independent of the energy. Thus if the energy difference of the i-th path pair is E_i and E_σ is the total energy difference of all trajectories traversing the σ-th encounter these products are

$$\prod_{i=1}^{L+n} \int_0^\infty \mathrm{d}t_i \mathrm{e}^{-(1-\mathrm{i}E_i\tau_\mathrm{D}/\hbar)t_i/\tau_\mathrm{D}} \qquad \text{for links,} \tag{4.6a}$$

$$\prod_{\sigma=1}^{V} \int_{-c}^{c} \mathrm{d}^{l_\sigma-1}s \mathrm{d}^{l_\sigma-1}u \frac{\exp\left(\mathrm{i}\sum_{j=1}^{l_\sigma-1} s_j u_j/\hbar\right) \mathrm{e}^{-(1-\mathrm{i}E_\sigma\tau_\mathrm{D}/\hbar)t_\sigma(\mathbf{s},\mathbf{u})/\tau_\mathrm{D}}}{\Omega^{l-1} t_\sigma(\mathbf{s},\mathbf{u})} \qquad \text{for encounters.} \tag{4.6b}$$

Here l_σ is the degree of the σ-th encounter. Note that we have left out the factor $(N\tau_\mathrm{D})^{-n}$ and the summation over the channels. The latter has been left out due to the fact that on the one hand the evaluation of this sum depends on the actual problem, *e.g* whether the channels may be in all leads or just in a certain one, and on the other hand we may later include additional factors depending only on the lead a channel is in.

We then expand the second exponential factor in the encounter-integral $\mathrm{e}^{-(1-\mathrm{i}E_\sigma\tau_\mathrm{D}/\hbar)t_\sigma(\mathbf{s},\mathbf{u})/\tau_\mathrm{D}} = 1 - (1-\mathrm{i}E_\sigma\tau_\mathrm{D})\, t_\sigma(\mathbf{s},\mathbf{u})/\tau_\mathrm{D}$. Due to the average the constant term of this expansion provides rapid oscillations as $\hbar \to 0$ [84] such that this contribution vanishes. Thus in the semiclassical limit the contribution of the encounter is solely determined by the linear term for which the denominator $t_\sigma(\mathbf{s},\mathbf{u})$ cancels out. The integral in the contributions can be easily evaluated and gives a factor $\tau_\mathrm{D}/(1-\mathrm{i}E_i\tau_\mathrm{D}/\hbar)$. The contribution of the encounters is determined by using $\int_{-c}^{c} \mathrm{d}s\mathrm{d}u \exp(\mathrm{i}su/\hbar) = (2\pi\hbar)$. The contribution of the σ-th l-encounter is therefore given by $-\tau_\mathrm{D}^{-1}(2\pi\hbar(1-\mathrm{i}E_\sigma\tau_\mathrm{D}/\hbar)/\Omega)^{l-1} = -N(1-\mathrm{i}E_\sigma\tau_\mathrm{D}/\hbar)/(N\tau_\mathrm{D})^l$ where we used that $\Omega = 2\pi\hbar\tau_\mathrm{D}/N$. When we make use of the definitions of L and V and include the original prefactor $(N\tau_\mathrm{D})^{-n}$ again we may attribute the factors of the channel numbers as well as the τ_D factors to the links and encounters in a slightly different way: First of all the τ_D factors cancel. The factors of the number of channels are all together $N^{-(L-V+n)} = N^V/N^{L+n}$. Therefore each encounter provides a factor of the number of channels while each link contributes a factor $\propto 1/N$. We may therefore write the diagrammatic rules in absence of a magnetic field and for the case that the energies of all trajectories are $\pm\epsilon\hbar/2\tau_\mathrm{D}$ where we have measured the energy in units of the Thouless energy $E_\mathrm{T} = \hbar/2\tau_\mathrm{D}$ as

> A link contributes a factor $[N(1-\eta_i\epsilon)]^{-1}$ with η_i=0 if the two paths have the same energy and $\eta_i = 1$ otherwise.
>
> An l-encounter contributes a factor $-N(1-\mathrm{i}\eta_\sigma\epsilon)$, where η_σ is the difference between the number of traversals of unprimed trajectories with energy $+\epsilon/2$ and the number of traversals of primed trajectories with energy $\epsilon/2$ in the encounter.

Consider for example the diagrams in figure 4.1b-h. If the blue solid lines denote electrons with energy $E_\mathrm{F}+\epsilon\hbar/2\tau_\mathrm{D}$ and the green dashed lines holes with energy $E_\mathrm{F}-\epsilon\hbar/2\tau_\mathrm{D}$ the links consisting of one blue solid line and one green dashed line contribute a factor $[N(1-\mathrm{i}\epsilon)]^{-1}$. In figure 4.1b there are two 2-encounters

(marked by the circles) consisting of two electron- and two hole-stretches such that $\eta_1 = \eta_2 = 2 - 0 = 2$ such that the contribution of both encounters is $-N(1 - 2\mathrm{i}\epsilon)$. The 3-encounter in figure 4.1c contributes a factor $-N(1 - 3\mathrm{i}\epsilon)$.

4.3 Diagrammatic rules including a magnetic field

Considering the dependence on a magnetic field B allows us to study the crossover from time reversal symmetry to fully broken time reversal symmetry and therefore - in the language of RMT - the crossover from orthogonal to unitary ensembles. However the treatment here only applies to magnetic fields weak enough not to influence the classical motion, such that we have to deal with the same trajectory sets as above. In this part we will drop the energy dependence since including energy dependences is straightforwad. The modifications to the diagrammatic rules we will consider here were introduced for the spectral form factor [89, 90]. In particular the effect of the magnetic field may be treated by considering parametric correlations [91, 92].

The action of a trajectory ζ is changed by the magnetic field by an amount proportional to the contour integral of the vector potential $\mathbf{A}$ along the trajectory, *i.e* by

$$\Theta_\zeta = \frac{\mathrm{e}}{\mathrm{c}} \int_\zeta \mathbf{A}(\mathbf{q}) \cdot \mathrm{d}\mathbf{q}. \tag{4.7}$$

Here, e is the elementary charge and c is the speed of light.

Therefore for path pairs traversed by both trajectories in the same direction as well as for encounters where all stretches are traversed in the same direction the action difference due to the magnetic field may be neglected and we get the same diagrammatic rules as above. However if there are trajectory stretches following the time reversal of an other trajectory stretch this situation changes. As is obvious from (4.7) the magnetic action changes its sign under time reversal leading to a significant action difference $\Theta_\zeta - \Theta_{\zeta'}$ between the trajectories ζ and ζ'.

4.3.1 Links

We will first consider the effect of the magnetic field on the i-th link traversed by the two trajectories ζ and ζ' in opposite direction. The magnetic action Θ_i' of ζ' provided by the link is then minus the magnetic action Θ_i of ζ provided by the link and therefore the total action difference of this link is $2\Theta_i$.

The magnetic action may effectively be seen as a random variable [82]. In alignment with the central limit theorem the magnetic action is Gaussian distributed with width $\sqrt{K}W$, where $K = t_i/t_{\mathrm{cl}}$ with the classical 'equilibration' time t_{cl} after which phase space points following each other may be seen as uncorrelated and W is proportional to the applied magnetic field. After averaging the phase factor arising from the magnetic action with the Gaussian probability distribution, this gives an additional phase factor of $\exp(-bt_i/\tau_{\mathrm{D}})$ with a system specific parameter $b \propto B^2/\hbar^2$ in (4.6a).

4.3.2 Encounters

For the encounters we first of all define the set of trajectories traversing the σ-th encounter whose action contributes with positive sign by $\gamma_\sigma = \{\zeta_{\sigma,1}, \ldots, \zeta_{\sigma,n}\}$ and equivalently the set of trajectories traversing the σ-th encounter whose action contributes with negative sign $\gamma_\sigma' = \{\zeta_{\sigma,1}', \ldots, \zeta_{\sigma,n}'\}$. Note that we allow that γ_σ and γ_σ' may have two identical entries $\zeta_{\sigma,i} = \zeta_{\sigma,j}$ with $i \neq j$ and $\zeta_{\sigma,k}' = \zeta_{\sigma,l}'$ with $k \neq l$ but each entry is treated as different from all the others since we are interested only in the part of the trajectory inside the encounter.

Assume that ν_σ of the l_σ trajectories in γ_σ traverses the encounter in a certain direction arbitrarily chosen as 'positive'. The remaining $l_\sigma - \nu_\sigma$ stretches are then traversed in the opposite 'negative' direction. The ν_σ trajectories provide approximately all the same magnetic action Θ_σ while the remaining $l_\sigma - \nu_\sigma$ ones provide the negative of this action. The same holds for the trajectories in γ_σ' but maybe with different

numbers ν'_σ and $l_\sigma - \nu'_\sigma$ and with Θ_σ replaced by $-\Theta_\sigma$. The total difference of the magnetic actions of γ_σ and γ'_σ is then given by $\Theta_{\gamma_\sigma} - \Theta_{\gamma'_\sigma} = 2\mu_\sigma\Theta_\sigma$ with $\mu_\sigma = \nu_\sigma - \nu'_\sigma$. When one again performs the average with the Gaussian probability distribution as in section 4.3.1 one gets an additional exponential factor $\exp\left(-\mu_\sigma^2 b t_\sigma\right)/\tau_\mathrm{D}$ in (4.6b).

4.3.3 Changed diagrammatic rules

By doing the expansion of the actions in the energy around E_0 one may again include the energy dependence also in presence of a magnetic field in the same way as in section 4.2.2. We again consider the case where the energy of a trajectory is given by $\pm\epsilon\hbar/2\tau_\mathrm{D}$. The complete diagrammatic rules where we have still not included the contribution from the sums over the channels are

> The i-th path pair gives a factor $\left[N\left(1 - \mathrm{i}\eta_i\epsilon + \mu_i b\right)\right]^{-1}$, where $\eta_i = 0$ if both trajectories have the same energy an $\eta_i = 1$ if one has energy $+\epsilon$ and the other one has energy $-\epsilon$ as well as $\mu_i = 0$ if the trajectories traverse the path pair in the same direction and $\mu_i = 1$ otherwise.
>
> The σ-th encounter gives a factor $-N(1 - \mathrm{i}\eta_\sigma\epsilon + \mu_\sigma^2 b)$ where η_σ is defined in the same way as in section 4.2.2.

5 Density of states with a single lead

We now turn back to the Andreev billiards and consider the density of states for the case of a single lead. For this we closely follow [52]. This part shall also show how the diagrammatic rules may be used.

5.1 Semiclassical correlation functions and tree recursions

The diagrammatic rules give rise to a simplifying picture of the trajectories which have to be treated for the density of states. We may replace each link by a straight line connecting two encounters which are represented by vertices of even degree. The degree of the vertices are even since an l-encounter is entered and left by l path pairs thus connecting in total $2l$ path pairs to each other. Therefore we will essentially treat graphs representing the actual trajectories. In order to become familiar with the diagrammatic rules derived above we will now show how to derive the correlation function C which inserted into (2.14) will later give the density of states. We first substitute the semiclassical expression for the scattering matrix (3.16) into the correlation function C:

$$C(\epsilon,n)\approx\frac{1}{NT_{\mathrm{H}}^{n}}\prod_{j=1}^{n}\sum_{i_j,o_j}\sum_{\substack{\zeta_j(i_j\to o_j)\\ \zeta'_j(o_j\to i_{j+1})}}\mathrm{e}^{\mathrm{i}\Phi}A_{\zeta_j}A^{*}_{\zeta'_j}\exp\left[\frac{\mathrm{i}}{\hbar}\left(S_{\zeta_j}(+\epsilon E_{\mathrm{T}})-S_{\zeta'_j}(-\epsilon E_{\mathrm{T}})\right)\right], \tag{5.1}$$

where $S_\zeta(+\epsilon E_{\mathrm{T}})$ is the action of the trajectory ζ traversed by an electron while $S_\zeta(-\epsilon E_{\mathrm{T}})$ corresponds to a hole following ζ and Φ is the total phase contributed by the Andreev reflections at the channels i_j, o_j which is given by the phase difference of the superconducting leads and the number of Andreev reflections at each single superconducting lead. We will call the channels i_j through which electrons enter the dot 'incoming channels' and o_j an 'outgoing' channel since the electrons leave the dot through these channels. For the holes however its the other way around: they enter through an outgoing channel and leave the dot at an incoming one. In (5.1) we have labelled the channels cyclic, *i.e.* $i_{n+1}=i_1$ and $o_{n+1}=o_1$, in order to account for the cyclicity induced by the trace in (2.15). Taking the trace means that the last outgoing channel has to be connected by an hole to the first incoming one. Thus the in total $2n$ trajectories form a complete cycle. Therefore before doing the averaging the trajectories look for example like in figure 5.1a,d. The averaging necessitates a collapse of the stretches onto each other creating path pairs and encounters as shown in figures 5.1b,c.

We will now derive the topology of the diagrams contributing in leading order in the total number of channels $N_{\mathrm{S}}=N_{\mathrm{S}_1}+N_{\mathrm{S}_2}$. This will be done following [88]. They started with non-diagonal diagrams and focussed on the contributed factors of the numbers of channels of the links, encounters and the distinct channels. The sum over the incoming and outgoing channels here runs over all channels in lead 1 and lead 2. Therefore these sums give (neglecting the phase contributed by Andreev reflection) $\prod_{j=1}^{n}\sum_{i_j,o,j}=N_{\mathrm{S}}^{2n}$. Additionally a graph with characteristic $\mathbf{v}$ has in total $n+L(\mathbf{v})=n+\sum_l lv_l$ links contributing a factor N_{S}^{-1} and $V(\mathbf{v})=\sum_l v_l$ encounters contributing a factor $-N_{\mathrm{S}}$. The total contributed numbers of channels is therefore $N_{\mathrm{S}}^{2n+V(\mathbf{v})-(L(\mathbf{v})+n)}$. Thus in order to get leading order in the channel number one has to maximise $n+V(\mathbf{v})-L(\mathbf{v})$. This yields the condition $n+V-L=1$ and therefore the diagrams correspond to rooted planar trees such as those shown in figure 5.1e,f [88].

As long as the phase difference is zero and all the channels are distinct the fact that the diagrams are trees also includes that the contributed number of channels cancel. The diagrammatic rules in section

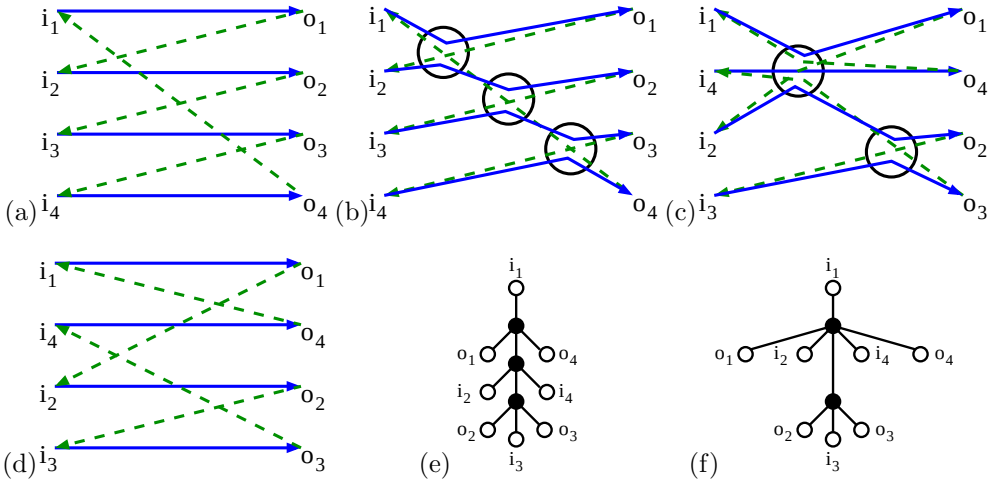

Figure 5.1: (a,d) 2D projections of the original trajectory structure of the correlation function $C(\epsilon, 4)$ where the incoming channels are drawn on the left, outgoing channels on the right, electrons as solid (blue) and holes as dashed (green) lines. (b) By pinching together the electron trajectories (pairwise here) we can create a structure which only differs in three small regions (encounters) and which can have a small action difference. (c) Sliding two of the encounters from (b) together (or originally pinching 3 electron trajectories together) creates this diagram. (e,f) Resulting rooted plane tree diagrams of (b,c) defining the top left as the first incoming channel (*i.e.* the channel ordering as depicted in (b,c)).

4.2.2 therefore give for a tree with characteristic $\mathbf{v}$ a contribution to $C(\epsilon, n)$ of

$$\frac{1}{(1-\mathrm{i}\epsilon)^n}\prod_{\alpha=1}^{V}-\frac{1-\mathrm{i}l_\alpha\epsilon}{(1-\mathrm{i}\epsilon)^{l_\alpha}} \tag{5.2}$$

A particularly important property of the trees is their amenability to recursive counting. The recursions behind our treatment of Andreev billiards were derived in [88] and we recall the main details here. First we can describe the encounters in a particular tree by a vector $\boldsymbol{v}$ whose elements v_l count the number of l-encounters in the tree (or diagram); this is often written as $2^{v_2}3^{v_3}\cdots$. An l-encounter is a vertex in the tree of degree $2l$ (*i.e.* connected to $2l$ links). The vertices of the tree that correspond to encounters will be called 'nodes', to distinguish them from the vertices of degree 1 which correspond to the incoming and outgoing channels and which will be called 'leaves'. The total number of nodes is $V = \sum_{l>1} v_l$ and the number of leaves is $2n$ where n is the order of the correlation function $C(\epsilon, n)$ to which the trees contribute. Defining $L = \sum_{l>1} l v_l$, we can express n as $n = (L - V + 1)$. Note that the total number of links is $L + n$ which can be seen as l links trailing each l-encounter plus another n from the incoming channels. For example, the $2^1 3^1$ tree in figure 5.1f has $L = 5$, $V = 2$ and contributes to the $n = 4$ correlation function. We always draw the tree with the leaves ordered $i_1, o_1, \ldots, i_n, o_n$ in anticlockwise direction. This fixes the layout of the tree in the plane, thus the name 'rooted plane trees' [93].

From the start tree, we can also move some encounters into the lead(s) and it is easy to read off when this is possible. If an l-encounter (node of degree $2l$) is adjacent to exactly l leaves with label i it may 'i-touch' the lead, *i.e.* the electron trajectories have an encounter upon entering the system and the corresponding incoming channels coincide. Likewise if a $2l$-node is adjacent to l o-leaves it may 'o-touch' the lead. For example, in figure 5.1f the top node has degree 6, is adjacent to 3 i-leaves (including the root) and can i-touch the lead as in figures 5.2b,e. The lower encounter can o-touch as in figures 5.2a,d. In addition, both encounters can touch the lead to create figures 5.2c,f.

Semiclassically, we add the contributions of all the possible trajectory structures (or trees) and the contribution of each is made up by multiplying the contributions of its constituent parts (links, encounters and leaves). First we count the orders of the number of channels N. As mentioned in [88] (see also

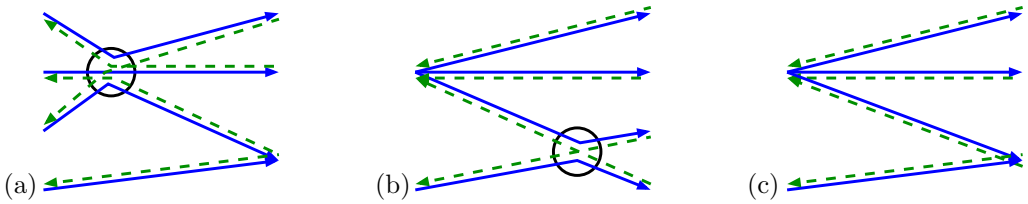

Figure 5.2: Further possibilities arise from moving encounters into the lead(s). Starting from figure 5.1c we can slide the 2-encounter into the outgoing channels on the right (called 'o-touching', see text) to arrive at (a) or the 3-encounter into the incoming channels on the left (called 'i-touching') to obtain (b). Moving both encounters leads to (c), but moving both to the same side means first combining the 3- and 2-encounter in figure 5.1c into a 4-encounter and is treated as such.

section 5.1 below) the multiplicative contribution of each encounter or leaf is of order N and each link gives a contribution of order $1/N$. Together with the overall factor of $1/N$, see equation (2.15), the total power of $1/N$ is ρ, the cyclicity of the diagram. Since our diagrams must be connected, the smallest cyclicity is $\rho = 0$ if the diagram is a tree. The trees can be generated recursively, since by cutting a tree at the top node of degree $2l$ (after the root) we obtain $2l - 1$ subtrees, as illustrated in figure 5.3.

To track the trees and their nodes, the generating function $F(\boldsymbol{x}, \boldsymbol{z}_i, \boldsymbol{z}_o)$ was introduced [88] where the powers of

- x_l enumerate the number of l-encounters,
- $z_{i,l}$ enumerate the number of l-encounters that i-touch the lead,
- $z_{o,l}$ enumerate the number of l-encounters that o-touch the lead.

Later we will assign values to these variables which will produce the correct semiclassical contributions of the trees. Note that the contributions of the links and leaves will be absorbed into the contributions of the nodes hence we do not directly enumerate the links in the generating function F. Inside F we want to add all the possible trees and for each have a multiplicative contribution of its nodes. For example, the tree in figure 5.1f and its relatives in figure 5.2 would contribute

$$x_3 x_2 + z_{i,3} x_2 + x_3 z_{o,2} + z_{i,3} z_{o,2} = (x_3 + z_{i,3})(x_2 + z_{o,2}). \tag{5.3}$$

A technical difficulty is that the top node may (if there are no further nodes) be able to both i-touch and o-touch, but clearly not at the same time. An auxiliary generating function $f = f(\boldsymbol{x}, \boldsymbol{z}_i, \boldsymbol{z}_o)$ is thus introduced with the restriction that the top node is not allowed to i-touch the lead. An empty tree is assigned the value 1 (*i.e.* $f(0) = 1$) to not affect the multiplicative factors. To obtain a recursion for f we separate the tree into its top node of degree $2l$ and $2l - 1$ subtrees as in figure 5.3. As can be seen from the figure, l of the new trees (in the odd positions from left to right) start with an incoming channel, while the remaining $l - 1$ even numbered subtrees start with an outgoing channel, and correspond to a tree with the i's and o's are reversed. For these we use the generating function $\hat{f}$ where the roles of the $\boldsymbol{z}$ variables corresponding to leaves of one type are switched so $\hat{f} = f(\boldsymbol{x}, \boldsymbol{z}_o, \boldsymbol{z}_i)$. The tree then has the contribution of the top node times that of all the subtrees giving $x_l f^l \hat{f}^{l-1}$.

The top node may also o-touch the lead, but for this to happen all the odd-numbered subtrees must be empty. When this happens we just get the contribution of $z_{o,l}$ times that of the $l - 1$ even subtrees: $z_{o,l} \hat{f}^{l-1}$. In total we have

$$f = 1 + \sum_{l=2}^{\infty} \left[x_l f^l \hat{f}^{l-1} + z_{o,l} \hat{f}^{l-1} \right], \tag{5.4}$$

and similarly

$$\hat{f} = 1 + \sum_{l=2}^{\infty} \left[x_l \hat{f}^l f^{l-1} + z_{i,l} f^{l-1} \right]. \tag{5.5}$$

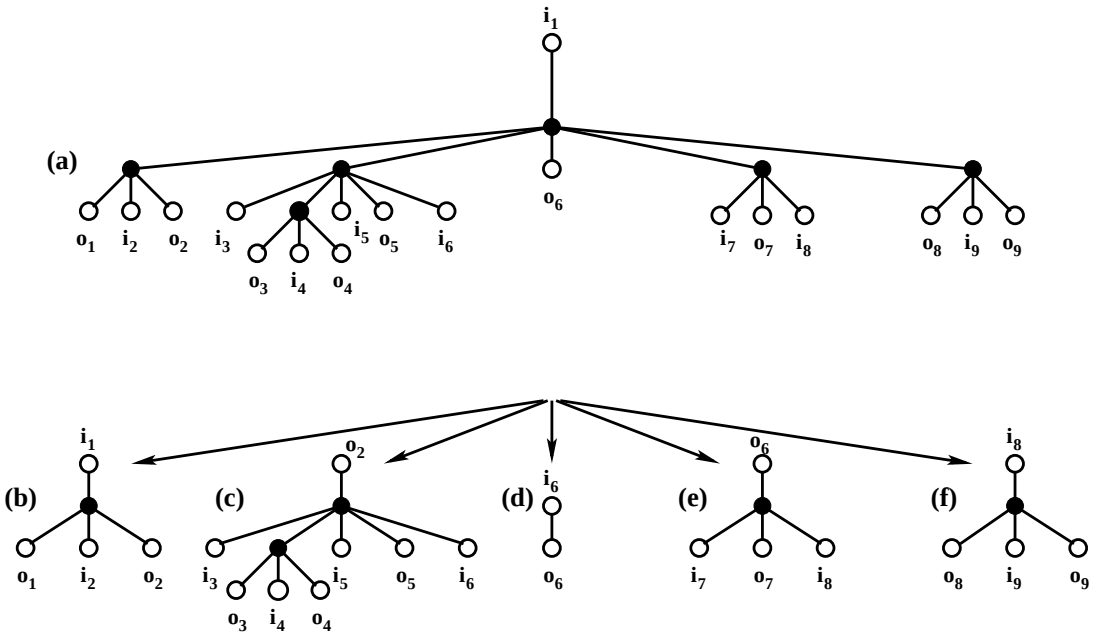

Figure 5.3: The tree shown in (a) is cut at its top node (of degree 6) such that the trees (b)-(f) are created. Note that to complete the five new trees we need to add to each tree the last leave of the previous tree as its root and that the trees (c) and (e) in the even positions have the incoming and outgoing channels reversed.

For F we then reallow the top node to i-touch the lead which means that the even subtrees must be empty and a contribution of $z_{i,l}f^l$, giving

$$F = f + \sum_{l=2}^{\infty} z_{i,l} f^l = \sum_{l=1}^{\infty} z_{i,l} f^l, \tag{5.6}$$

if we let $z_{i,1} = 1$ (and also $z_{o,1} = 1$ for symmetry). Picking an o-leaf as the root instead of an i-leaf should lead to the same trees and contributions so F should be symmetric upon swapping $\boldsymbol{z}_i$ with $\boldsymbol{z}_o$ and f with $\hat{f}$. These recursions enumerate all possible trees (which represent all diagrams at leading order in inverse channel number). We will now first review the results for the density of states of an Andreev billiard with just one superconducting lead reported in [48]. We can then choose the phase of the superconductor to be zero and $N_{\mathrm{S}_1} = N_{\mathrm{S}}$ and $N_{\mathrm{S}_2} = 0$.

Putting the diagrammatic rules of section 4.3 into the recursions in section 5.1 then simply means setting

$$x_l = \frac{-(1 - \mathrm{i}l\epsilon)}{(1 - \mathrm{i}\epsilon)^l} \cdot \tilde{r}^{l-1}, \qquad z_{i,l} = z_{o,l} = 1 \cdot \tilde{r}^{l-1}, \tag{5.7}$$

where we additionally include powers of $\tilde{r}$ to track the order of the trees and later generate the semiclassical correlation functions. The total power of $\tilde{r}$ of any tree is $\sum_{l>1}(l-1)v_l = L - V = n - 1$. To get the required prefactor of $(1 - \mathrm{i}\epsilon)^{-n}$ in (5.2) we can then make the change of variable

$$f = g(1 - \mathrm{i}\epsilon), \qquad \tilde{r} = \frac{r}{1 - \mathrm{i}\epsilon}, \tag{5.8}$$

so that the recursion relation (5.4) becomes

$$g(1 - \mathrm{i}\epsilon) = 1 - \sum_{l=2}^{\infty} r^{l-1} g^l \hat{g}^{l-1}(1 - \mathrm{i}l\epsilon) + \sum_{l=2}^{\infty} r^{l-1}\hat{g}^{l-1}, \tag{5.9}$$

and similarly for $\hat{g}$. Using geometric sums (the first two terms are the $l = 1$ terms of the sums) this is

$$\frac{g}{1 - rg\hat{g}} = \frac{\mathrm{i}\epsilon g}{(1 - rg\hat{g})^2} + \frac{1}{1 - r\hat{g}}. \tag{5.10}$$

We note that since $\hat{f}$ is obtained from f by swapping $\boldsymbol{z}_i$ and $\boldsymbol{z}_o$ and in our substitution (5.7) $\boldsymbol{z}_i = \boldsymbol{z}_o$, the functions $\hat{f}$ and f are equal. Taking the numerator of the equation above and substituting $\hat{g} = g$ leads to

$$g - \frac{1}{1 - \mathrm{i}\epsilon} = \frac{rg^2}{1 - \mathrm{i}\epsilon}\left[g - 1 - \mathrm{i}\epsilon\right]. \tag{5.11}$$

To obtain the desired generating function of the semiclassical correlation functions we set $F = G\,(1 - \mathrm{i}\epsilon)$ in (5.6), along with the other substitutions in (5.7) and (5.8),

$$G(\epsilon, r) = \frac{g}{1 - rg}, \qquad G(\epsilon, r) = \sum_{n=1}^{\infty} r^{n-1} C(\epsilon, n), \tag{5.12}$$

so that by expanding g and hence G in powers of r we obtain all the correlation functions $C(\epsilon, n)$. This can be simplified by rearranging (5.12) and substituting into (5.11) to get the cubic for G directly

$$r(r-1)^2 G^3 + r(3r + \mathrm{i}\epsilon - 3)G^2 + (3r + \mathrm{i}\epsilon - 1)G + 1 = 0. \tag{5.13}$$

5.2 Universal regime

The density of states of a chaotic Andreev billiard with one superconducting lead (2.14) can be rewritten as

$$d(\epsilon) = 1 - 2\mathrm{Im}\frac{\partial}{\partial \epsilon}\sum_{n=1}^{\infty}\frac{(-1)^{n-1}C(\epsilon, n)}{n}, \tag{5.14}$$

where without the $1/n$ the sum would just be $G(\epsilon, -1)$ in view of (5.12). To obtain the $1/n$ we can formally integrate to obtain a new generating function $H(\epsilon, r)$,

$$H(\epsilon, r) = \frac{1}{\mathrm{i}r}\frac{\partial}{\partial \epsilon}\int G(\epsilon, r)\mathrm{d}r, \qquad H(\epsilon, r) = \sum_{n=1}^{\infty}\frac{r^{n-1}}{\mathrm{i}n}\frac{\partial C(\epsilon, n)}{\partial \epsilon}, \tag{5.15}$$

so the density of states is given simply by

$$d(\epsilon) = 1 - 2\mathrm{Re}H(\epsilon, -1). \tag{5.16}$$

To evaluate the sum in (5.14) we now need to integrate the solutions of (5.13) with respect to r and differentiate with respect to ϵ. Since G is an algebraic generating function, *i.e.* the solution of an algebraic equation, the derivative of G with respect to ϵ is also an algebraic generating function [94]. However, this is not generally true for integration, which can be seen from a simple example of $f = 1/x$, which is a root of an algebraic equation, unlike the integral of f. Solving equation (5.13) explicitly and integrating the result is also technically challenging, due to the complicated structure of the solutions of the cubic equations. Even if it were possible, this approach would fail in the presence of magnetic field, when G is a solution of a quintic equation, see section 5.3, or in the presence of a phase difference between two superconductors.

The approach we took is to conjecture that $H(\epsilon, r)$ is given by an algebraic equation, perform a computer-aided search over equations with polynomial coefficients and then prove the answer by differentiating appropriately. We found that

$$(\epsilon r)^2(1-r)H^3 + \mathrm{i}\epsilon r[r(\mathrm{i}\epsilon - 2) + 2(1 - \mathrm{i}\epsilon)]H^2 + [r(1 - 2\mathrm{i}\epsilon) - (1 - \mathrm{i}\epsilon)^2]H + 1 = 0, \tag{5.17}$$

when expanded in powers of r, agrees for a range of values of n with the expansion of (5.15) derived from the correlation functions obtained from (5.13). In order to show that (5.17) agrees with (5.15) to all orders in r we use a differentiation algorithm to find an equation for the intermediate generating function

$$I(\epsilon,r)=\frac{1}{\mathrm{i}}\frac{\partial G(\epsilon,r)}{\partial\epsilon}=\frac{\partial[rH(\epsilon,r)]}{\partial r},\qquad I(\epsilon,r)=\sum_{n=1}^{\infty}\frac{r^{n-1}}{\mathrm{i}}\frac{\partial C(\epsilon,n)}{\partial\epsilon}, \tag{5.18}$$

both starting from (5.13) and from (5.17) and verifying that the two answers agree.

The differentiation algorithm starts with the algebraic equation for a formal power series η in the variable x which satisfies an equation of the form

$$\Phi(x,\eta):=p_0(x)+p_1(x)\eta+\ldots+p_m(x)\eta^m=0, \tag{5.19}$$

where $p_0(x),\ldots,p_m(x)$ are some polynomials, not all of them zero. The aim is to find an equation satisfied by $\xi=\mathrm{d}\eta/\mathrm{d}x$, of the form

$$q_0(x)+q_1(x)\xi+\ldots+q_m(x)\xi^m=0, \tag{5.20}$$

where $q_0(x),\ldots,q_m(x)$ are polynomials. Differentiating (5.19) implicitly yields

$$\xi=-\frac{\partial\Phi(x,\eta)}{\partial x}\left(\frac{\partial\Phi(x,\eta)}{\partial\eta}\right)^{-1}=\frac{P(\eta,x)}{Q(\eta,x)}, \tag{5.21}$$

where P and Q are again polynomial. After substituting this expression into the algebraic equation for ξ and bringing everything to the common denominator we get

$$q_0(x)Q^m(x,\eta)+q_1(x)P(x,\eta)Q^{m-1}(x,\eta)+\ldots+q_m(x)P^m(x,\eta)=0. \tag{5.22}$$

However, this equation should only be satisfied modulo the polynomial $\Phi(x,\eta)$. Namely, we use polynomial division and substitute $P^j(x,\eta)Q^{m-j}(x,\eta)=T(x,\eta)\Phi(x,\eta)+R_j(x,\eta)$ into (5.22). Using (5.19) we arrive at

$$q_0(x)R_0(x,\eta)+q_1(x)R_1(x,\eta)+\ldots+q_m(x)R_m(x,\eta)=0. \tag{5.23}$$

The polynomials R_j are of degree of $m-1$ in η. Treating (5.23) as an identity with respect to η we thus obtain m linear equations on the coefficients q_j. Solving those we obtain q_j as rational functions of x and multiplying them by their common denominator gives the algebraic equation for ξ.

Performing this algorithm on G from (5.13), with $x=\mathrm{i}\epsilon$, and on rH from (5.17), with $x=r$, leads to the same equation, given as (A.1) in Appendix A, for the intermediate function defined in (5.18) and therefore proves the validity of the equation (5.17). Setting $\epsilon=0$ in (5.17) then shows that $\partial C(\epsilon,n)/\partial\epsilon|_{\epsilon=0}=\mathrm{i}n$ To compare the final result (5.16) with the RMT prediction we can substitute $H(\epsilon,-1)=\left[-\mathrm{i}W(\epsilon)+1\right]/2$ into (5.17). The density of states is then given in terms of W as $d(\epsilon)=-\mathrm{Im}W(\epsilon)$. The equation for W simplifies to the RMT result (2.23), and the density of states then reads [33]

$$d(\epsilon)=\begin{cases}0 & \epsilon\le 2\left(\frac{\sqrt{5}-1}{2}\right)^{5/2}\\ \frac{\sqrt{3}}{6\epsilon}\left[Q_+(\epsilon)-Q_-(\epsilon)\right] & \epsilon>2\left(\frac{\sqrt{5}-1}{2}\right)^{5/2}\end{cases}, \tag{5.24}$$

where $Q_\pm(\epsilon)=\left(8-36\epsilon^2\pm3\epsilon\sqrt{3\epsilon^4+132\epsilon^2-48}\right)^{1/3}$. This result is plotted in figure 5.4 and shows the hard gap extending up to around $0.6E_\mathrm{T}$.

5.3 Magnetic field

As derived in section 4.3 in presence of a magnetic field the diagrammatic rules have to be changed. According to the modified diagrammatic rules in the recursion relation in section 5.1 we have to set

$$x_l=\frac{-\left(1-\mathrm{i}l\epsilon+l^2b\right)}{\left(1-\mathrm{i}\epsilon+b\right)^l}\cdot\tilde{r}^{l-1},\qquad z_{i,l}=z_{o,l}=1\cdot\tilde{r}^{l-1}, \tag{5.25}$$

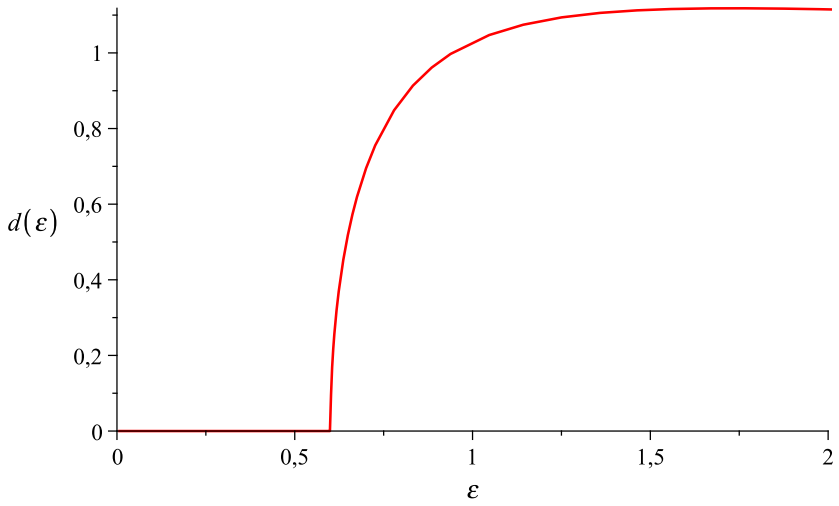

Figure 5.4: The density of states of a chaotic quantum dot coupled to a single superconductor at $E = \epsilon E_{\mathrm{T}} \ll \Delta$.

and

$$f = g(1 - \mathrm{i}\epsilon + b), \qquad \tilde{r} = \frac{r}{1 - \mathrm{i}\epsilon + b}. \tag{5.26}$$

The intermediate generating function is then given by the implicit equation

$$-r^2g^5 + (1 + \mathrm{i}\epsilon + b)r^2g^4 + (2 - \mathrm{i}\epsilon - b)rg^3 - (2 + \mathrm{i}\epsilon - b)rg^2 - (1 - \mathrm{i}\epsilon + b)g + 1 = 0, \tag{5.27}$$

and the generating function $G(\epsilon, b, r)$ of the magnetic field dependent correlation functions $C(\epsilon, b, n)$, which is still connected to g via $G = g/(1 - rg)$, is given by

$$\begin{aligned} r^2(r-1)^3G^5 + \left(\mathrm{i}\epsilon r - \mathrm{i}\epsilon + 5r^2 - 10r + 5 - br - b\right) r^2G^4 \\ + \left(3\mathrm{i}\epsilon r - \mathrm{i}\epsilon + 10r^2 - 12r + 2 - 3br - b\right) rG^3 \\ + (3\mathrm{i}\epsilon + 10r - 6 - 3b)rG^2 - (1 - 5r - \mathrm{i}\epsilon + b)G + 1 = 0. \end{aligned} \tag{5.28}$$

Removing the magnetic field by setting $b = 0$ reduces both these equations (after factorising) to the previous results (5.11) and (5.13). Next we again search for and verify an algebraic equation for $H(\epsilon, b, r) = 1/(\mathrm{i}r)\int[\partial G(\epsilon, b, r)/\partial\epsilon]\mathrm{d}r$, though the higher order makes this slightly more complicated, finding

$$\begin{aligned} 4b^2r^4(r-1)H^5 + 4br^3\left[\mathrm{i}\epsilon - 3b + r(2b - \mathrm{i}\epsilon)\right]H^4 \\ + r^2\left[\epsilon^2(1-r) + 2\mathrm{i}\epsilon b(5 - 3r) - b(13b + 4) + br(5b + 4)\right]H^3 \\ + r\left[2(\mathrm{i}\epsilon - 3b)(1 - \mathrm{i}\epsilon + b) + r\left((1 - \mathrm{i}\epsilon + b)^2 + 4b - 1\right)\right]H^2 \\ - \left[(1 - \mathrm{i}\epsilon + b)^2 - r(1 - 2\mathrm{i}\epsilon + 2b)\right]H + 1 = 0. \end{aligned} \tag{5.29}$$

In order to check the agreement with the RMT result we substitute $H(\epsilon, b, -1) = [-\mathrm{i}W(\epsilon, b) + 1]/2$ into (5.29). This leads to

$$b^2W^5 - 2b\epsilon W^4 - \left(4b - b^2 - \epsilon^2\right)W^3 + 2(2 - b)\epsilon W^2 + \left(4 - 4b + \epsilon^2\right)W + 4\epsilon = 0, \tag{5.30}$$

which corresponds to the RMT result (2.22) with no phase ($\phi = 0$). The density of states calculated from this equation is shown in figure 5.5 for different values of b. The gap reduces for increasing b, closes exactly at the critical flux ($b = 1$) and the density of states becomes flat (at 1) as $b \to \infty$.

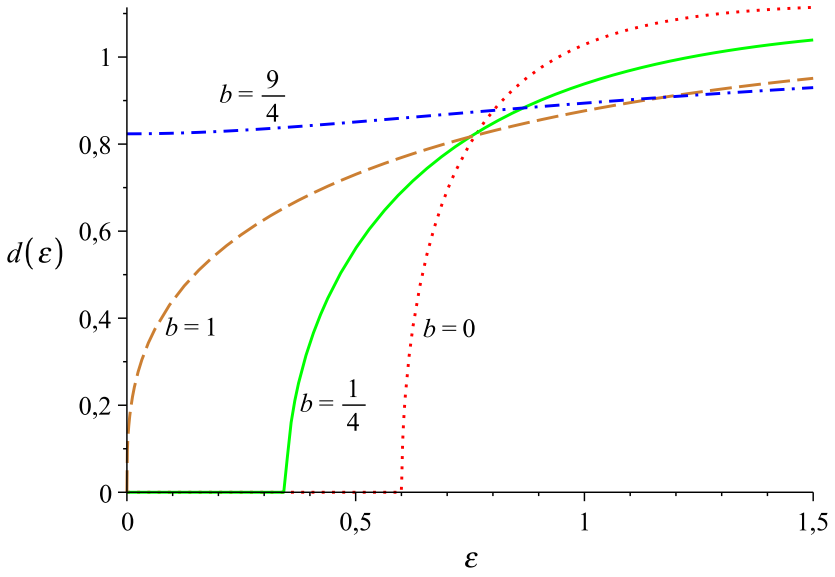

Figure 5.5: The effect of a time reversal symmetry breaking magnetic field on the density of states of a chaotic Andreev billiard with a single superconducting lead for $b = 0$ (dotted line), $b = 1/4$ (solid line), $b = 1$ (dashed line) and $b = 9/4$ (dashed dotted line).

5.4 Ehrenfest time dependence

So far we have been looking at the regime where the Ehrenfest time $\tau_{\mathrm{E}} \sim |\ln \hbar|$, the time below which wave packets propagate essentially classically (and above which wave interference dominates), is small compared to the dwell time τ_{d}, the typical time the trajectories spend inside the scattering region. This is the same limit described by RMT and we have seen the agreement between semiclassics and RMT in sections 5.1 and 6 above. Moving away from this limit we can treat the typical effect of the Ehrenfest time on the correlation functions $C(\epsilon, n)$, for now for the simplest case of a single lead and no magnetic field. To contribute in the semiclassical limit, the correlated trajectories should have an action difference of the order of $\hbar$ which in turn means that the encounters have a duration of the order of the Ehrenfest time. Increasing this relative to the dwell time, or increasing the ratio $\tau = \tau_{\mathrm{E}}/\tau_{\mathrm{d}}$, then increases the possibility that all the trajectories travel together for their whole length in a correlated band. Likewise the probability of forming the diagrams (as in figure 5.1) considered before reduces. All told, the Ehrenfest time dependence [95] leads to the simple replacement

$$C(\epsilon, \tau, n) = C(\epsilon, n)\mathrm{e}^{-(1-\mathrm{i}n\epsilon)\tau} + \frac{1 - \mathrm{e}^{-(1-\mathrm{i}n\epsilon)\tau}}{1 - \mathrm{i}n\epsilon}. \tag{5.31}$$

This replacement leaves the $n = 1$ term unchanged and had previously been shown for $n = 2$ [96] and $n = 3$ [45]. The exponential growth of differences between trajectories due to the chaotic motion means that we just add the first term from the previous diagrams with encounters in (5.31) to the second term from the bands as their opposing length restrictions lead to a negligible overlap. In fact this separation into two terms was shown [97, 98] to be a direct consequence of the splitting of the classical phase space into two virtually independent subsystems.

We leave the technical demonstration of (5.31) to [95] but the result follows by treating the diagrams considered before, which are created by sliding encounters together or into the lead (like the process depicted in figures 5.1 and 5.2) , as part of a continuous deformation of a single diagram. With a suitable partition of this family one can see that each set has the same τ_{E} dependence and hence that (5.31) holds for all n. It is clear that in the limit $\tau = 0$ (5.31) reduces to the previous (and hence RMT) results while

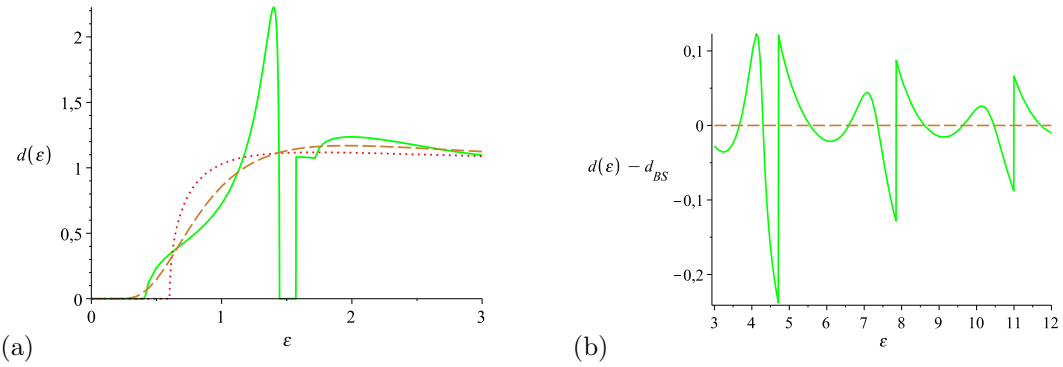

Figure 5.6: (a) Density of states for $\tau = \tau_{\rm E}/\tau_{\rm d} = 2$ (solid line), along with the BS (dashed) limit $\tau \to \infty$ and the RMT (dotted) limit $\tau = 0$, showing a second gap just below $\epsilon\tau = \pi$. (b) Ehrenfest time related $2\pi/\tau$-periodic oscillations in the density of states after subtracting the BS curve.

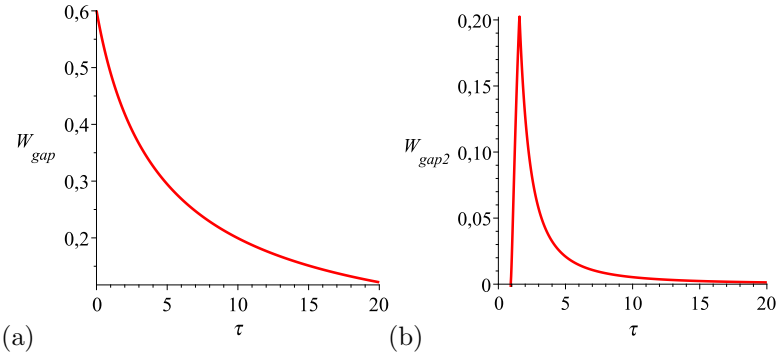

Figure 5.7: (a) Width (and end point) of the first gap and (b) width of the second gap as a function of τ.

in the opposite limit, $\tau = \infty$, substituting (5.31) into (5.14) and performing a Poisson summation we obtain the Bohr-Sommerfeld (BS) [35] result

$$d_{\rm BS}(\epsilon) = \left(\frac{\pi}{\epsilon}\right)^2 \frac{\cosh(\pi/\epsilon)}{\sinh^2(\pi/\epsilon)}. \tag{5.32}$$

This result was previously found semiclassically by [36] and corresponds to the classical limit of bands of correlated trajectories.

For arbitrary Ehrenfest time dependence we simply substitute the two terms in (5.31) into (5.14). With the second term we include $1-(1+\tau){\rm e}^{-\tau}$ from the constant term (this turns out to simplify the expressions) and again perform a Poisson summation to obtain

$$\begin{aligned} d_2(\epsilon,\tau) &= 1-(1+\tau){\rm e}^{-\tau} + 2{\rm Im}\sum_{n=1}^{\infty}\frac{(-1)^n}{n}\frac{\partial}{\partial\epsilon}\left(\frac{1-{\rm e}^{-(1-{\rm i}n\epsilon)\tau}}{1-{\rm i}n\epsilon}\right) \\ &= d_{\rm BS}(\epsilon) - \exp\left(-\frac{2\pi k}{\epsilon}\right)\left(d_{\rm BS}(\epsilon) + \frac{2k(\pi/\epsilon)^2}{\sinh(\pi/\epsilon)}\right), \end{aligned} \tag{5.33}$$

where $k = \lfloor(\epsilon\tau+\pi)/(2\pi)\rfloor$ involves the floor function, and we see that this function is zero for $\epsilon\tau < \pi$.

Of course the first term in (5.31) also contributes and when we substitute into (5.14) we obtain two further terms from the energy differential. These however may be written, using our semiclassical generating

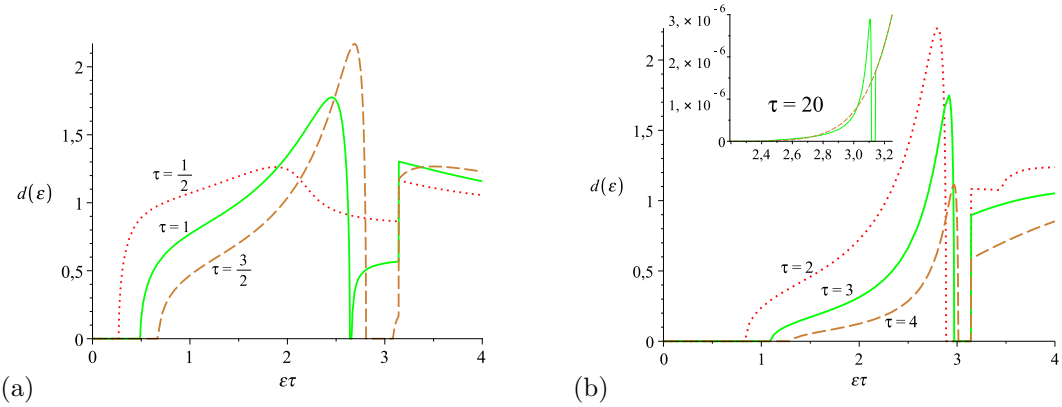

Figure 5.8: Density of states as a function of $\epsilon\tau = E/E_\mathrm{E}$ for various values of τ showing the appearance of a second gap below $\epsilon\tau = \pi$. Inset: Density of states for $\tau = 20$ (solid line) together with the BS limit (dashed).

functions, as

$$d_1(\epsilon,\tau) = \mathrm{e}^{-\tau}\left[1 - 2\mathrm{Re}\,\mathrm{e}^{\mathrm{i}\epsilon\tau}H(\epsilon,-\mathrm{e}^{\mathrm{i}\epsilon\tau})\right] + \tau\mathrm{e}^{-\tau}\left[1 - 2\mathrm{Re}\,\mathrm{e}^{\mathrm{i}\epsilon\tau}G(\epsilon,-\mathrm{e}^{\mathrm{i}\epsilon\tau})\right]. \tag{5.34}$$

Because G and H are given by cubic equations, we can write this result explicitly as

$$d_1(\epsilon,\tau) = \frac{\sqrt{3}\mathrm{e}^{-\tau}}{6\epsilon}\mathrm{Re}\left[Q_+(\epsilon,\tau) - Q_-(\epsilon,\tau)\right] + \frac{\sqrt{3}\tau\mathrm{e}^{-\tau}}{6}\mathrm{Re}\left[P_+(\epsilon,\tau) - P_-(\epsilon,\tau)\right], \tag{5.35}$$

where

$$Q_\pm(\epsilon,\tau) = \left[8 - \frac{24\epsilon\left(1-\cos(\epsilon\tau)\right)}{\sin(\epsilon\tau)} - 24\epsilon^2 - \frac{24\epsilon^2\left(1-\cos(\epsilon\tau)\right)}{\sin^2(\epsilon\tau)} + \frac{6\epsilon^3\left(1-\cos(\epsilon\tau)\right)}{\sin(\epsilon\tau)} + \frac{2\epsilon^3\left(2-3\cos(\epsilon\tau)+\cos^3(\epsilon\tau)\right)}{\sin^3(\epsilon\tau)} \pm \frac{6\epsilon\sqrt{3D}\left(1-\cos(\epsilon\tau)\right)}{\sin^2(\epsilon\tau)}\right]^{\frac{1}{3}}, \tag{5.36}$$

$$P_\pm(\epsilon,\tau) = \left[\frac{36\epsilon}{\left(1+\cos(\epsilon\tau)\right)^2} - \frac{9\epsilon^2\sin(\epsilon\tau)}{\left(1+\cos(\epsilon\tau)\right)^3} + \frac{\epsilon^3}{\left(1+\cos(\epsilon\tau)\right)^3} \pm \frac{3\sqrt{3D}}{\left(1+\cos(\epsilon\tau)\right)^2}\right]^{\frac{1}{3}}. \tag{5.37}$$

These all involve the same discriminant D and so the differences in (5.35) are only real (and hence $d_1(\epsilon,\tau)$ itself is non-zero) when

$$D(\epsilon,\tau) = \epsilon^4 - 8\epsilon^3\sin(\epsilon\tau) + 4\epsilon^2\left[5 + 6\cos(\epsilon\tau)\right] + 24\epsilon\sin(\epsilon\tau) - 8\left[1+\cos(\epsilon\tau)\right], \tag{5.38}$$

is positive. Recalling that the second contribution is zero up to $\epsilon\tau = \pi$, the complete density of states is therefore zero up to the first root of $D(\epsilon,\tau)$. The width of this gap is then solely determined by the contribution from quantum interference terms given by the trajectories with encounters. The hard gap up to the first root shrinks as τ increases (see figure 5.7a) and when taking the limit $\tau\to\infty$ while keeping the product $\epsilon\tau$ constant (5.38) reduces to $-8\left[1+\cos(\epsilon\tau)\right]$ which has its first root at $\epsilon\tau = \pi$. The gap then approaches $E = \pi E_\mathrm{E}$ for $\tau \gg 1$ where $E_\mathrm{E} = 2\hbar/\tau_\mathrm{E}$ is the Ehrenfest energy. So one indeed observes a hard gap up to πE_E in the limit $\tau\to\infty$ at fixed $\epsilon\tau$ in agreement with the quasiclassical result of [47].

Alongside this reduction in size of the first gap, which was predicted by effective RMT [25], when $\tau \geq 0.916$ the discriminant (5.38) has additional roots. Between the second and third root $D(\epsilon,\tau)$ is also negative and a second gap appears. As τ increases the roots spread apart so the gap widens. For example, the complete density of states for $\tau = 2$ is shown in figure 5.6a along with the oscillatory behaviour visible

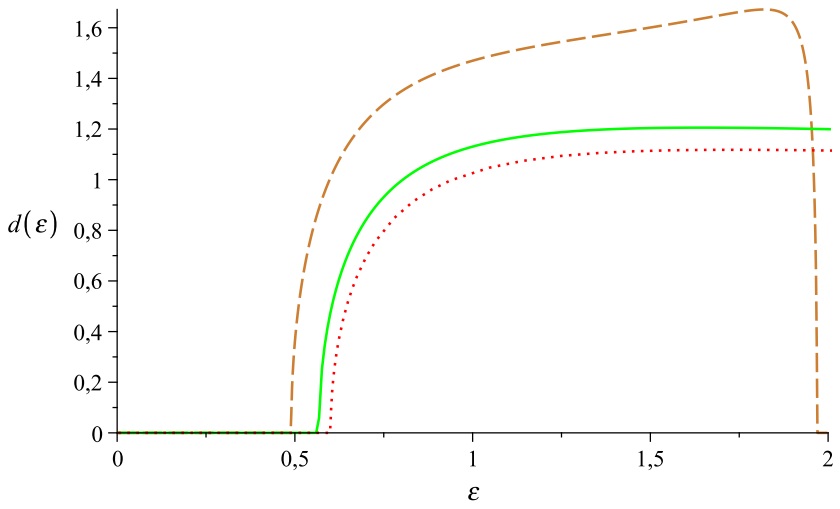

Figure 5.9: The density of states with a finite bulk superconducting gap $\Delta = 2E_\mathrm{T}$ (dashed line) and $\Delta = 8E_\mathrm{T}$ (solid line) compared to the previous case in figure 5.4 with $\Delta \to \infty$ (dotted line).

at larger energies (with period $2\pi/\tau$) in figure 5.6b. There the second gap is clearly visible and only ends when the second contribution $d_2(\epsilon,\tau)$ becomes non-zero at $\epsilon\tau = \pi$. In fact for $\tau > \pi/2$ the third root of $D(\epsilon,\tau)$ is beyond $\epsilon\tau = \pi$ so the second gap is cut short by the jump in the contribution $d_2(\epsilon,\tau)$. Since the second root also increases with increasing τ the gap shrinks again, as can be seen in figure 5.7b.

To illustrate this behaviour further, the density of states is shown for different values of τ in figure 5.8. One can see first the formation and then the shrinking of the second gap. As can be seen in the inset of figure 5.8b the second gap persists even for large values of τ and the size of the first hard gap converges slowly to $\epsilon\tau = \pi$. The plot for $\tau = 20$ also shows how the density of states converges to the BS result.

5.5 Small bulk superconducting gap

The effect of a small bulk superconducting gap on the density of states was not considered in [48]. The calculation of the density of states above used the approximation that the energy was well below the bulk superconductor gap, $E \ll \Delta$ or $\epsilon \ll \delta$ (for $\delta = \Delta/E_\mathrm{T}$), so that the phase shift at each Andreev reflection was $\arccos(\epsilon/\delta) \approx \pi/2$ (see section 2.1.2). For higher energies or smaller superconducting gaps, however, the density of states should be modified [99] to

$$d(\epsilon) = 1 + \mathrm{Re}\frac{2}{\sqrt{\delta^2-\epsilon^2}} + 2\mathrm{Im}\sum_{n=1}^{\infty}\frac{\partial}{\partial\epsilon}\left[\frac{\alpha(\epsilon)^{2n}C(\epsilon,n)}{n}\right], \tag{5.39}$$

where $\alpha(\epsilon) = \delta/(\epsilon + \mathrm{i}\sqrt{\delta^2-\epsilon^2})$ as in (2.7). When taking the energy derivative in the sum in (5.39) we can split the result into two sums and hence two contributions to the density of states

$$d(\epsilon) = 1 + 2\mathrm{Im}\sum_{n=1}^{\infty}\frac{\alpha(\epsilon)^{2n}}{n}\frac{\partial C(\epsilon,n)}{\partial\epsilon} + \mathrm{Re}\frac{2}{\sqrt{\delta^2-\epsilon^2}}\left[1 + 2\sum_{n=1}^{\infty}\frac{\alpha(\epsilon)^{2n}C(\epsilon,n)}{n}\right]. \tag{5.40}$$

Here the first term, which comes from applying the energy derivative to $C(\epsilon,n)$, gives an analogous contribution to the case $E \ll \Delta$ but with $r = \alpha^2$ instead of -1 and involving $H(\epsilon,\alpha^2)$ from (5.15) and (5.17). The second term in (5.40) comes from the energy derivative of α^{2n} and can be written using

$G(\epsilon, \alpha^2)$ from (5.12) and (5.13):

$$d(\epsilon) = \mathrm{Re}\left[1 + 2\alpha^2 H(\epsilon, \alpha^2)\right] + \mathrm{Re}\frac{2}{\sqrt{\delta^2 - \epsilon^2}}\left[1 + 2\alpha^2 G(\epsilon, \alpha^2)\right]. \tag{5.41}$$

The effect of a finite bulk superconducting gap on the hard gap in the density of states of the Andreev billiard is fairly small, for example as shown in figure 5.9 even for $\delta = \Delta/E_\mathrm{T} = 2$ the width just shrinks to around $0.5E_\mathrm{T}$. For $\delta = 2$ the shape of the density of states is changed somewhat (less so for $\delta = 8$) and we can see just before $\epsilon = 2$ it vanishes again giving a second thin gap. This gap, and even the way we can separate the density of states into the two terms in (5.41), foreshadows the effects of the Ehrenfest time (in section 5.4). For energies above the bulk superconducting gap ($\epsilon > \delta$) we see a thin singular peak from the $\sqrt{\delta^2 - \epsilon^2}$ which quickly tends to the density of states of an Andreev billiard with an infinite superconducting gap as the energy becomes larger.

6 Density of states with two leads

Next we consider a classically chaotic quantum dot connected to two superconductors with N_{S_1} and $N_{S_2} = N_S - N_{S_1}$ channels respectively and a phase difference ϕ, as depicted in figure 2.2a. For the density of states we we now have to include the phase factors in (2.14) again. Thus we will have to evaluate

$$C(\epsilon, \phi, n) = \frac{1}{N_S} \mathrm{Tr} \left[S^* \left(-\frac{\epsilon \hbar}{2\tau_d} \right) \mathrm{e}^{-\mathrm{i}\tilde{\phi}} S \left(+\frac{\epsilon \hbar}{2\tau_d} \right) \mathrm{e}^{\mathrm{i}\tilde{\phi}} \right]^n , \tag{6.1}$$

where $\tilde{\phi}$ is again a diagonal matrix whose first N_{S_1} elements from the first superconductor S_1 are $\phi/2$ and the remaining N_{S_2} elements from S_2 are $-\phi/2$. Note that the case $\phi = 0$ corresponds to the previous case of a single superconductor with $N_S = N_{S_1} + N_{S_2}$ channels. Since exchanging the leads gives the opposite phase, we expect the solution to be symmetric if we instantaneously exchange N_{S_1} with N_{S_2} and change ϕ to $-\phi$. When we substitute the semiclassical approximation for the scattering matrix (3.16) into (6.1), and especially if we write the scattering matrix in terms of its reflection and transmission subblocks, the effect of the superconductors' phase difference becomes simple. Namely, each electron (unprimed) trajectory which starts in lead 1 and ends in lead 2 picks up the phase factor $\exp(-\mathrm{i}\phi)$ while each unprimed trajectory going from lead 2 to lead 1 receives the factor $\exp(\mathrm{i}\phi)$. Reflection trajectories which start and end in the same lead have no additional phase factor, as depicted in figure 6.1. These paths are related to Andreev bound states [100, 101, 102, 103] appearing if a normal conducting region is coupled to two superconductors.A current carrying Andreev bound states has been proven spectroscopically *e.g.* in carbon nanotubes embedded between two superconductors [104].

As these factors are multiplicative, we can equivalently say that each electron trajectory leaving superconductor 1 or 2 picks up $\exp(-\mathrm{i}\phi/2)$ or $\exp(\mathrm{i}\phi/2)$ while each one entering lead 1 or 2 picks up $\exp(\mathrm{i}\phi/2)$ or $\exp(-\mathrm{i}\phi/2)$. To include these factors in our semiclassical diagrams, we can simply remember that in our tree recursions in section 5.1 the channels we designated as 'incoming' channels have electrons leaving them while electrons always enter the outgoing channels. Each incoming channel (in the original channel sum in (5.1)) can still come from the N_S possible, but with the trajectory leaving it now provides the factor $N_{S_1} \exp(-\mathrm{i}\phi/2) + N_{S_2} \exp(\mathrm{i}\phi/2)$. Similarly each outgoing channel now provides the complex conjugate of this factor. Recalling the power of N_S^{-2n} coming from the links and encounters, we can update the contribution of each diagram or tree (5.2) to

$$\frac{\left(N_{S_1} \mathrm{e}^{-\frac{\mathrm{i}\phi}{2}} + N_{S_2} \mathrm{e}^{\frac{\mathrm{i}\phi}{2}} \right)^n \left(N_{S_1} \mathrm{e}^{\frac{\mathrm{i}\phi}{2}} + N_{S_2} \mathrm{e}^{-\frac{\mathrm{i}\phi}{2}} \right)^n}{N_S^{2n} \left(1 - \mathrm{i}\epsilon\right)^n} \prod_{\alpha=1}^{V} \frac{-\left(1 - \mathrm{i}l_\alpha \epsilon\right)}{\left(1 - \mathrm{i}\epsilon\right)^{l_\alpha}}. \tag{6.2}$$

However, moving an l-encounter into lead 1 means combining l incoming channels, l links and the encounter itself. These combined incoming channels, with l electron trajectories leaving, will now only give the factor $N_{S_1} \exp(-\mathrm{i}l\phi/2) + N_{S_2} \exp(\mathrm{i}l\phi/2)$ where the important difference is that l is inside the exponents. We therefore make the replacement

$$\frac{\left(N_{S_1} \mathrm{e}^{-\frac{\mathrm{i}\phi}{2}} + N_{S_2} \mathrm{e}^{\frac{\mathrm{i}\phi}{2}} \right)^l}{N_S^l} \to \frac{\left(N_{S_1} \mathrm{e}^{-\frac{\mathrm{i}l\phi}{2}} + N_{S_2} \mathrm{e}^{\frac{\mathrm{i}l\phi}{2}} \right)}{N_S} \tag{6.3}$$

as well as removing the encounter from (6.2). Similarly when we move the encounter into the outgoing leads we take the complex conjugate of (6.3).

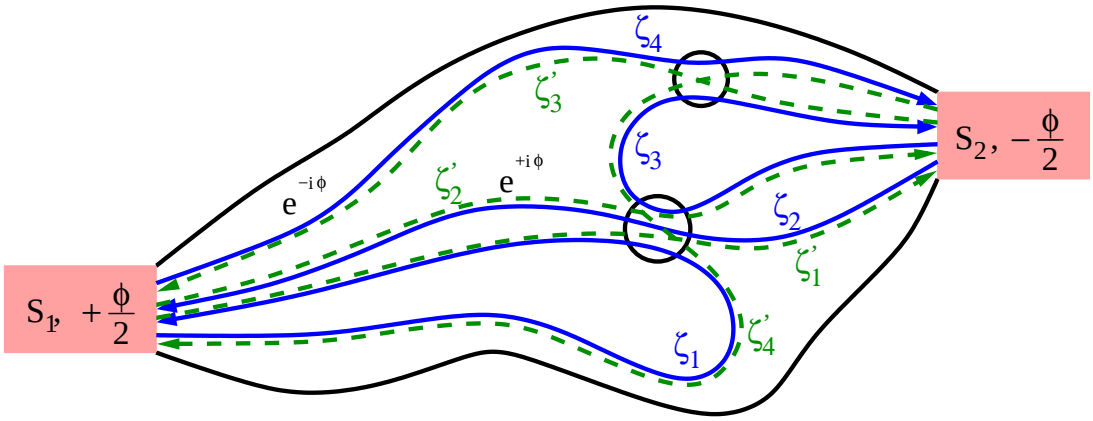

Figure 6.1: The paths may start and end in either of the two leads as shown. ζ_4 as it travels from lead 1 to lead 2 obtains a phase factor $\exp(-\mathrm{i}\phi)$, ζ_2 travelling back contributes $\exp(\mathrm{i}\phi)$ while the others does not contribute any phase. The encounters are again marked by circles and S_1 and S_2 denote the two superconducting leads at the corresponding superconducting phases $\pm\phi/2$. This diagram is equivalent to the one in figure 5.1c.

To mimic these effects in the semiclassical recursions we can set

$$x_l = \frac{-(1-\mathrm{i}l\epsilon)}{(1-\mathrm{i}\epsilon)^l}\cdot\tilde{r}^{l-1}, \qquad \beta = \frac{\left(N_{\mathrm{S}_1}\mathrm{e}^{-\frac{\mathrm{i}\phi}{2}} + N_{\mathrm{S}_2}\mathrm{e}^{\frac{\mathrm{i}\phi}{2}}\right)}{N_{\mathrm{S}}}, \tag{6.4}$$

$$z_{i,l} = \frac{\left(N_{\mathrm{S}_1}\mathrm{e}^{-\frac{\mathrm{i}l\phi}{2}} + N_{\mathrm{S}_2}\mathrm{e}^{\frac{\mathrm{i}l\phi}{2}}\right)}{N_{\mathrm{S}}\beta^l}\cdot\tilde{r}^{l-1}, \qquad z_{o,l} = \frac{\left(N_{\mathrm{S}_1}\mathrm{e}^{\frac{\mathrm{i}l\phi}{2}} + N_{\mathrm{S}_2}\mathrm{e}^{-\frac{\mathrm{i}l\phi}{2}}\right)}{N_{\mathrm{S}}\left(\beta^*\right)^l}\cdot\tilde{r}^{l-1}, \tag{6.5}$$

$$f = g\frac{(1-\mathrm{i}\epsilon)}{\beta\beta^*}, \qquad \tilde{r} = r\frac{\beta\beta^*}{(1-\mathrm{i}\epsilon)}, \tag{6.6}$$

in section 5.1. Including these substitutions in the recursion relation (5.4) and summing we obtain

$$\frac{g}{\beta\beta^* - rg\hat{g}} = \frac{\mathrm{i}\epsilon\beta\beta^* g}{\left(\beta\beta^* - rg\hat{g}\right)^2} + \frac{N_{\mathrm{S}_1}}{N_{\mathrm{S}}}\frac{1}{\beta^*\mathrm{e}^{-\frac{\mathrm{i}\phi}{2}} - r\hat{g}} + \frac{N_{\mathrm{S}_2}}{N_{\mathrm{S}}}\frac{1}{\beta^*\mathrm{e}^{\frac{\mathrm{i}\phi}{2}} - r\hat{g}}, \tag{6.7}$$

and a similar equation from (5.5). The generating function of the correlation functions $C(\epsilon,\phi,n)$ is then given from (5.6) by

$$G = \frac{N_{\mathrm{S}_1}}{N_{\mathrm{S}}}\frac{g}{\beta\mathrm{e}^{\frac{\mathrm{i}\phi}{2}} - rg} + \frac{N_{\mathrm{S}_2}}{N_{\mathrm{S}}}\frac{g}{\beta\mathrm{e}^{\frac{-\mathrm{i}\phi}{2}} - rg}. \tag{6.8}$$

Returning to (6.7) and multiplying through by $\hat{g}$, we can see that the first two terms are symmetric in g and $\hat{g}$. Combining the other two and taking the difference from the corresponding equation for $\hat{g}$ we have

$$\frac{\hat{g}\left[\left(\beta^*\right)^2 - r\hat{g}\right]}{\left(\beta^*\mathrm{e}^{-\frac{\mathrm{i}\phi}{2}} - r\hat{g}\right)\left(\beta^*\mathrm{e}^{\frac{\mathrm{i}\phi}{2}} - r\hat{g}\right)} = \frac{g\left[\beta^2 - rg\right]}{\left(\beta\mathrm{e}^{\frac{\mathrm{i}\phi}{2}} - rg\right)\left(\beta\mathrm{e}^{-\frac{\mathrm{i}\phi}{2}} - rg\right)}. \tag{6.9}$$

The resulting quadratic equation, when substituted back into (6.7) leads to a sixth order equation for g. Note that the right hand side of (6.9) is (recalling (6.4) and that $N_{\mathrm{S}_1} + N_{\mathrm{S}_2} = N_{\mathrm{S}}$) the same as (6.8) so it is clear that G satisfies the required symmetry upon swapping the leads (*i.e.* swapping N_{S_1} with N_{S_2} and ϕ with $-\phi$).

6.1 Equal leads

To make the equations more manageable we focus for now on the simpler case where the leads have equal size and $N_{S_1} = N_{S_2} = N_S/2$. Then $\beta = \cos(\phi/2)$ is real and we can see from (6.9) or $\boldsymbol{z}_i = \boldsymbol{z}_o$ that $g = \hat{g}$ is a solution. Putting this simplification into (6.7) we can obtain the following quartic

$$r^2 g^4 - r(1 + r + \mathrm{i}\epsilon r)g^3 + 2\mathrm{i}\epsilon\beta^2 r g^2 + (1 - \mathrm{i}\epsilon + r)\beta^2 g - \beta^4 = 0. \tag{6.10}$$

We may also find an algebraic equation of fourth order for G if we solve (6.8) for g and substitute the solution

$$g = \frac{\beta}{2}\frac{2r\beta G + \beta - \sqrt{\beta^2 + 4rG\,(1 + rG)\,(\beta^2 - 1)}}{r(1 + rG)}, \tag{6.11}$$

into (6.10). Note that we take the negative square root to agree with the previous result when the phase is 0 (*i.e.* $\beta = 1$) though this sign does not affect the equation one finally finds for G. After the fourth order equation for G has been found we can again search for and verify an equation for $H(\epsilon, \phi, r) = 1/(\mathrm{i}r)\int(\partial G(\epsilon, \phi, r)/\partial\epsilon)\mathrm{d}r$,

$$\begin{aligned}\epsilon^2 r^3\left[1 - 2r\left(2\beta^2 - 1\right) + r^2\right]H^4 + \mathrm{i}\epsilon r^2\left[2 - 3\mathrm{i}\epsilon - 4r\,(1 - \mathrm{i}\epsilon)\left(2\beta^2 - 1\right) + r^2\,(2 - \mathrm{i}\epsilon)\right]H^3 \\ - r\left[1 - 4\mathrm{i}\epsilon - 3\epsilon^2 - 2r\left(1 - 3\mathrm{i}\epsilon - \epsilon^2\right)\left(2\beta^2 - 1\right) + r^2\,(1 - 2\mathrm{i}\epsilon)\right]H^2 \\ - \left[(1 - \mathrm{i}\epsilon)^2 - 2r\,(1 - \mathrm{i}\epsilon)\left(2\beta^2 - 1\right) + r^2\right]H + \beta^2 = 0.\end{aligned} \tag{6.12}$$

In order to see the agreement of our result with the RMT prediction we again substitute $H(\epsilon, \phi, -1) = [-\mathrm{i}W(\epsilon, \phi) + 1]/2$ such that $d(\epsilon) = -\mathrm{Im}W(\epsilon, \phi)$. If we do so we find

$$\epsilon^2\beta^2 W^4 + 4\epsilon\beta^2 W^3 + (4\beta^2 - \epsilon^2 + 2\epsilon^2\beta^2)W^2 + 4\epsilon\beta^2 W - \epsilon^2 + \epsilon^2\beta^2 = 0, \tag{6.13}$$

which corresponds to (2.22) for zero magnetic field. Moreover, if the phase difference is zero (and $\beta = 1$), we can take out the factor W and recover (2.23).

Solving this equation yields the density of states. If we insert different values for the phase ϕ one finds that the hard gap in the density of states decreases with increasing phase difference while the density of states has a peak at the end of the gap which increases and becomes sharper with increasing phase. Finally when the phase difference is equal to π the gap closes and the peak vanishes so the density of states becomes identical to 1. This can all be seen in figure 6.2. Moreover (6.13) is the same as (2.22) expanded and therefore we have reproduced the RMT prediction [41] for the density of states of an Andreev billiard with two leads.

6.2 Magnetic field.

In the presence of a magnetic field, we again have to change the diagrammatic rules as in section 5.3. Doing the calculation above with these modified diagrammatic rules leads to a sixth order equation for g:

$$\begin{aligned}r^3 g^6 - r^2\left[1 + r\,(1 + \mathrm{i}\epsilon + b)\right]g^5 - r^2\beta^2\,(1 - 2\mathrm{i}\epsilon - 2b)\,g^4 \\ + r\beta^2\left[2 - \mathrm{i}\epsilon - b + r\,(2 + \mathrm{i}\epsilon - b)\right]g^3 - r\beta^4\,(1 + 2\mathrm{i}\epsilon - 2b)\,g^2 \\ - \beta^4\,(1 + r - \mathrm{i}\epsilon + b)\,g + \beta^6 = 0.\end{aligned} \tag{6.14}$$

The relation (6.8) between G and g remains unchanged and therefore we may find a sixth order equation for G. We find the corresponding H, which is recorded as (A.2) in Appendix A, using a computer search over sixth order equations with polynomial (in ϵ, ϕ, b and r) coefficients whose expansion in r (5.15) matches the correlation functions calculated by expanding G. We note that for this order polynomial it was not feasible (in terms of computational time and memory) to solve the equations resulting from

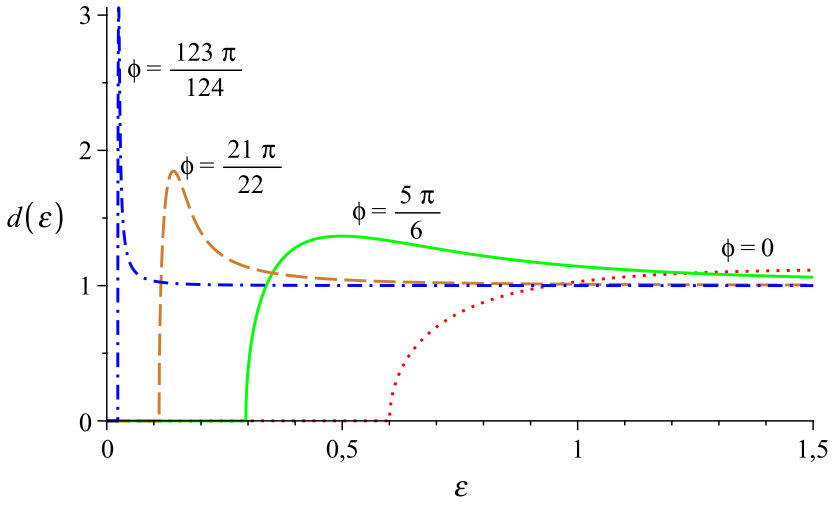

Figure 6.2: The density of states of a chaotic quantum dot coupled to two superconductors with the same numbers of channels and phase differences 0 (dotted line), $5\pi/6$ (solid line), $21\pi/22$ (dashed line) and $123\pi/124$ (dashed dotted line).

the differentiation algorithm described in section 5.2 and to find the intermediate generating function I in all generality. However, we succeeded to find a polynomial equation for I that was satisfied by the derivatives of both rH and G for a large number of numerical values of the parameters (ϵ, ϕ, b). For each parameter involved, the number of the values checked was larger than the maximum degree of the parameter in the conjectured equation. While we cannot rule out the possibility that the true equation for I has a higher order, given the large number of numerical values checked this is highly unlikely.

From H we obtain the equation for $W(\epsilon, \phi, b)$,

$$\begin{aligned} b^2\beta^2 W^6 - 2\epsilon b\beta^2 W^5 + \left(2b^2\beta^2 + \epsilon^2\beta^2 - 4b\beta^2 - b^2\right) W^4 \\ + 2\left(\epsilon b + 2\epsilon\beta^2 - 2\epsilon b\beta^2\right) W^3 + \left(4\beta^2 - b^2 - \epsilon^2 - 4b\beta^2 + b^2\beta^2 + 2\epsilon^2\beta^2\right) W^2 \\ + 2\left(\epsilon b + 2\epsilon\beta^2 - \epsilon b\beta^2\right) W - \epsilon^2 + \epsilon^2\beta^2 = 0, \end{aligned} \tag{6.15}$$

which corresponds exactly to the full RMT result (2.22) expanded.

As an example, the magnetic field dependence of the density of states is shown at the phase difference of $5\pi/6$ in figure 6.3. As the magnetic field is increased one finds a reduction of the gap and the peak appearing for a phase difference $\phi > 0$ vanishes again. Moreover the higher the phase difference the lower the magnetic field needed in order to close the gap. While for $\phi = 0$ the gap closes at $b = 1$ in the case of a phase difference of $5\pi/6$ one needs $b \approx 0.4096$ and for $\phi = 21\pi/22$ a magnetic field corresponding to $b \approx 0.1024$ closes the gap. In particular the critical magnetic field for which the gap closes is given by [41]

$$b_c = \frac{2\cos(\phi/2)}{1 + \cos(\phi/2)}. \tag{6.16}$$

For ever increasing magnetic field the density of states approaches 1 and we can see that a higher phase difference causes a faster convergence to this limit. Some examples are plotted in figure 6.4 and there we see that for $b = 1$ the curve for $\phi = 21\pi/22$ is nearly constant.

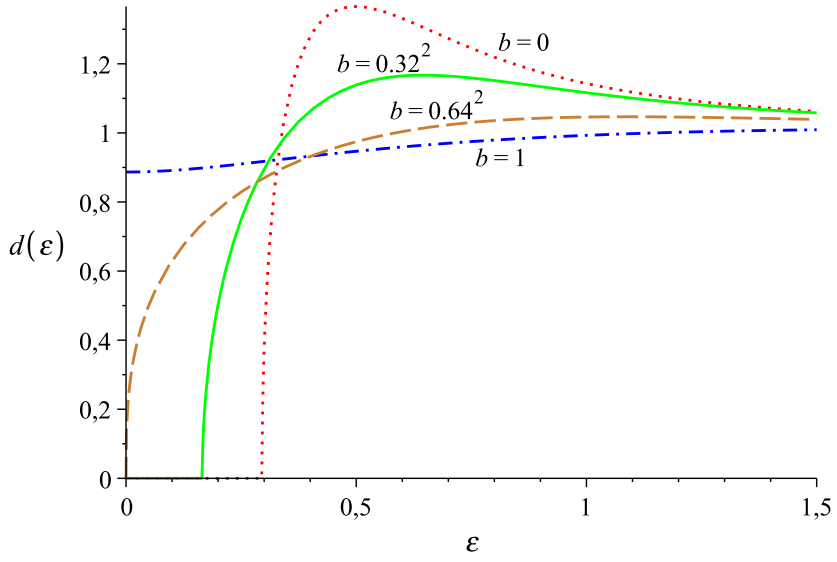

Figure 6.3: Magnetic field dependence of the density of states of a chaotic Andreev billiard with phase difference $\phi = 5\pi/6$ for $b = 0$ (dotted line), $b = 0.1024$ (solid line), $b = 0.4096$ (dashed line) and $b = 1$ (dashed dotted line).

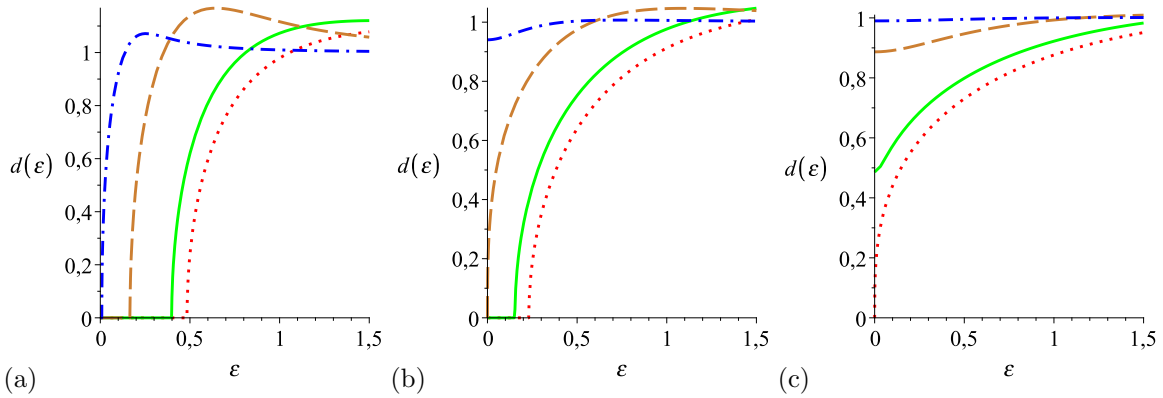

Figure 6.4: Phase dependence of the density of states of a chaotic Andreev billiard with phase difference $\phi = 0$ (dotted line), $\phi = \pi/2$ (solid line), $\phi = 5\pi/6$ (dashed line) and $\phi = 21\pi/22$ (dashed dotted line). (a) At magnetic field $b = 0.1024$, (b) at $b = 0.4096$ and (c) at $b = 1$.

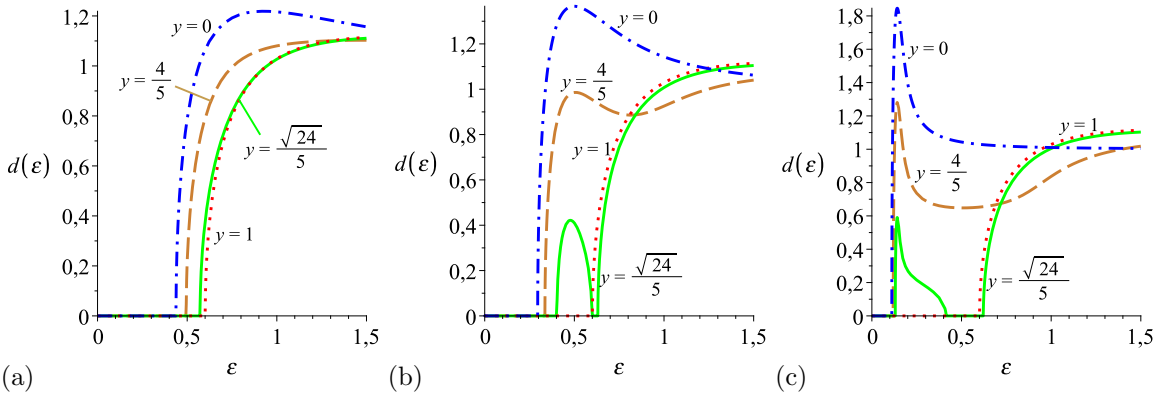

Figure 6.5: Dependence of the density of states of an Andreev billiard on the difference $y = (N_{S_1} - N_{S_2})/N_S$ in size of the leads with $y = 0$ (dashed dotted line), $y = 4/5$ (dashed line), $y = \sqrt{24}/5$ (solid line) and $y = 1$ (dotted line). (a) At phase difference $\phi = 2\pi/3$, (b) at $\phi = 5\pi/6$ and (c) at phase difference $\phi = 21\pi/22$.

6.3 Unequal leads

Removing the restriction that the leads have equal size we return to a sixth order polynomial for g and G when substituting (6.9) into (6.7) and then (6.8). Expanding G as a power series in r via $G = \sum r^{n-1} C(\epsilon, \phi, n)$ now gives three starting values for $C(\epsilon, \phi, 1)$ and we choose the one that coincides with the result from the semiclassical diagrams, namely $\beta\beta^*/(1 - \mathrm{i}\epsilon)$. Choosing the variable y to represent the relative difference in the lead sizes

$$y = \frac{N_{S_1} - N_{S_2}}{N_S}, \qquad \beta = \cos\left(\frac{\phi}{2}\right) + \mathrm{i}y \sin\left(\frac{\phi}{2}\right), \tag{6.17}$$

leads to a particularly compact solution, and as before, we can go through our roundabout route of finding the generating function of interest $H(\epsilon, \phi, y, r)$, which is recorded as (A.3) in Appendix A. Although it also was not possible to verify (other than at a large number of parameter values) this sixth order equation, from it we can obtain the polynomial satisfied by $W(\epsilon, \phi, y)$:

$$\left[\epsilon^2\beta^2 W^4 + 4\epsilon\beta^2 W^3 + \left(4\beta^2 - \epsilon^2 + 2\epsilon^2\beta^2\right) W^2 + 4\epsilon\beta^2 W - \epsilon^2 + \epsilon^2\beta^2\right](2 + \epsilon W)^2 + 4\epsilon^2 y^2 \left(1 - \beta^2\right) = 0, \tag{6.18}$$

where we have redefined β to just its real part, $\beta = \cos(\phi/2)$ as in the case with equal leads, and the evenness in y follows from the symmetry under swapping the leads and ϕ to $-\phi$. The term in the square brackets is simply (6.13) and so we recover the result with equal leads when $y = 0$. Likewise we can check that when we only have a single lead ($y = \pm 1$) we recover a factor corresponding to (2.23) so that the phase, as expected, no longer plays a role. From this equation we can plot the density of states as in figure 6.5 and see how the difference in lead sizes y interpolates between the result with equal leads above and the density of states with a single lead in (5.24). Note in particular that the peak in the density of states as the phase difference nears π vanishes slowly as y approaches ± 1 so that we can see a second gap appear in the density of states for leads differing distinctly in channel numbers (for example the solid line in figures 6.5b and c).

6.4 Ehrenfest time dependence

The effect of non-zero Ehrenfest time can be included in the channel sum and treated as above (the effective RMT result can be found by a simple modification of the treatment in [105]). Important to

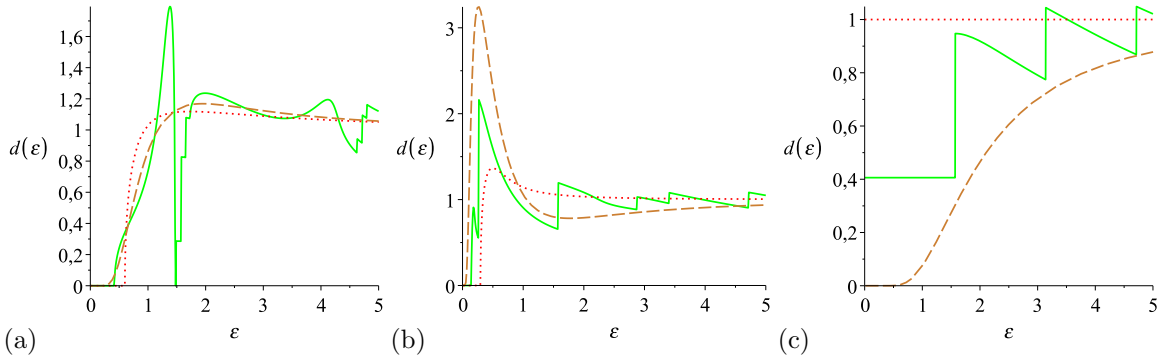

Figure 6.6: Density of states for $\tau = 2$ (solid line) along with the $\tau = 0$ (dotted) and $\tau = \infty$ (dashed) limits for a chaotic Andreev billiard with phase difference (a) $\phi = \pi/18$, (b) $\phi = 5\pi/6$ and (c) $\phi = \pi$.

remember is that the second part (of (5.31)) corresponds to bands of trajectories which are correlated for their whole length and so they all start and end together (in the same leads). Therefore the second contribution has to be multiplied by $[1 + \cos(n\phi)]/2$ leading to

$$C(\epsilon, \phi, \tau, n) = C(\epsilon, \phi, n)\mathrm{e}^{-(1-\mathrm{i}n\epsilon)\tau} + \frac{1 + \cos(n\phi)}{2} \frac{1 - \mathrm{e}^{-(1-\mathrm{i}n\epsilon)\tau}}{1 - \mathrm{i}n\epsilon}. \tag{6.19}$$

The first part of the density of states for non zero Ehrenfest time then remains as in (5.34) but with $G(\epsilon, r)$ and $H(\epsilon, r)$ replaced by $G(\epsilon, \phi, r)$ and $H(\epsilon, \phi, r)$, respectively. The second contribution in this case however may be written as the average of the $\phi = 0$ contribution and a contribution with the full phase difference ϕ,

$$d_2(\epsilon, \phi, \tau) = \frac{1}{2}\left[d_2'(\epsilon, 0, \tau) + d_2'(\epsilon, \phi, \tau)\right]. \tag{6.20}$$

Here $d_2'(\epsilon, \phi, \tau)$ may be again written as the sum of the $\tau = \infty$ result

$$d_2'^{(1)}(\epsilon, \phi, \tau) = \frac{\pi}{2\epsilon^2 \sinh^2(\pi/\epsilon)} \left[(\pi + 2\pi k_1 - \phi)\cosh\left(\frac{\pi - 2\pi k_1 + \phi}{\epsilon}\right) + (\pi - 2\pi k_1 + \phi)\cosh\left(\frac{\pi + 2\pi k_1 - \phi}{\epsilon}\right)\right], \tag{6.21}$$

and some correction

$$d_2'^{(2)}(\epsilon, \phi, \tau) = -\frac{\pi}{2\epsilon^2 \sinh^2(\pi/\epsilon)} \left\{\left[\pi\cosh\left(\frac{\pi}{\epsilon}\right) + (2\pi k_2 - \phi)\sinh\left(\frac{\pi}{\epsilon}\right)\right]\mathrm{e}^{-\frac{2\pi k_2 - \phi}{\epsilon}} + \left[\pi\cosh\left(\frac{\pi}{\epsilon}\right) + (2\pi k_3 + \phi)\sinh\left(\frac{\pi}{\epsilon}\right)\right]\mathrm{e}^{-\frac{2\pi k_3 + \phi}{\epsilon}}\right\}, \tag{6.22}$$

with $k_1 = \lfloor(\pi + \phi)/(2\pi)\rfloor$, $k_2 = \lfloor(\epsilon\tau + \pi + \phi)/(2\pi)\rfloor$ and $k_3 = \lfloor(\epsilon\tau + \pi - \phi)/(2\pi)\rfloor$. Since the k_i and ϕ only occur in the combinations $2\pi k_1 - \phi$, $2\pi k_2 - \phi$ and $2\pi k_3 + \phi$ it is obvious that these contributions have oscillations in the phase ϕ with period 2π. It can also be easily seen that for $\phi = 0$ the previous result for the density of states in the Ehrenfest regime is reproduced.

With $|\phi| < \pi$ we have $k_1 = k_2 = k_3 = 0$ for $\epsilon\tau < \pi - |\phi|$. Therefore one again sees that $d_2 = 0$ as long as $\epsilon\tau < \pi - |\phi|$. The first part $d_2'^{(1)}$ equals the Bohr-Sommerfeld result (5.32), so in the limit $\tau = \infty$ this result is reproduced again. The oscillations in ϵ seen in the $\phi = 0$ case which have a period of $2\pi/\tau$ can still be seen due to the fact that the $\phi = 0$ result enters $d_2(\epsilon, \phi, \tau)$ even if $\phi \neq 0$. However one gets additional (but smaller) steps at energies satisfying $\epsilon = [(2n - 1)\pi \mp \phi]/\tau$.

We plot the density of states for $\tau = 2$, along with the $\tau = 0$ and $\tau = \infty$ limits in figure 6.6 for different values of the phase difference. We can see that as the phase difference increases the second intermediate

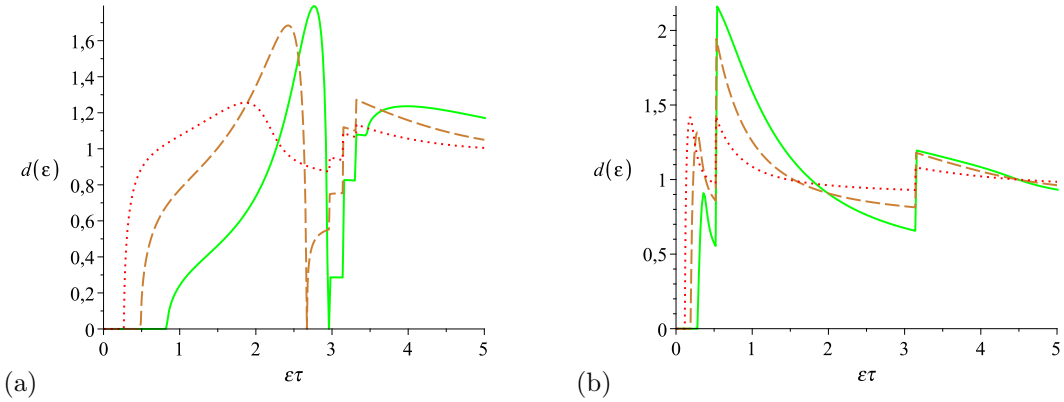

Figure 6.7: Density of states for $\tau = 1/2$ (dotted line), $\tau = 1$ (dashed) and $\tau = 2$ (solid) showing the phase dependent jumps for phase difference (a) $\phi = \pi/18$ and (b) $\phi = 5\pi/6$.

gap (*c.f.* figure 5.6a) shrinks quickly. The reason for this shrinking is twofold: On one hand the gap in the RMT-like contribution shrinks and on the other the second contribution is zero only up to $\epsilon\tau = \pi - |\phi|$. Moreover if $\phi \to \pi$ the modified correlation function tends to zero so the density of states converges to $(1+\tau)\mathrm{e}^{-\tau} + d_2(\epsilon, \tau)$. For a finer look at the Ehrenfest time dependence and the phase dependent jumps we plot the density of states for $\tau = 1/2$, 1 and 2 for phases $\phi = \pi/18$ and $5\pi/6$ in figure 6.7.

7 Conductance of Andreev Interferometers

Another important topic in solid state physics is the electronic transport which is often described by the conductance $G = \frac{\partial I}{\partial V}$ which may be seen as the inverse resistance. To calculate the conductance one essentially has to evaluate the coefficients for transmission between two normal conducting leads [29]. If we have not only normal leads but also superconducting ones in the linear response regime we still have to calculate coefficients $T_{ij}^{\beta\alpha}$ for transmission from the normal metal lead $j \in \{1,2\}$ to the normal metal lead $i \in \{1,2\}$ while converting an α-type quasiparticle into a β-type quasiparticle where $\alpha, \beta \in \{e,h\}$ denote electrons and holes (see figure 2.4). The transmissions are essentially given by (3.18):

$$T_{ij}(E) = \frac{1}{T_\mathrm{H}} \sum_{o\in i} \sum_{i\in j} \sum_{\zeta(i\to o)} \sum_{\zeta'(i\to o)} A_\zeta A_{\zeta'}^* \mathrm{e}^{\mathrm{i}\left(S_\zeta(E) - S_{\zeta'}(E)\right)/\hbar}. \tag{7.1}$$

However we will have to decide whether the trajectories ζ and ζ' contribute to $T_{ij}^{\alpha\alpha}$ ($\alpha \in \{e,h\}$) or $T_{ij}^{\bar{\alpha}\alpha}$ where $\bar{\alpha}$ denotes a hole if α denotes an electron and vice versa. The trajectory pair contributes to $T_{ij}^{\alpha\alpha}$ if both ζ and ζ' undergo an even number of Andreev reflections and to $T_{ij}^{\bar{\alpha}\alpha}$ otherwise.

The paths depend on the actual system we are looking at. Here we will investigate the conductance between two normal metal leads providing N_1 and N_2 channels, respectively, coupled to a ballistic quantum dot which is additionally connected to two superconducting leads having N_{S_1} and N_{S_2} channels, respectively, as well as a phase difference $\phi = \phi_1 - \phi_2$ as shown in figure 7.1.

The presence of Andreev reflection again causes the formation of links and encounters. This is that we start with a link traversed by ζ and ζ' in the same direction which may then hit the superconductor. The Andreev reflected trajectories may now separate from each other and form individual stretches but in order to ensure a small action difference these stretches have to be retraced by the opposite quasiparticle as indicated in figure 7.3. If these stretches come close to each other again this makes the formation of encounters possible. We will show which trajectory pairs contribute in leading order in section 7.1.

However we start with considering the result provided by the diagonal approximation $\zeta = \zeta'$. The trajectory pairs contributing to the diagonal approximation are drawn schematically for up to three Andreev reflections in figure 7.2. These consist of links traversed by trajectories with the same energy in the same direction yielding a factor N^{-1} and Andreev reflections at the superconductors yielding a factor N_{S_i}, $i \in \{1,2\}$. If the number of Andreev reflections is even the incoming and outgoing quasiparticles are the same while if it is odd they are different. Since a diagonal pair hitting the superconductor does not contribute any phase the sum over the superconducting channels for the diagonal diagrams can be combined and therefore the Andreev reflections give a factor $N_\mathrm{S} = N_{\mathrm{S}_1} + N_{\mathrm{S}_1}$. Thus the transmission

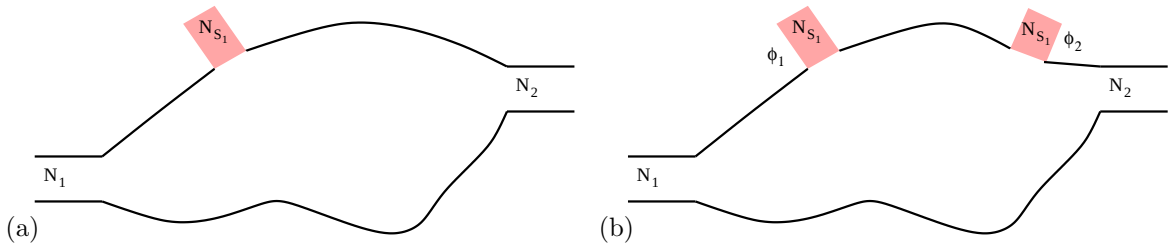

Figure 7.1: The two cases we will consider here: (a) Ballistic chaotic quantum dot with one superconducting lead. (b)Ballistic chaotic quantum dot with two superconducting leads.

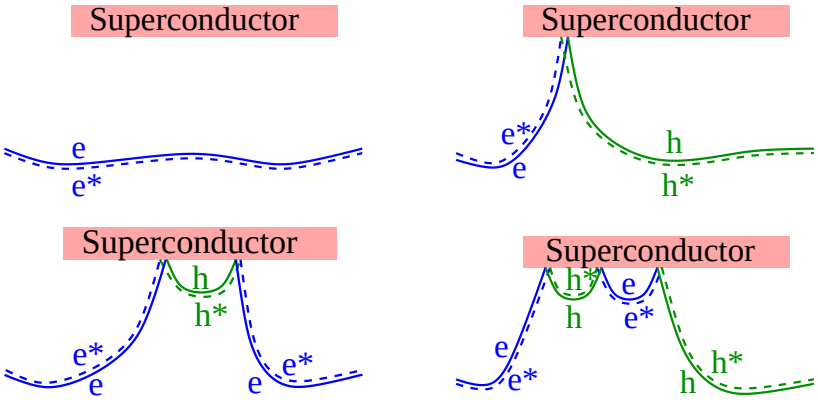

Figure 7.2: The diagonal diagrams up to third order in the number of channels of the superconductor contributing to the conductance.

coefficients given by the diagonal contributions are

$$T_{ij}^{\alpha\alpha} = N_i N_j \sum_{n=0}^{\infty} \left(\frac{N_\mathrm{S}}{N}\right)^{2n} \tag{7.2a}$$

$$T_{ij}^{\alpha\bar{\alpha}} = N_i N_j \sum_{n=0}^{\infty} \left(\frac{N_\mathrm{S}}{N}\right)^{2n+1}, \tag{7.2b}$$

where again $\alpha \in \{e, h\}$ and $\bar{\alpha}$ denotes a hole if α denotes an electron and vice versa. Inserting these transmission coefficients into (2.31) and (2.35) provides the classical dimensionless conductances [49]

$$g_\mathrm{cl} = \frac{N_1 N_2}{N_\mathrm{N}} \qquad \text{if the superconductors are isolated (superconducting islands)} \tag{7.3a}$$

$$g_\mathrm{cl} = \frac{N_1\,(N_2 + 2N_\mathrm{S})}{N_\mathrm{N} + 2N_\mathrm{S}} \qquad \text{if } \mu_\mathrm{S} = \mathrm{e}V_2 \text{ (superconducting leads)}, \tag{7.3b}$$

where $N_\mathrm{N} = N_1 + N_2$, μ_S the chemical potential of the superconductor, V_2 the voltage applied to the normal lead 2 and e the negative of the charge of an electron.

7.1 Contributing diagrams

In what follows we will identify the possible trajectories contributing to the conductance beyond the diagonal approximation in leading order in the inverse number of channels $1/N$ with diagrams. The trajectories contributing in third order in $x = N_\mathrm{S}/N_\mathrm{N}$, *i.e.* trajectories with three Andreev reflections, are shown in figure 7.3 while the trajectories with two Andreev reflections may be found in [49]. The first task is to find a structure in the diagrams contributing at leading order in the channel number. Therefore we first consider just the channel numbers contributed by certain diagrams, *i.e.* we use the diagrammatic rules in section 4.2.2 and described in [82] without an energy difference and magnetic field and not worrying about any signs for the moment. A path pair hitting lead l then contributes a factor of the number of channels N_l. The path pair which will also be called a 'link' itself however contributes a factor $1/N$ where $N = N_\mathrm{N} + N_\mathrm{S}$ while each encounter contributes a factor N. From the trajectory pairs shown in figure 7.3 we see that if we cut off all e-h and e*-h*pairs we again get a diagonal like contribution as depicted in figure 7.6. For example if we cut the e-h pair at the very left of ee3I we get the diagonal contribution to the second order in $x = N_\mathrm{S}/N_\mathrm{N}$ since there are two Andreev reflections and if we cut the 'off-diagonal' parts in say ee3III we get a diagonal contribution to first order in x.

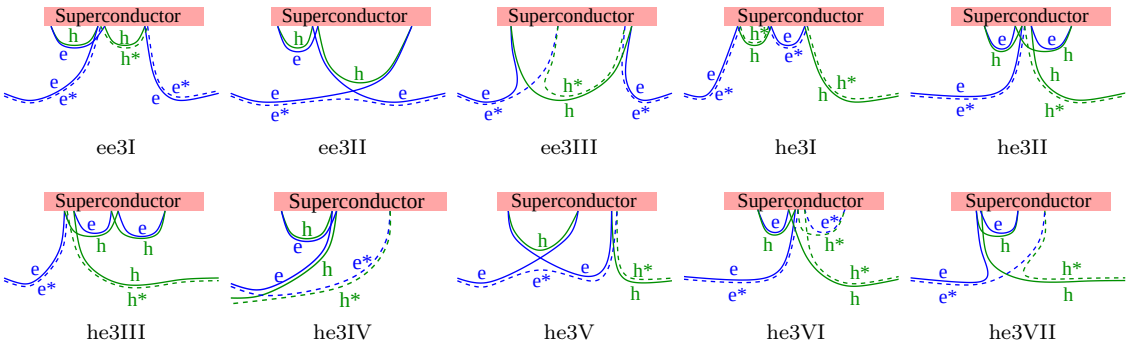

Figure 7.3: Paths contributing to the third order term in N_S/N_N of the transmission. The electron paths are drawn green while the hole paths are drawn red. The solid lines belong to ζ and the paths belonging to ζ' are drawn dashed. A trajectory pair entering on the left and exiting on the right may connect the two normal conducting leads to each other while a trajectory pair entering and exiting at the same side only contributes if the incoming and outgoing channel belong both to the same lead.

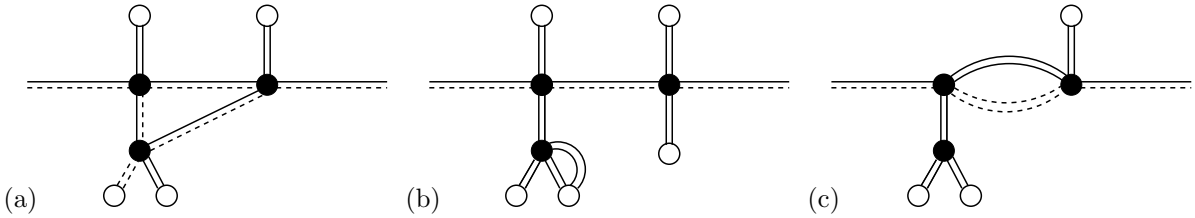

Figure 7.4: Diagrams we neglect in leading order in $1/N$ due to the formation of loops: (a) A non-diagonal ζ-ζ' pair causes the formation of a loop. (b) A loop formed by an off-diagonal e-h path pair. (c) A loop formed due to the lack of a diagonal-type ζ-ζ' path pair.

This is that the 'off-diagonal' path pairs can not consist of one ζ- and one ζ'-stretch since each of those path pairs has to be traversed by ζ and ζ' in the same direction. Thus in order to come back from the off-diagonal part starting with an ζ-ζ' pair we have to connect this off-diagonal part to the diagonal 'backbone' by a second ζ-ζ' path pair thus forming a loop as indicated in figure 7.4a. This loop however decreases the number of Andreev reflections by at least one and therefore the contribution to the conductance is suppressed by a factor of the order $1/N_S$ such that it would contribute to sub-leading order in the inverse channel number. Therefore the 'off-diagonal' parts may only consist of e-h or e*-h*pairs. In the same way we may neglect loops formed by e-h or e*-h*path pairs such as the one in figure 7.4b and the 'off-diagonal' parts again become rooted plane trees as in section 5.1. However the trees here - we will call them 'side-trees' - start at the 'diagonal encounter' such that their root does not touch a channel.

The fact that the path pairs of the backbone have to be ζ-ζ' pairs is again due to the neglect of loops: The two trajectories ζ and ζ' both have to start at lead l and end at lead k. Thus the path pairs hitting the normal leads have to be ζ-ζ' pairs and thus if there is a 'diagonal' encounter entered by a ζ-ζ' pair and left only by e-h and e*-h*pairs there has to be an encounter entered only by e-h and e*-h*pairs and left by a ζ-ζ' pair. Therefore we again would get a loop essentially formed by one e-h and one e*-h*pair as shown in figure 7.4c. Therefore the diagrams have to consist of a diagonal type 'backbone' consisting of ζ-ζ' path pairs and encounters and ζ- and ζ'-side trees emerging from these diagonal encounters.

Note that when pairing a ζ with a ζ' stretch these stretches have to be traversed by the same kind of quasiparticle, *i.e.* it has to be an e-e*or a h-h*pair. This is related to the fact that each encounter has an even number of entering and exiting path pairs. With these considerations we find for the contributions

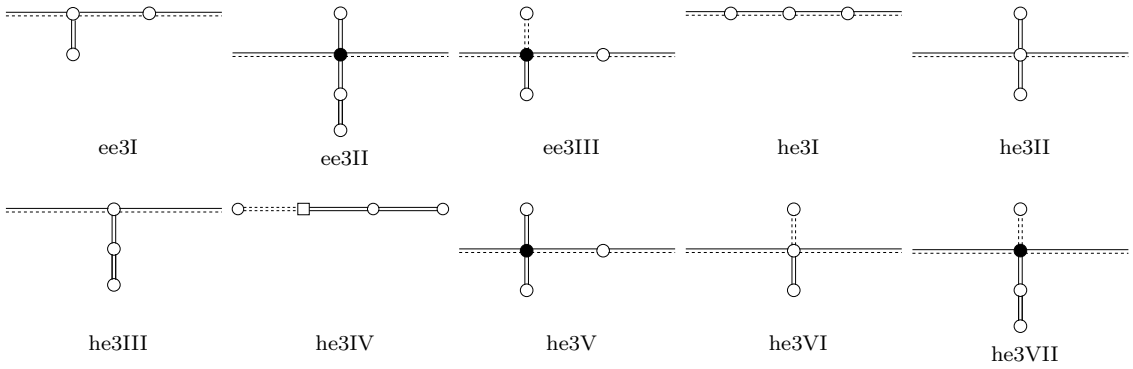

Figure 7.5: Diagrams corresponding to the trajectory pairs shown in figure 7.3. The full circles denote encounters while the empty circles denote Andreev reflection. Note that an encounter touching the superconductor is also shown as Andreev reflection. An encounter touching a normal conducting lead is shown as an empty box. The solid line represents ζ while the dashed line denotes ζ'.

in third order in x the diagrams in figure 7.5 which represent the trajectories shown in figure 7.3.

Since there are no loops in the 'off-diagonal' parts an l-encounter creates $(2l-1)$ additional path pairs. If we denote the total number of encounters by $V = \sum_{l\geq 2} v_l$ where v_l denotes the number of l-encounters (and is the l-th entry of the vector $\mathbf{v}$) and define $L(\mathbf{v}) = \sum_{l\geq 2} l v_l$ the total channel number provided by one specific 'off-diagonal' part originating from one specific path pair exiting an 'diagonal' encounter is $N_{\mathrm{S}}^{2L-2V+1}/N^{2L-2V+1}$. In terms of graphs an 'off-diagonal' part is a rooted planar tree [88] and therefore we will refer to it as a 'side tree'. The above considerations still hold, if one of the encounters of an 'off-diagonal' part is moved inside the superconducting lead.

However, there is still one possibility left we have not mentioned yet but that needs a special treatment. If the 'diagonal' part consists of only two path pairs and one 2-encounter with one ζ-side tree (a side tree formed by ζ) and one ζ'-side tree this encounter can be moved into one of the normal conducting leads, say lead i. An example for an 2-encounter touching the incoming lead is the trajectory labelled by he3IV in figure 7.3 which arises from the trajectory labelled by he3VII by moving the encounter into the lead. However this is only possible if the trajectory connects lead i to itself and thus if the electron is scattered back coherently. In this case we have only one side tree and one complex conjugated side tree but no 'diagonal' part.

7.2 Side tree contributions

Since we know the structure of the trajectory pairs contributing in leading order in the channel number we can start evaluating them. Since the contributions of the encounters and the stretches are multiplicative we may factorise the contribution of a given diagram into the contributions of side trees starting at the first encounter with an α-type quasiparticle, $P^{\alpha}(\epsilon, x)$, the first encounter and the diagram remaining when cutting off the diagram after the first encounter. We will first evaluate the contribution arising from the summation over a possible side tree. Here we consider all side trees starting with an electron, since the complex conjugated side tree only gives the complex conjugated contribution and the side trees starting with a hole have ϕ replaced by $-\phi$.

We restrict ourself to sufficiently low temperatures such that in (2.31) only energies ϵE_{T} (measured with respect to the Fermi energy and in units of the Thouless energy $E_{\mathrm{T}} = \hbar/2\tau_{\mathrm{D}}$ where τ_{D} is the mean dwell time) much smaller than the superconducting gap Δ have to be taken into account. $\epsilon E_{\mathrm{T}} \ll \Delta$ allows us to approximate $\exp[-\mathrm{i}\arccos(\epsilon/\Delta)] \approx -\mathrm{i}$ such that the scattering matrix of Andreev reflection becomes independent of the energy [54]. Thus the diagrammatic rules for the ζ-side trees read [82, 52]

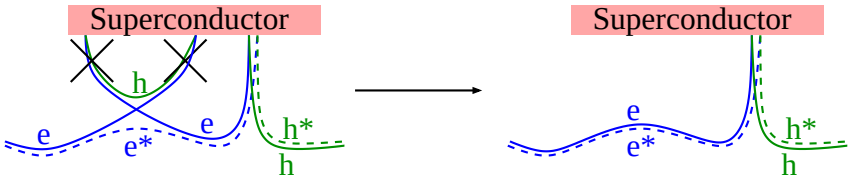

Figure 7.6: If the e-h path pairs are cut off a diagonal type diagram remains.

- An e-h path pair contributes $\left[N\left(1+\mathrm{i}\epsilon+b^2\right)\right]^{-1}$
- An l-encounter contributes $-N\left(1+\mathrm{i}l\epsilon+l^2b^2\right)$
- An e-h path pair hitting the superconductor S_j contributes N_{S_j}.
- An l-encounter touching the superconductor S_j contributes N_{S_j}.
- Each Andreev reflection at the superconducting lead j converting an electron into a hole contributes $-\mathrm{i}\mathrm{e}^{-\mathrm{i}\phi_j}$.
- Each Andreev reflection at the superconducting lead j converting a hole into an electron contributes $-\mathrm{i}\mathrm{e}^{\mathrm{i}\phi_j}$.

where b represents a magnetic field as described in section 4.3. These diagrammatic rules have to be complex conjugated for a ζ'-side tree and imply that when exchanging electrons and holes we just have to replace $\phi \leftrightarrow -\phi$. Thus a side tree starting with a hole gives the same contribution of a side tree starting with an electron but with negative phase.

The evaluation of the side trees then follows essentially those in sections 5 and 6 and Refs. [88], [52] and [106]. However here the root of the tree does not hit any channel and therefore can not touch the superconductor which simplifies the calculation. Moreover for a path pair hitting a channel in the superconductor S_1 we get a factor $-\mathrm{i}\mathrm{e}^{-\mathrm{i}\phi/2}N_{\mathrm{S}_1}$ if an electron hits the channel and $-\mathrm{i}\mathrm{e}^{\mathrm{i}\phi/2}N_{\mathrm{S}_1}$ if a hole hits the channel rather than just a factor of the numbers of channels and equivalently for a path pair hitting S_2.

Similar to section 5 as long as the phase difference is zero and all $2n-1$ channels are distinct the contribution of a side tree with characteristic $\mathbf{v}$ is

$$\prod_{\alpha=1}^{V(\mathbf{v})} \frac{\left(1+\mathrm{i}l_\alpha\epsilon+l_\alpha^2b^2\right)}{\left(1+\mathrm{i}\epsilon+b^2\right)^{2l_\alpha-1}} = \left(1+\mathrm{i}\epsilon+b^2\right)^{-n} \prod_{\alpha=1}^{V(\mathbf{v})} \frac{\left(1+\mathrm{i}l_\alpha\epsilon+l_\alpha^2b^2\right)}{\left(1+\mathrm{i}\epsilon+b^2\right)^{l_\alpha}},$$

where the encounters have been labelled by α.

We then again enumerate the number of l-encounters by x_l and the number of l-encounters touching the superconductor S_i at an odd numbered channel by $z_{o,l}^{(i)}$. Note that due to the fact that the root is not in a channel we do not need the further variable $z_{i,l}$. This simplifies the evaluation a little bit because there are not the two possibilities of 'o-touching' and 'i-touching' for the top encounter as it was for the density of states. We therefore may look at the generating function $F(\mathbf{x}, \mathbf{z}_o^{(1)}, \mathbf{z}_o^{(2)})$ directly and will derive a recursion relation for it by again cutting the side tree at its top node. If the top node has degree $2l$ and does not touch the superconductor the tree then has the contribution of the top node times that of all $2l-1$ subtrees giving $x_l F^l \hat{F}^{l-1}$, where $\hat{F}$ is the same as F but with ϕ replaced by $-\phi$ accounting for the fact that each even numbered subtree starts with a hole instead of an electron thus yielding an exchange $\phi \leftrightarrow -\phi$. If the top node however is a node of degree $2l$ touching S_i its contribution is $z_{o,l}^{(i)}\hat{F}^{l-1}$. In total

we therefore have

$$F = -\mathrm{i}\frac{N_{\mathrm{S}_1}}{N}\mathrm{e}^{-\mathrm{i}\phi/2} - \mathrm{i}\frac{N_{\mathrm{S}_2}}{N}\mathrm{e}^{\mathrm{i}\phi/2} + \sum_{l=2}^{\infty}\left[x_l F^l \hat{F}^{l-1} + \left(z_{o,l}^{(1)} + z_{o,l}^{(2)}\right)\hat{F}^{l-1}\right] \tag{7.4c}$$

$$\hat{F} = \mathrm{i}\frac{N_{\mathrm{S}_1}}{N}\mathrm{e}^{-\mathrm{i}\phi/2} + \mathrm{i}\frac{N_{\mathrm{S}_2}}{N}\mathrm{e}^{\mathrm{i}\phi/2} + \sum_{l=2}^{\infty}\left[x_l \hat{F}^l F^{l-1} + \left(\hat{z}_{o,l}^{(1)} + \hat{z}_{o,l}^{(2)}\right)F^{l-1}\right] \tag{7.4d}$$

where the first two terms account for empty side trees which consist of one link and one Andreev reflection at S_1 or S_2 and $\hat{z}_{o,l}^{(i)}$ is the same as $z_{o,l}^{(i)}$ but with ϕ replaced by $-\phi$.

Due to the fact that the links of the side trees are traversed by one electron at energy $+\epsilon\hbar/2\tau_{\mathrm{D}}$ and one hole at energy $-\epsilon\hbar/2\tau_{\mathrm{D}}$ in opposite directions an l-encounter consists of l electron-stretches traversing the encounter in the same direction and l hole-stretches traversing the encounter in the opposite direction. Thus we have $x_l = -\left(1+\mathrm{i}l\epsilon+l^2b^2\right)/\left(1+\mathrm{i}\epsilon+b^2\right)^l\tilde{r}^{l-1}$. The powers of $\tilde{r}$ are again included in order to keep track of the order of the trees. If the encounter touches the superconductor S_i the encounter itself and the initial link contribute a factor N_{S_i}/N. However we get additional factors from the Andreev reflections we will evaluate by looking at the side tree before sliding the encounter into the superconductor since the Andreev reflections do not change. The relevant Andreev reflections are those of the odd numbered subtrees which have zero characteristic. Thus if the top node has degree $2l$ the odd numbered side trees provide in total l Andreev reflections involving a conversion $e \to h$. Thus the Andreev reflections at the encounter touching S_i is $-\mathrm{i}\mathrm{e}^{-\mathrm{i}l\phi_i}$ and thus $z_{o,l}^{(1)} = (-\mathrm{i})^l N_{\mathrm{S}_1}\mathrm{e}^{-\mathrm{i}l\phi/2}\tilde{r}^{l-1}/N$ and $z_{o,l}^{(2)} = (-\mathrm{i})^l N_{\mathrm{S}_2}\mathrm{e}^{\mathrm{i}l\phi/2}\tilde{r}^{l-1}/N$.

The total power of a tree with $2n-1$ Andreev reflections is again $\sum_l (l-1)v_l = L - V = n-1$. Thus in order to get the required prefactor of $(1+\mathrm{i}\epsilon+b^2)^{-n}$ we can again do the change of variables

$$F = g(1+\mathrm{i}\epsilon+b^2), \qquad \tilde{r} = \frac{r}{1+\mathrm{i}\epsilon+b^2} \tag{7.5}$$

After doing this change of variables and performing the summations in (7.4c,b) using geometric series we get

$$\begin{aligned}&\frac{\left(1+\mathrm{i}\epsilon+b^2\right)g}{1-rg\hat{g}} + \frac{\left(2b^2+\mathrm{i}\epsilon\right)r\hat{g}g^2}{\left(1-rg\hat{g}\right)^2} + \frac{b^2\left(1+rg\hat{g}\right)r\hat{g}g^2}{\left(1-rg\hat{g}\right)^3}\\ &+\frac{\mathrm{i}x(1+y)}{2(1+x)\left(\mathrm{e}^{\mathrm{i}\phi/2}+\mathrm{i}r\hat{g}\right)} + \frac{\mathrm{i}x(1-y)}{2(1+x)\left(\mathrm{e}^{-\mathrm{i}\phi/2}+\mathrm{i}r\hat{g}\right)} = 0\end{aligned} \tag{7.6}$$

and the same equation with $\hat{g}$ and g exchanged and ϕ replaced by $-\phi$. Here we used $N_{\mathrm{S}}/N_{\mathrm{N}} = x$ and introduced the difference of the numbers of channels of the two superconductors $y = (N_{\mathrm{S}_1} - N_{\mathrm{S}_2})/N_{\mathrm{S}}$ such that $y = 0$ corresponds to the case of equal numbers of channels and $y = \pm 1$ to the case of just one superconductor.

In the case that the two superconductors provide the same number of channels, *i.e.* $y = 0$, those two equations are the same implying $\hat{g} = g$ and (7.6) is equivalent to an algebraic equation of 7th order in g. This increase in the order of the equation with respect to the same case at the density of states is due to the effect that in the case of the density of states we had no normal leads.

The contribution P^e of the side trees starting with an electron is then obtained by giving all trees the same weight by setting $r = 1$ in g. The contribution of the side trees starting with an hole are then given by replacing ϕ by $-\phi$ or setting $r = 1$ in $\hat{g}$. The general equation for the case $N_{\mathrm{S}_1} = N_{\mathrm{S}_2}$ as well as the equation for different numbers of channels with $\epsilon = 0$ and $b = 0$ are given in section Appendix A.

If the Andreev interferometer consists of two superconductors with the same numbers of channels the side tree contributions only depend on $\beta = \cos(\phi/2)$ rather than on ϕ itself. Therefore in this case the side tree contributions are symmetric in ϕ and the contribution of a side tree starting with a hole is the same as that of a side tree starting with an electton. In the most simple case of the absence of a magnetic field, zero temperature (*i.e.* $\epsilon = 0$) and zero phase difference we find $P^e = P^h = P$ and (A.4) reduces to an second order equation:

$$-P^2 + \mathrm{i}P + \mathrm{i}Px - x \tag{7.7}$$

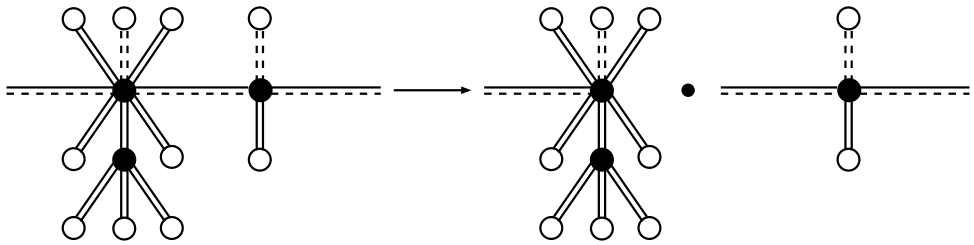

Figure 7.7: A diagram contributing to X_4 is split right after the first 4-encounter and decomposes into two separate diagrams where the second one contributes to T_{ij}^{eh}.

yielding

$$P(0,x) = \frac{\mathrm{i}}{2}\left(1 + x - \sqrt{1+6x+x^2}\right) \tag{7.8}$$

Note that we take the solution satisfying $P(0,0) = 0$ since for the case that there is no superconductor the correction of leading order in the channel number has to be zero.

7.3 Transmission coefficients

We will now demonstrate how to calculate the transmission coefficients using T_{ij}^{ee} as an example, as the evaluation of the other transmission coefficients will be similar.

We first order the sum over all diagrams contributing in leading order in the channel number with respect to the first encounter. Then the first summand of course is the diagram corresponding to the upper left trajectory in figure 7.2. Next there are all diagrams which first encounter is a 2-encounter followed by all diagrams which first encounter is a 3-encounter etc. Note that we also allow for the first encounter to touch the lead. We denote the contribution of the sum over all diagrams having an l-encounter as their first encounter and contributing to T_{ij}^{ee} in leading order in the number of channels by X_l. We may include the diagonal diagram without any encounter by setting $X_1 = N_i N_j/N$. The transmission coefficients are then given by $T_{ij}^{ee} = \sum_{l\geq 1} X_l$. Now we fix X_l with $l \geq 2$ and split all diagrams contributing to X_l right after the first encounter into one part consisting of the first path pair and the first encounter together with its side trees and the remaining part such as indicated in figure 7.8 and figure 7.7. Note that with this the diagonal type path pair leaving the first encounter is completely included in the second part. Since the diagrammatic rules are multiplicative the contribution of a diagram is given by the product of the two parts and hence they all have a common factor which is given by the first diagonal type link, the first encounter and the side trees emerging from it. Therefore we may pull this factor out of the sum implicitly included in X_l. Since this sum runs over all diagrams starting with an l-encounter the remaining second part is again the sum over all possible diagrams contributing to T_{ij}^{ee} if the first encounter is left by an electron and to T_{ij}^{eh} if it is left by a hole as indicated by figure 7.8. However in order to be able to fully identify the sum over the second parts as the transmission we have to reassign the contributed number of channels of the first part to the second part. X_l is then equal to the product of the first part without the factor of N_j contributed by the first path pair hitting lead j all the diagrams have in common and one of the two transmission coefficients T_{ij}^{ee} and T_{ij}^{eh}. Due to these two possibilities to which transmission coefficient the remaining diagrams contributes we split X_l into two parts

$$X_l = A_l^e T_{ij}^{ee} + B_l^e T_{ij}^{eh},$$

where A_l^e is the contribution of the first e-e*pair and the l-encounter the path pair enters together with all side trees and with the entering and exiting quasiparticle being the same. B_l^e is the same but the entering and exiting quasiparticle being different.

So far we left out the possibility that the initial path pair does not enter any encounter but connects directly the incoming and outgoing lead. This possibility however arises only for the transmission coef-

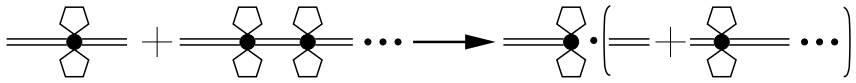

Figure 7.8: When the diagrams are split right after the first l-encounter the remaining diagram again contributes to one of the considered transmissions. The pentagons represent an arbitrary side tree.

ficients $T_{ij}^{\alpha\alpha}$ since the transmission including a conversion from one quasiparticle to its counter particle needs at least one Andreev reflection and therefore one encounter. The transmission coefficients may therefore be written as

$$T_{ij}^{ee} = \frac{N_i N_j}{N} + \sum_{l=2}^{\infty} A_l^e T_{ij}^{ee} + \sum_{l=2}^{\infty} B_l^e T_{ij}^{eh} \tag{7.9a}$$

$$T_{ij}^{eh} = \sum_{l=2}^{\infty} A_l^h T_{ij}^{eh} + \sum_{l=2}^{\infty} B_l^h T_{ij}^{ee}. \tag{7.9b}$$

A_l^h and B_l^h are the same as A_l^e and B_l^e, respectively, but with electrons and holes exchanged. Equation (7.9b) is obtained in the same way as (7.9a) but with the additional condition that there is no diagram without any Andreev reflection contributing to it. The formulae for T_{ij}^{hh} and T_{ij}^{he} are the same but with e and h exchanged.

Due to the multiplicativity A_l^α and B_l^α are products with a factor $1/N$ coming from the first path pair, a factor coming from the encounter which contributed number of channels cancels the factor provided by the first path pair and factors of side tree contributions. The first task is to find out what causes the encounter to be entered by an electron and left by an electron or a hole. The trajectories in figure 7.3 and their corresponding diagrams in figure 7.5 indicate that, as long as the first encounter does not touch the superconductor, an encounter entered by an electron is left by an electron if the number of side trees emerging from this encounter is even (such as in the diagrams ee3II and he3V) and by a hole if it is odd (such as in the diagrams ee3III and he3VII). If the first encounter however touches the superconductor the encounter is always left by a hole if it was entered by an electron. This is also indicated in figure 7.9

We will now show that this indeed holds for all 'diagonal encounters' entered by an diagonal type e-e*pair by starting with considering encounters not touching the superconductor. Since an l-encounter connects $2l$ links to each other, each diagonal l-encounter, where 2 of the links belong to the backbone, provides in total $(2l-2)$ side trees implying that if the number of ζ-side trees is even the number of ζ'-side trees is even, too, and vice versa. Furthermore each side tree provides an odd number of Andreev reflection and therefore a convertion of an electron into a hole or vice versa, since each l-encounter is left by $(2l-1)$ additional path pairs and each path pair increases the number of Andreev reflections by one (this is closely related to the fact that we consider diagrams contributing in leading order in the number of channels). Thus, as long as the first encounter does not touch the superconductor, the entering electron leaves the encounter as an electron if the number of side trees $\tilde{p}$ built by ζ is even and as a hole if the number of side trees built by ζ is odd.

However if the first diagonal l-encounter touches the superconductor the first side tree starts with a hole instead of an electron and is therefore left by an electron. Since the electron leaving the first side tree hits the superconductor the second side tree again starts with a hole. If one proceeds inductively one finds that every side tree starts with a hole and is left by an electron which after that undergoes again an Andreev reflection. Therefore if the first encounter entered by an electron touches the superconductor it is always left by a hole and we can look at it as arising from an l-encounter with an odd number $\tilde{p}$ of ζ-side trees slided into the superconductor as indicated in figure 7.10 and contributes to B_l^e. Therefore an l-encounter may touch the superconductor if the number of ζ-side trees $\tilde{p}$ is odd and the odd numbered ζ-side trees, which are the side trees traversed by ζ after an odd number of traversals of the encounter, as well as the odd numbered ζ'-side trees have zero characteristic, *i.e.* consist of just one link and one Andreev reflection. Moreover the links of the odd numbered side trees have to hit the same superconductor such

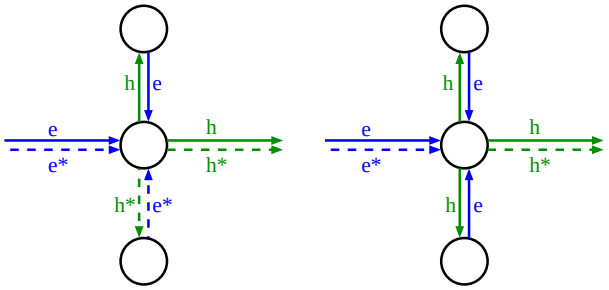

Figure 7.9: Simple examples for encounters touching a superconductor. The electron paths are shown green while the hole paths are shown red. The solid lines belong to ζ while the dashed ones belong to ζ'. If the quasiparticles entering an encounter touching the superconductor following an diagonal-type path pair the diagonal-type path pairs leaving it are traversed by holes and vice versa.

that the channels can coincide. When sliding such an encounter into the superconductor the channels at which the odd numbered side trees hit the superconductor coincide and the links vanish. Therefore beside the diagonal-type path pairs from such a diagonal l-encounter touching the superconductor $p = (\tilde{p}-1)/2$ even numbered ζ-side trees starting with a hole and the $[(2l-2-\tilde{p})-1]/2 = l-2-p$ ζ'-side trees, which also start with a hole emerge.

Thus if we denote the contribution of the first α-α^* pair and of the first l-encounter inside the dot with $\tilde{p}$ ζ-side trees by $z^{\alpha}_{l,\tilde{p}}$ and the contribution of the Andreev reflections provided by the first l-encounter touching the superconductor S_j created by sliding an l-encounter with originally $\tilde{p}$ ζ-side trees into the superconductor S_j by $\tilde{z}^{\alpha}_{l,p,j}$ with $p = (\tilde{p}+1)/2$, we find

$$A^e_l = \sum_{p=0}^{l-1} z^e_{l,2p} \left(P^e\right)^p \left(P^h\right)^p \left[\left(P^e\right)^*\right]^{l-1-p} \left[\left(P^h\right)^*\right]^{l-1-p} \tag{7.10a}$$

$$B^e_l = \sum_{p=0}^{l-2} \left[z^e_{l,2p+1} \left(P^e\right)^{p+1} \left(P^h\right)^p \left[\left(P^e\right)^*\right]^{l-1-p} \left(\left(P^h\right)^*\right)^{l-2-p} + \sum_j \tilde{z}^e_{l,p,j} \left(P^h\right)^p \left[\left(P^h\right)^*\right]^{l-2-p} \right] \tag{7.10b}$$

$$A^h_l = \sum_{p=0}^{l-1} z^h_{l,2p} \left(P^h\right)^p \left(P^e\right)^p \left[\left(P^h\right)^*\right]^{l-1-p} \left[\left(P^e\right)^*\right]^{l-1-p} \tag{7.10c}$$

$$B^h_l = \sum_{p=0}^{l-2} \left[z^h_{l,2p+1} \left(P^h\right)^{p+1} \left(P^e\right)^p \left[\left(P^h\right)^*\right]^{l-1-p} \left(\left(P^e\right)^*\right)^{l-2-p} + \sum_j \tilde{z}^h_{l,p,j} \left(P^e\right)^p \left[\left(P^e\right)^*\right]^{l-2-p} \right], \tag{7.10d}$$

where we have used that $\tilde{p}$ has to be even for A^{α}_l and thus replaced $\tilde{p} = 2p$ and odd for B^{α}_l with $\tilde{p} = 2p+1$. In the case of an electron entering the dot the side trees arising from an encounter touching the superconductor are always entered by a hole since each side tree ends with the opposite quasiparticle than the one it started with. Since the entering electron undergoes an Andreev reflection before entering the first side tree, the first side tree starts with a hole and ends with an electron. This electron again undergoes an Andreev reflection and the second side tree is entered by a hole etc. Thus, inductively, each side tree is entered by a hole and thus contributes P^h rather than P^e. In the case that the dot is entered by a hole we have to exchange ϕ by $-\phi$ in the side tree contributions and thus we have to replace $P^e \leftrightarrow P^h$. Note that as already mentioned above if the two superconductors provide the same numbers of superconducting channels the side tree contribution is an even function of ϕ and thus $P^h = P^e$.

The next and final step is to find the contribution of the encounters. For that we would like to recall the diagrammatic rule for an l-encounter traversed by trajectories with energies $\pm\epsilon$ and in presence of a magnetic field b [82]:

An l-encounter inside the dot contributes a factor $-N\left(1+\eta\epsilon+\mu^2 b^2\right)$.

Here η is the difference between the number of traversals of e-stretches and the number of traversals of e*-stretches and μ is the difference between the number of ζ-stretches traversed in a certain direction and the number of ζ'-stretches traversed in the same direction. Since every electron path of the side tree is retraced by a hole every second stretch connected to a ζ-side tree is an e-stretch and they are all traversed in the same direction we choose arbitrarily as 'positive'. Therefore if the number of ζ-side trees is even the number of e-stretches traversed in positive direction is simply $\tilde{p}/2$. If $\tilde{p}$ is odd we have to account for the fact that the first ζ-side tree starts with an electron and the last also does. Thus there are $(\tilde{p}+1)/2$ e-stretches traversed in positive direction in the encounter. In the same way one finds that the number of e*-stretches are $(2l-2-\tilde{p})/2$ and $[(2l-2-\tilde{p})+1]/2$, respectively. Since the diagonal path pair is traversed by ζ and ζ' in the same direction the directions of the e*-paths are also positive. Since the holes retrace the electron paths their directions in the encounters is negative. Thus if one replaces $\tilde{p}$ by $2p$ for the case that $\tilde{p}$ is even and by $2p+1$ otherwise, one finds that $\eta = \mu = (\tilde{p} - l + 1)$.

What is left now is the derivation of the contribution $\tilde{z}^{\alpha}_{l,p,j}$ which arises by sliding an l-encounter into the superconductor [88] as shown in figure 7.10. As already mentioned this requires that the number of ζ-side trees $\tilde{p}$ emerging from it is odd and the odd numbered ζ-side trees as well as the odd numbered ζ'-side trees consist of only one path pair and one Andreev reflection, *i.e.* they have zero characteristic. Moreover the Andreev reflections of the odd numbered side tress have to be all at the same superconductor. The contribution of the encounter itself and the first path pair is then N_{S_j}/N. However we also included the factors contributed by the Andreev reflections we already stated in section 7.2 in $\tilde{z}^{\alpha}_{l,\tilde{p},j}$, too. Similar as for the side trees these phase factors may be determined by looking to the odd numbered side trees before sliding the encounter into the superconductor since the number of Andreev reflection of the ζ- and ζ'-trajectory can not change when sliding the encounter into the superconductor. Consider the $p+1 = (\tilde{p}+1)/2$ odd numbered side tree which have zero characteristic and hit say S_i. The Andreev reflections provided by these side trees convert an electron into a hole and thus the Andreev reflections provide a factor $-\mathrm{i}\mathrm{e}^{-\mathrm{i}\phi_i}$. Thus in total the Andreev reflections of the odd numbered ζ-side trees provide a factor $(-\mathrm{i})^{p+1}\,\mathrm{e}^{-\mathrm{i}(p+1)\phi_i}$. Analogously the Andreev reflections of the odd numbered ζ'-side trees contribute a factor $\mathrm{i}^{l-p-1}\mathrm{e}^{\mathrm{i}(l-p-1)\phi_i}$. Thus in the case of two superconductors with phases $\phi_1 = -\phi_2 = \phi/2$ the phase factor included in $\tilde{z}^{e}_{l,p,1}$ is given by $(-\mathrm{i})^p\mathrm{i}^{l-p-2}\mathrm{e}^{-\mathrm{i}(2p-l+2)\phi/2}$. For $\tilde{z}^{e}_{l,p,2}$ we have to exchange $\phi \leftrightarrow -\phi$. Moreover $\tilde{z}^{h}_{l,p,j} = \tilde{z}^{e}_{l,p,j}|_{\phi\to-\phi}$. Therefore we have

$$A^e_l = -\sum_{p=0}^{l-1}\left[1+\mathrm{i}\,(2p-l+1)\,\epsilon + (2p-l+1)^2\,b^2\right](P^e)^p\left(P^h\right)^p\left[(P^e)^*\right]^{l-p-1}\left[\left(P^h\right)^*\right]^{l-p-1} \tag{7.11a}$$

$$\begin{aligned} B^e_l = -\sum_{p=0}^{l-2}\Bigg[&\left(1+\mathrm{i}\,(2p-l+2)\,\epsilon + (2p-l+2)^2\,b^2\right)(P^e)^{p+1}\left(P^h\right)^p\left[(P^e)^*\right]^{l-p-1}\left[\left(P^h\right)^*\right]^{l-p-2} \\ &- \frac{x(1+y)\mathrm{e}^{-\mathrm{i}(2p-l+2)\phi/2}\left(-\mathrm{i}P^h\right)^p\left(\mathrm{i}\left(P^h\right)^*\right)^{l-p-2}}{2\,(1+x)} \\ &- \frac{x(1-y)\mathrm{e}^{\mathrm{i}(2p-l+2)\phi/2}\left(-\mathrm{i}P^h\right)^p\left(\mathrm{i}\left(P^h\right)^*\right)^{l-p-2}}{2\,(1+x)}\Bigg]. \end{aligned} \tag{7.11b}$$

where we defined $y = (N_{\mathrm{S}_1} - N_{\mathrm{S}_2})/N_{\mathrm{S}}$. The case $N_{\mathrm{S}_1} = N_{\mathrm{S}_2}$ is then obtained by setting $y = 0$ while the case of just one superconducting lead corresponds to $y = \pm 1$. Since exchanging electrons and holes corresponds to replacing ϕ by $-\phi$ A^h_l and B^h_l are obtained by the same formulae but with ϕ replaced by $-\phi$ including an exchange $P^e \leftrightarrow P^h$. The sums may be performed using geometric series.
Note that if the numbers of channels of the superconducting leads are equal the symmetry of P towards the phase implies that A^{α}_l and B^{α}_l are symmetric in ϕ yielding $A^e_l = A^h_l$ and $B^e_l = B^h_l$ and thus $T^{ee}_{ij} = T^{hh}_{ij}$ and $T^{he}_{ij} = T^{eh}_{ij}$.

Therefore we now have all the necessary utilities to calculate the conductance of Andreev billiards with two superconducting islands. However there is one possibility we have not taken into account, yet. This

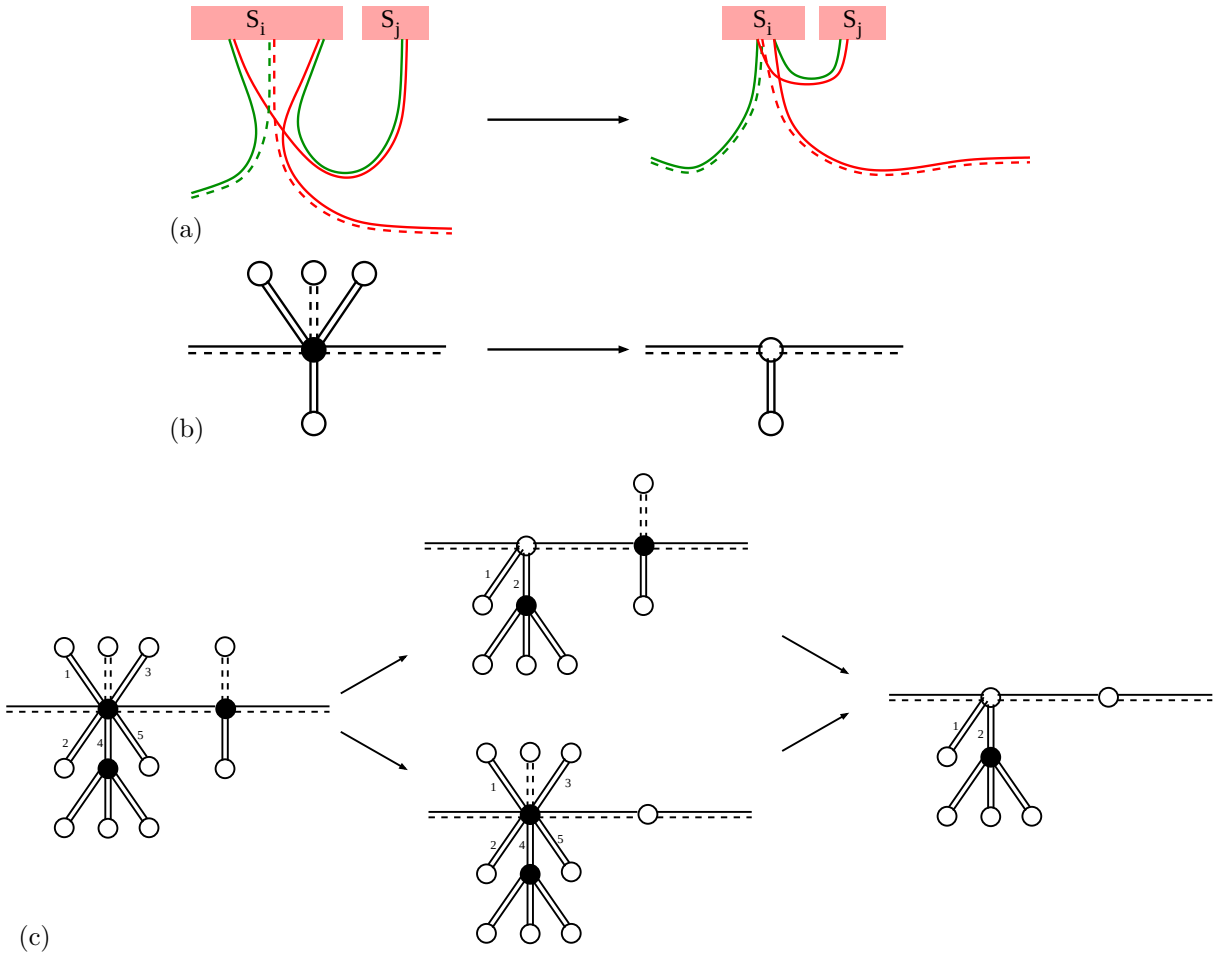

Figure 7.10: (a) An 3-encounter may touch the superconductor S_i if the odd numbered side trees have zero characteristic and hit the same superconductor. The number of Andreev reflections stays the same. (b) Diagrams corresponding to the trajectories in (a). (c) A more complicated diagram with two diagonal encounters that may touch the superconductor. The numbers at the solid side trees give the order of the traversals. Note that additionally the fourth side tree may also touch the superconductor but this does not affect the diagonal encounter but is instead included in the side tree recursion.

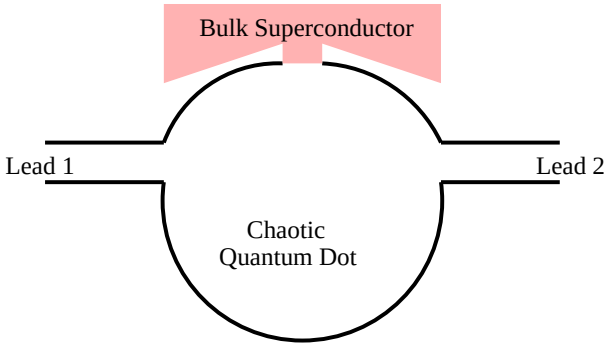

Figure 7.11: Schematic picture of a chaotic quantum dot coupled to one superconducting island.

is the first encounter being an 2-encounter and touching the normal conducting lead i requiring $i = j$. In this case however the encounter simply contributes N_i and the diagrams consist of one side tree and one ζ_2-side tree. The contribution of these diagrams is therefore simply

$$\delta_{ij} N_i |P^e|^2 \qquad \text{if the dot is entered by an electron} \tag{7.12a}$$

$$\delta_{ij} N_i |P^h|^2 \qquad \text{if the dot is entered by a hole.} \tag{7.12b}$$

Thus the transmission coefficients necessary for calculating the conductance may be calculated by evaluating the side tree contribution by essentially solving (7.6) for the side tree contribution, inserting this into (7.9a,b) and solving this for the transmission coefficients.

7.4 Superconducting islands

We may now start evaluating the conductance of Andreev billiards with two normal leads. We first consider a chaotic quantum dot coupled to two normal conducting leads and one or two isolated superconductors with equal number of channels as shown in figure 7.11. The chemical potential of the superconducting lead is then adjusted by the dot such that the net current in the superconductor vanishes. The dimensionless conductance $g = \pi\hbar I/(\mathrm{e}^2 V)$ with I the current, V the voltage drop between the two normal leads, $\hbar$ Planck's constant, in this case is given at zero temperature by [107]

$$g = T_{21}^{ee} + T_{21}^{he} + 2\frac{T_{11}^{he}T_{22}^{he} - T_{21}^{he}T_{12}^{he}}{T_{11}^{he} + T_{22}^{he} + T_{21}^{he} + T_{12}^{he}} \tag{7.13}$$

7.4.1 Low temperature

One superconductor

Using this result in the simplest case without phase difference the random matrix result for the conductance correction $\delta g = g - g_{cl}$ [50] could be reproduced:

$$\delta g = \frac{N_1 N_2}{N_\mathrm{N}} \left[x + \frac{1}{2}(1+x)^2 - \frac{1}{2}(1+x)\sqrt{1+6x+x^2} \right] \tag{7.14}$$

The conductance correction is shown in figure 7.12 as a function of $x = N_\mathrm{S}/N_\mathrm{N}$. From (7.14) it can be easily seen that the conductance in this case is symmetric in exchanging N_1 and N_2, as one would expect due to the symmetry of the setup. Moreover in this case the superconductor always increases the conductance. In the limit of large numbers of superconducting channels we find that the conductance is doubled compared to the classical limit $x = 0$ and hence approaches the conductance of a N-S interface [28].

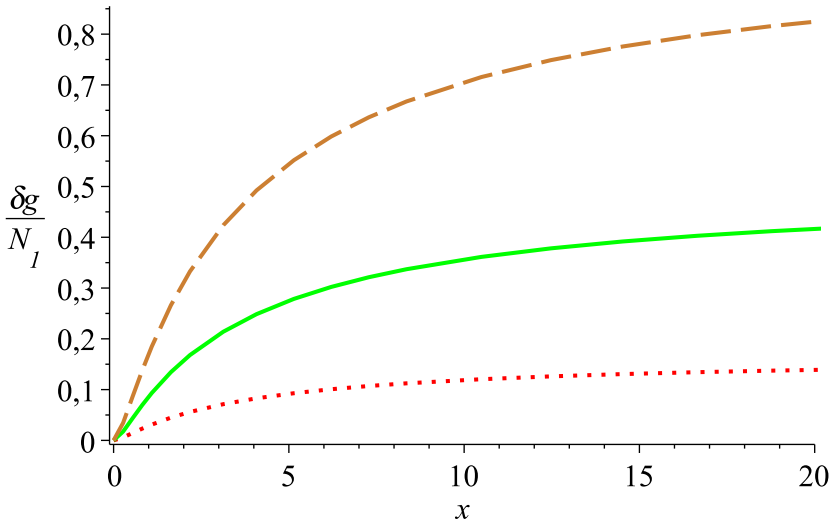

Figure 7.12: Conductance correction as a function of the number of channels of the isolated superconductor $x = N_S/N_N$ for $N_2/N_1 = 0.2$ (dotted line), $N_2/N_1 = 1$ (solid line) and $N_2/N_1 = 100$ (dashed line)

Two superconductors with phase difference

In Ref. [50] for a finite phase difference the authors could calculate the transmission only numerically but for all N. Moreover they restricted themselves to the case $N_{S_1} = N_{S_2}$. With our semiclassical approach however we are able to calculate it at zero temperature analytically for all cases. Using this we could reproduce the large-N limit in Ref. [50] shown in figures 7.13a,b for the case $N_{S_1} = N_{S_2}$. Moreover figures 7.13c,d show the dependence of the conductance on the difference of the numbers of channels in the superconductors. The conductance correction vanishes for $\phi \to \pi$ since the phase accumulated at each Andreev reflection causes destructive interference. In this case the conductance is up to π a monotonic function of the phase difference ϕ.

The symmetry found in figures 7.13a,b and 7.14a,b results from the fact that electrons and holes contribute symmetrically to the conductance as indicated by (2.31). The 2π-periodicity may also be found using (7.11a,b): If we increase ϕ by 2π the side tree contribution changes its sign. Thus this does not affect A_l^α and the first part of B_l^α. If l is odd in the last two terms in B_l^α changing the sign of the side tree contribution results in a change of the sign of these two parts. However increasing the phase by 2ϕ also yields an exchange of the sign of the phase factors cancelling the change of sign of the side tree contributions. If l is even we again have an even number of side tree contributions and the phase factors also contribute a different sign.

The crossover from two superconductors to just one superconductor is smooth as shown in figures 7.14a,b. We found that the bigger the difference in the numbers of channels the faster the amplitude changes.

Magnetic field

Whitney and Jacquod found in Ref. [49] that for small x the conductance of an Andreev quantum dot with an isolated superconductor decays at $T = 0$ with increasing magnetic field as $(1+b^2)^{-2}$. For higher orders in x the $(1+b^2)^{-2}$-decay mixes up with terms decaying as $1/(1+b^2)^{-n}$ with $n \geq 2$. This leads to the behaviour shown in figure 7.15. It can be seen that the conductance correction decays very fast.

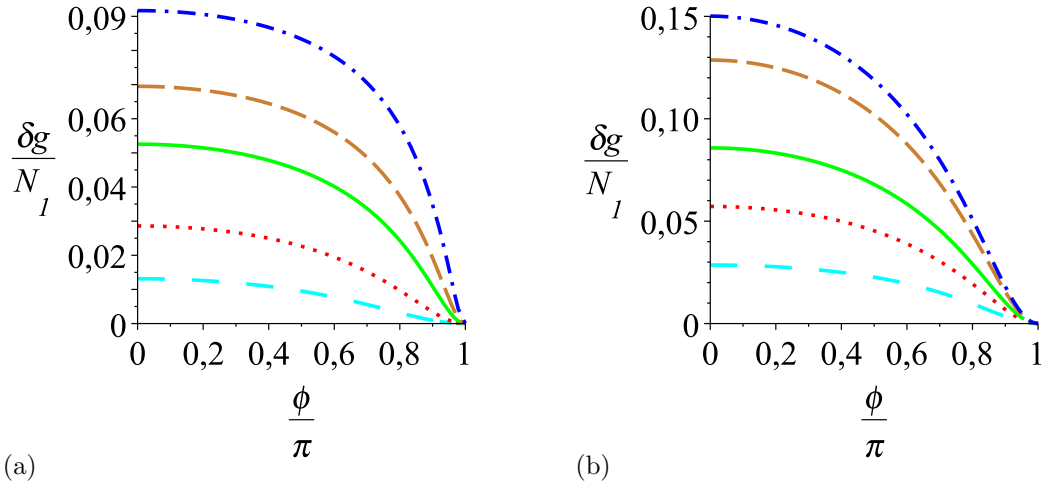

Figure 7.13: The conductance correction as a function of the phase difference. (a) $N_{S_1} = N_{S_2}$, $N_2/N_1 = 0.2$ and $x = 0.5$ (space dashed line), $x = 1$ (dotted line), $x = 2$ (solid line), $x = 3$ (dashed line), $x = 5$ (dashed dotted line). (b) $N_{S_1} = N_{S_2}$, $x = 1$ and $N_2/N_1 = 0.2$ (space dashed line), $N_2/N_1 = 0.5$ (dotted line), $N_2/N_1 = 1$ (solid line), $N_2/N_1 = 3$ (dashed line) and $N_2/N_1 = 7$ (dashed dotted line).

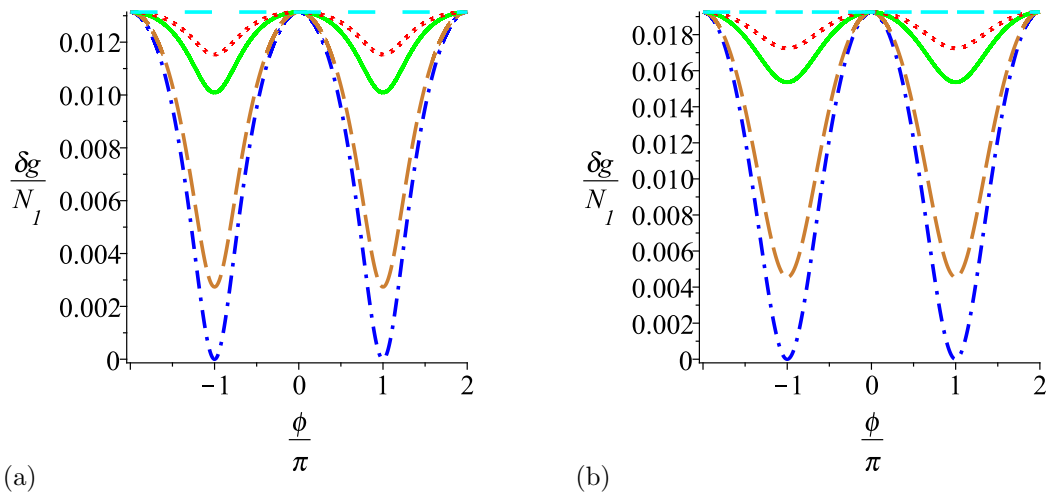

Figure 7.14: Dependence on the difference of the numbers of superconducting channels. (c) $N_2/N_1 = 0.2$, $x = 0.5$ and $y = 1$ (space dashed line), $y = 0.95$ (dotted line), $y = 0.9$ (solid line), $y = 0.5$ (dashed line) and $y = 0$ (dashed dotted line) and (d) $N_2/N_1 = 7$, $x = 0.2$ and $y = 1$ (space dashed line), $y = 0.95$ (dotted line), $y = 0.9$ (solid line), $y = 0.5$ (dashed line) and $y = 0$ (dashed dotted line).

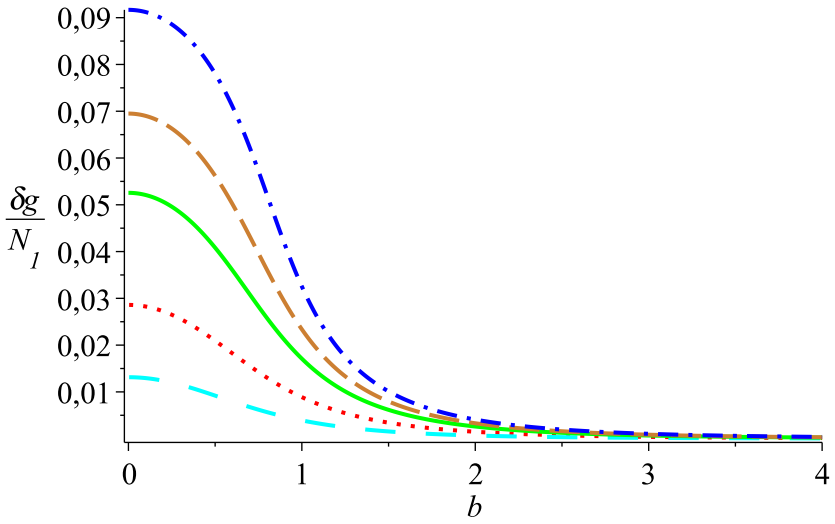

Figure 7.15: The conductance correction for the setup with one superconducting island as a function of the magnetic field dependence for $N_2/N_1 = 0.2$ and $x = 0.5$ (space dotted line), $x = 1$ (dotted line), $x = 2$ (solid line), $x = 3$ (dashed line) and $x = 5$ (dashed dotted line)

7.4.2 Temperature dependence

If we want to allow non-zero temperature each transmission and reflection coefficient in (7.13) has to be multiplied by the negative derivative of the Fermi function and integrated over energy. With evaluating these integrals numerically using gaussian quadrature with a total accuracy 10^{-10} and a truncation of the integral at $\epsilon = 100\theta$ with $\theta = k_{\mathrm{B}}T/E_{\mathrm{T}}$ the temperature measured in units of the temperature corresponding to the Thouless energy we find that the superconducting island obeys a monotonic temperature dependence: The conductance correction has its maximum at $T = 0$. For higher temperature it is damped due to the mixing with higher energies for which the side tree contributions become smaller because of the loss of coherence of the electrons and holes. As the temperature tends to infinity the conductance correction vanishes slowly. In figure 7.16 we plotted the conductance correction of the setup with one superconducting island versus the temperature $\theta = k_{\mathrm{B}}T/E_{\mathrm{T}}$.

7.5 Superconducting leads

Next we consider superconductors with externally controlled chemical potential. In particular we will consider superconductors lying on the same chemical potential as one of the two normal conducting leads, say lead 2. Such a setup is schematically shown for the case of one superconducting lead in figure 7.17. The current in lead i may than be calculated by the Landauer-type expression [108, 61]

$$I_i = \frac{e}{\hbar}\sum_{j=1}^{2}\int_0^\infty \mathrm{d}\epsilon \left[2N_i\delta_{ij} - T_{ij}^{ee} + T_{ij}^{he} - T_{ij}^{hh} + T_{ij}^{eh}\right]\left(-\frac{\partial f}{\partial \epsilon}\right)(\mu_j - \mu_S) \tag{7.15}$$

where $f = [\exp(-\epsilon/\theta) + 1]$ is the Fermi function with the temperature again measured in units of the Thouless energy E_{T}, μ_j and μ_S are the chemical potentials in the normal conducting lead j and in the superconductor respectively.

Of course we could use the transmission coefficients themselves calculated in section 7.3. However we would like to present a slightly different way to calculate the conductance here which in the case of the superconducting leads simplifies the calculation a little bit. For simplicity we will present this way only

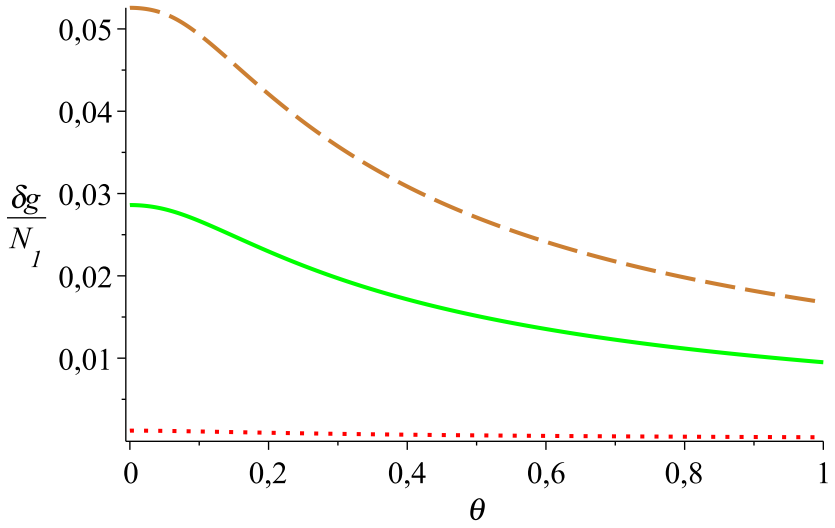

Figure 7.16: Temperature dependence of the conductance correction for the setup with an superconducting island for $N_2/N_1 = 0.2$ and $x = 0.1$ (dotted line), $x = 1$ (solid line) and $x = 2$ (dashed line).

for the case that the numbers of channels of the superconducting leads are equal since the modifications one would have to do in order to include different numbers of channels are the same as in section 7.3. According to (7.15) we have to calculate the difference between the Andreev and normal transmission, namely $\tilde{T}^e_{ij} = T^{he}_{ij} - T^{ee}_{ij}$ and $\tilde{T}^h_{ij} = T^{eh}_{ij} - T^{hh}_{ij}$. To do this (we again consider only the case of an incident electron) we essentially do the same steps as before and split the diagrams at their first l-encounter. In the same way as above we find that the sum over the remaining diagrams again contribute to $\tilde{T}^e_{ij}$ or $-\tilde{T}^h_{ij}$ depending on whether the quasiparticle leaving the encounter is an electron or a hole. The additional signs arise as follows: Consider for example a diagram contributing to T^{ee}_{ij} thus contributing to $\tilde{T}^e_{ij}$ with a minus sign. Then if the number of ζ-side trees arising from the first encounter is even the remaining diagrams contribute to T^{ee}_{ij}, too, and therefore it again contributes with a negative sign to $\tilde{T}^e_{ij}$. However if the number of ζ-side trees is odd the remaining diagrams contribute to T^{eh}_{ij} but with the additional minus sign of the original diagram. Hence it contributes to $-\tilde{T}^h_{ij}$.

Taking into account the diagram connecting lead i and lead j directly, which has no Andreev reflection this diagram contributes to T^{ee}_{ij} and therefore with a minus sign. According to the diagrammatic rules this contribution is simply given by $-N_iN_j/[N_\mathrm{N}(1+x)]$. The transmission differences $\tilde{T}^{e,h}_{ij}$ therefore read

$$\tilde{T}^e_{ij} = -\frac{N_iN_j}{N_\mathrm{N}(1+x)} + \sum_{l=2}^{\infty} A^e_l \tilde{T}^e_{ij} - \sum_{l=2}^{\infty} B^e_l \tilde{T}^h_{ij} \tag{7.16}$$

with A^e_l and B^e_l given by (7.11a) and (7.11b), respectively, and the same equation holds for $\tilde{T}^h_{ij}$ with an exchange of e and h yielding a replacement of ϕ by $-\phi$ in the coefficients A and B including an exchange $P^e \leftrightarrow P^h$. If the numbers of channels of the superconductors are the same this also implies a symmetry in the exchange of electrons and holes and $\tilde{T}^e_{ij} = \tilde{T}^h_{ij}$.

Thus we are readily prepared for calculating the conductance of the Andreev billiard with two superconducting leads. Since we consider the chemical potential of the superconductors being the same as that of the second lead the contribution to the conductance is given by the transmission coefficient for reflecting an electron entering the cavity from lead 1 back into lead 1 again. The conductance g, defined

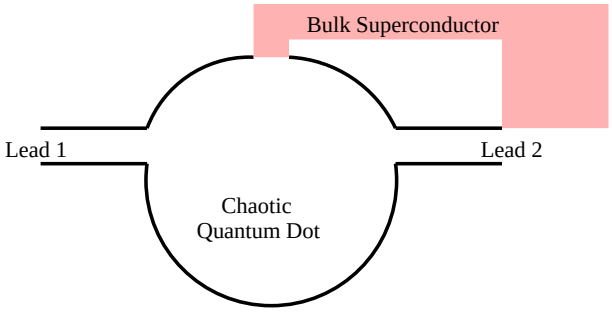

Figure 7.17: Schematic setup for the case of a superconducting lead with the same chemical potential as the right lead.

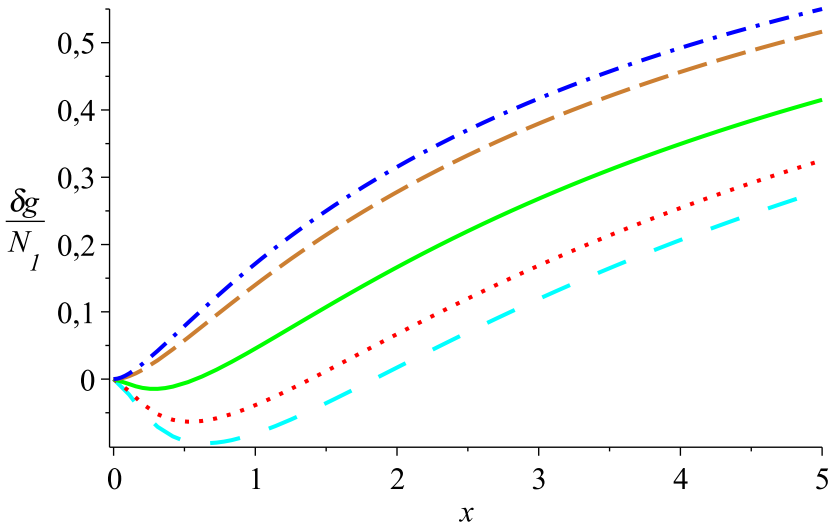

Figure 7.18: The quantum correction to the conductance of an Andreev billiard with one superconducting and two normal conducting leads at low temperature and in absence of an magnetic field as a function of the number of channels of the superconductor for $N_2/N_1 \to 0$ (space dashed line), $N_2/N_1 = 0.2$ (dotted line), $N_2/N_1 = 1$ (solid line), $N_2/N_1 = 7.2$ (dashed line) and $N_2/N_1 \to \infty$ (dashed dotted line).

by $I_1 = eg\left(\mu_1 - \mu_S\right)/\pi\hbar$, therefore reads

$$g = -2\int_0^\infty \mathrm{d}\epsilon \left(N_1 - \frac{N_1^2}{N\left(1 - A + B\right)} + N_1\left|P\right|^2\right)\frac{\partial f}{\partial \epsilon}. \tag{7.17}$$

Note that this setup induces an asymmetry due to the channel numbers: Since the chemical potential of the superconductor is the same as that of lead 2 one can not exchange the two channels and therefore the solution will (in general) not be symmetric in the exchange of N_1 and N_2.

7.5.1 Low temperatures

One superconductor

Let us consider first the simplest case of no phase difference and the absence of magnetic fields. Moreover we consider sufficiently low temperatures to approximate $-\partial f/\partial\epsilon \approx \delta(\epsilon)$. The contributions of the side

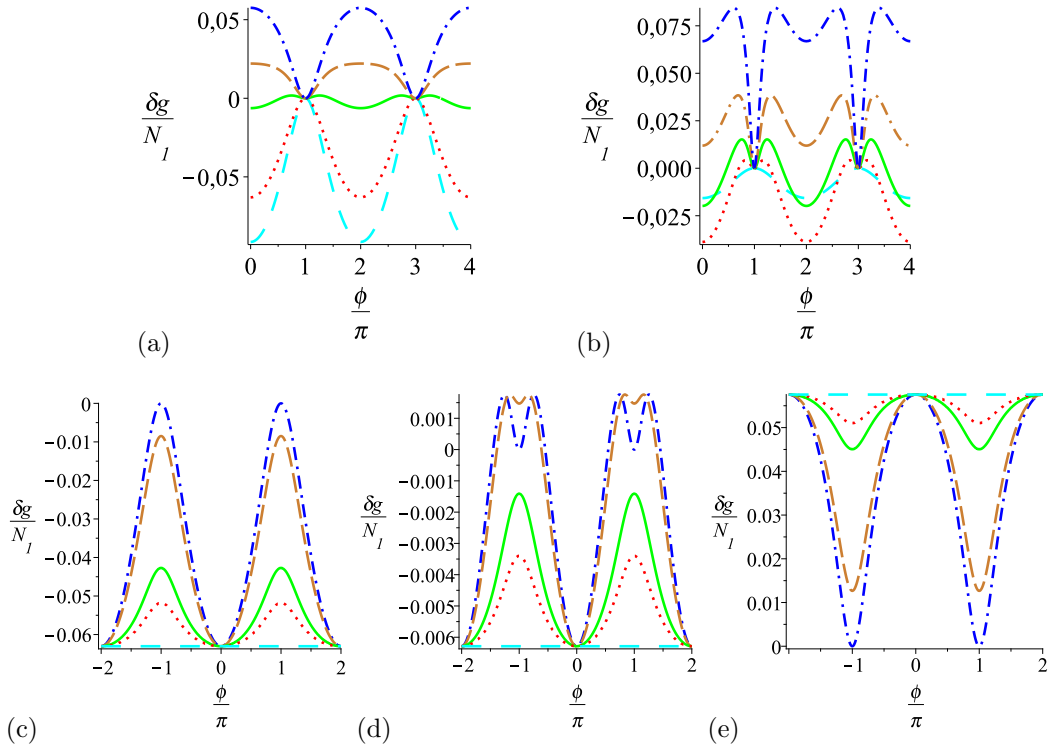

Figure 7.19: Phase dependence of the conductance correction. (a) $x = 0.5$ and $N_2/N_1 \to 0$ (space dashed line), $N_2/N_1 = 0.2$(dotted line), $N_2/N_1 = 1$ (solid line), $N_2/N_1 = 2$ (dashed line) and $N_2/N_1 = 7$ (dashed dotted line). (b) $N_2/N_1 = 0.2$ and $x = 0.1$ (space dashed line), $x = 1$ (dotted line), $x = 1.2$ (solid line), $x = 1.5$ (dashed line) and $x = 2$ (dashed dotted line). (c) $N_2/N_1 = 0.2$, $x = 0.5$ and $y = 1$ (space dashed line), $y = 0.95$ (dotted line), $y = 0.9$ (solid line), $y = 0.5$ (dashed line) and $y = 0$ (dashed dotted line). (d) $N_2/N_1 = 1.0$, $x = 0.5$ and $y = 1$ (space dashed line), $y = 0.95$ (dotted line), $y = 0.9$ (solid line), $y = 0.5$ (dashed line) and $y = 0$ (dashed dotted line). (e) $N_2/N_1 = 7$, $x = 0.5$ and $y = 1$ (space dashed line), $y = 0.95$ (dotted line), $y = 0.9$ (solid line), $y = 0.5$ (dashed line) and $y = 0$ (dashed dotted line).

trees are therefore given by (7.8).

We can easily compare our result for the conductance correction $\delta g = g - g_{cl}$ to those found for small superconductors in Ref. [49] by expanding our result in a Taylor series in $x = N_S/N_N$. The first non-vanishing term in the Taylor expansion is exactly the contribution found by Jacquod and Whitney:

$$\delta g^{(2)} = \frac{N_1 \left(N_2 - 4N_1\right) N_S^2}{N_N^3} \tag{7.18}$$

Therefore for small superconducting leads the correction becomes negative if lead 1 carries a sufficiently large amount of modes compared to lead 2. However if the number of superconducting channels increases the superconductor enhances the conductance again as shown in figure 7.18. Moreover we again found a doubling of the conductance for $N_S/N_N \to \infty$, *i.e.* $g = 2N_1$, independently of the ration N_1/N_2 in alignment with previous results for quantum dots with only one normal conducting lead[109].

Two superconductors with a phase difference

The effect of a phase difference between two superconducting leads depends sensitively on the ratios x and N_2/N_1. The result is pretty similar to the phase dependence of the conductance of an normal conducting region with one normal conducting lead and two superconducting leads with a phase difference ϕ found by

different approaches [110, 111]. While for most combinations the effect of the superconductor decreases with increasing phase difference due to the destructive interference in some cases the conductance becomes a nonmonotonic function of the phase difference as shown in figures 7.19a,b. In some cases the phase difference may even cause a change of the sign of the conductance correction. In figures 7.19a,b this can be seen for the case $N_2 = N_1$ and $x = 0.5$ as well as for the cases $N_2 = 0.2N_1$ and $x = 1$ and $x = 1.2$.

However if the number of channels of the superconducting leads are equal all possible combinations of x and N_2/N_1 have in common that the conductance correction becomes zero for a phase difference $\phi = \pi$ and that the conductance is symmetric and periodic in ϕ with period 2π. This can also be seen from (7.11a,b) and (7.6): The symmetry follows from the symmetry of B_l and P as well as the fact that A_l does not depend on ϕ explicitly. If ϕ is replaced by $\phi + 2\pi$ the side tree contribution changes its sign. A_l and the first part of B_l are symmetric in P and therefore give the same contribution as before. However the last two parts of B_l are antisymmetric in P but when increasing the phase difference by 2π the phase factors contribute an additional minus sign such that the total contribution stays the same.

This symmetry towards ϕ still holds if the two superconducting leads provide different numbers of channels. We show the crossover from a setup with two superconducting leads having the same number of channels to the setup with just one superconducting lead for different cases in figure 7.19c-e. As in (7.11b) $y = (N_{S_1} - N_{S_2})/N_S$ is the difference between the numbers of channels in the superconducting leads such that $y = 0$ corresponds to the symmetric case $N_{S_1} = N_{S_2}$ and $y = \pm 1$ to the case of just one superconducting lead. We found that in the cases where the conductance correction had a dip at $\phi = \pm\pi$ first of all this dip vanishes and after that the conductance correction tends to the $\phi = 0$ result for all ϕ if y is increased. If there were no dip the result would converge monotonically to the result for the case with just one superconducting lead.

Weak magnetic field

If a magnetic field is applied time reversal symmetry is broken. Therefore building side trees becomes less likely and their contribution vanishes as $b \to \infty$ as can be seen in figure 7.20. In particular for small superconducting channel numbers Whitney and Jacquod [49] predicted that the conductance correction decreases at zero temperature with $1/(1 + b^2)^2$. However we found a nonmonotonic behaviour for the dependence of the conductance correction on the magnetic field similar to that found for the case of one normal conducting lead [112] and for the magnetic field dependence of the excess current [109]. It may even happen that the conductance correction is negative for $b \neq 0$ although it is positive at $b = 0$. Since the diagrammatic rules depend on b^2 rather than b the conductance is a symmetric function of b and therefore satisfies the Onsager relation [113, 114] for a two terminal setup $g(b) = g(-b)$.

7.5.2 Temperature dependence

If we want to include the effect of finite temperature we have to include the energy dependence of the side tree contribution and the central encounters. For zero phase the sixth order equation for the side tree contribution factorizes and one has to solve a quartic equation. In leading order in N_S/N_N the temperature dependence is given by the generalised zeta function. However as can be seen from figure 7.21 see when including higher order terms strong derivations from this behaviour may occur again.

The integral in (7.15) of course can not be performed analytically. Therefore we calculated the integral numerically using gaussian quadrature with a total accuracy of 10^{-10}. The integral has been truncated at $\epsilon = 100\theta$ where $\theta = k_B T/E_T$ is again the temperature measured in units of the Thouless energy. In figure 7.21 we plotted the conductance correction versus the temperature.

As one might expect from the Sommerfeld expansion the conductance correction has a local extremum at $\theta = 0$ but not necessarily a global one as can be seen from the solid and the dash dotted curves in figure 7.21a. For a certain range of combinations of the ratios x and N_2/N_1 the conductance correction increases with increasing temperature although it is positive for $T = 0$. A similar effect known as the reentrance of the metallic conductance has previously found in NS-structures [115, 116]. Moreover it may

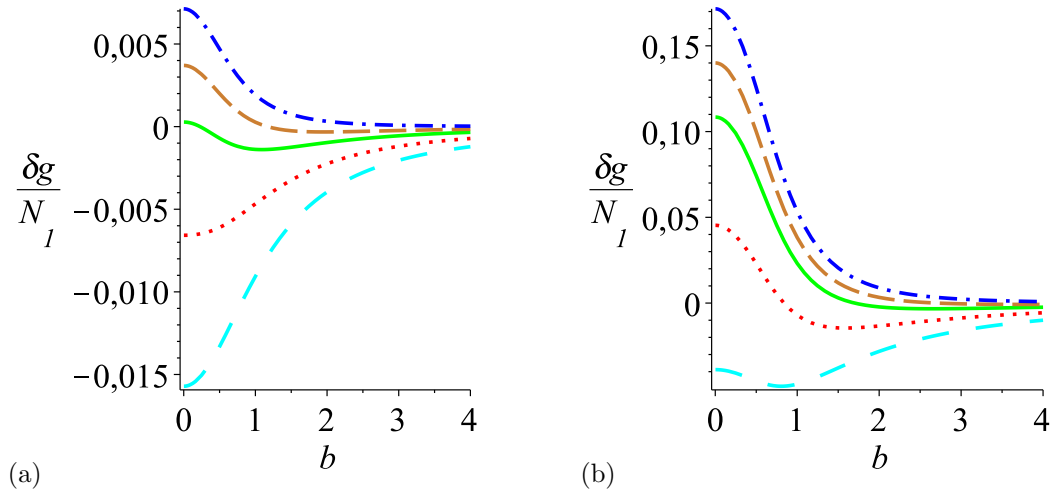

Figure 7.20: Magnetic field dependence of the conductance correction for (a) $x = 0.1$ and (b) $x = 1$ with $N_2/N_1 = 0.2$ (space dashed line), $N_2/N_1 = 1$ (dotted line, $N_2/N_1 = 3$ (solid line), $N_2/N_1 = 7$ (dashed line) and $N_2/N_1 \to \infty$ (dashed dotted line)

happen that the conductance correction changes its sign when the temperature is increased such as in the case $N_2/N_1 = 0.2$ and $x = 1.4$ shown by the solid line in figure 7.21a.

When including a phase difference again this affects the temperature dependence. It may again cause a nonmonotonic temperature dependence even if it is monotonic at $\phi = 0$. Moreover in contrast to the case $\phi = 0$ where the sign of the conductance correction with increasing temperature may only change from positive to negative it can be the other way around for $\phi \neq 0$. The temperature dependence of the conductance correction for different phases is shown in figure 7.21b,c.

In all cases for large temperatures the conductance correction tends to zero. However this limit is approached only very slowly.

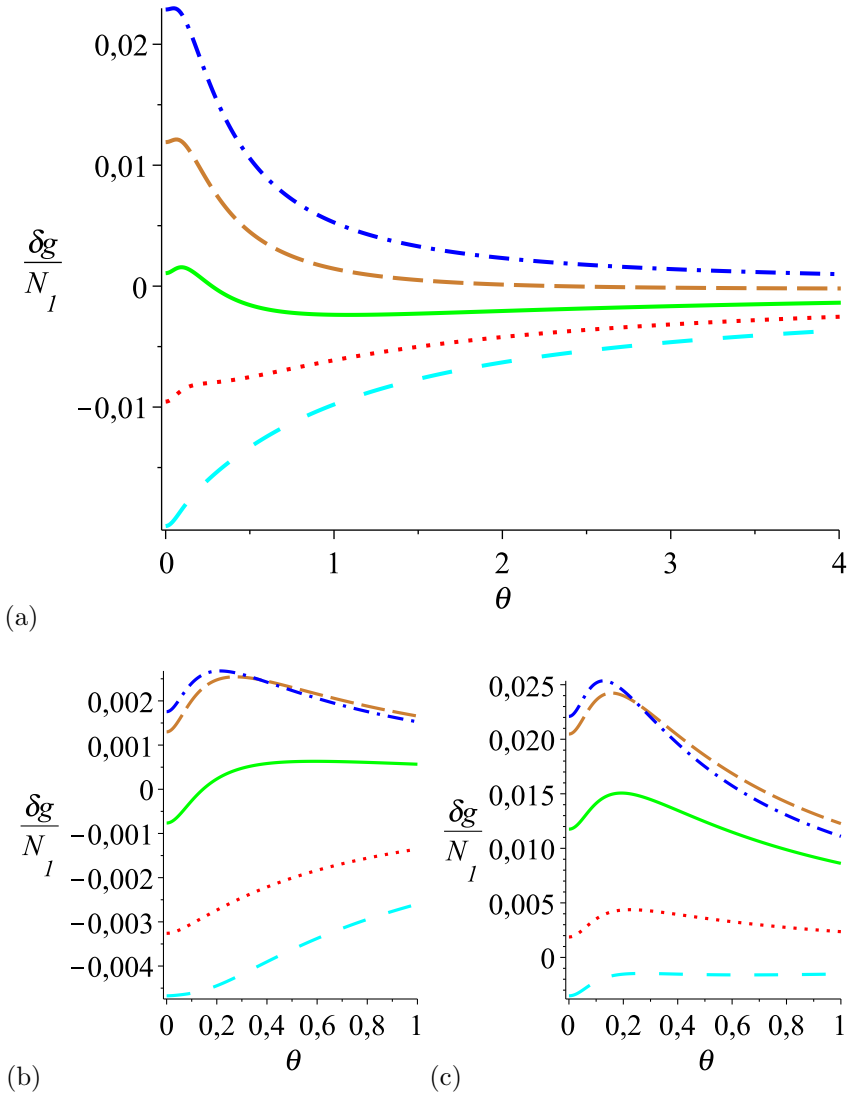

Figure 7.21: The conductance correction as a function of the temperature $\theta = k_B T/E_T$. (a)$N_2/N_1 = 0.2$, $\phi = 0$ and $x = 1.2$ (space dashed line), $x = 1.3$ (dotted line), $x = 1.4$ (solid line), $x = 1.5$ (dashed line) and $x = 1.6$ (dashed dotted line). (b) $N_2/N_1 = 1$, $x = 0.5$ and $\phi = \pi/4$ (space dashed line), $\phi = 7\pi/20$ (dotted line), $\phi = \pi/2$ (solid line), $\phi = 13\pi/20$ (dashed line) and $\phi = 3\pi/4$ (dashed dotted line). (c)$N_2/N_1 = 0.2$, $x = 1.3$ and $\phi = \pi/4$ (space dashed line), $\phi = 7\pi/20$ (dotted line), $\phi = \pi/2$ (solid line), $\phi = 13\pi/20$ (dashed line) and $\phi = 3\pi/4$ (dashed dotted line).

8 Thermopower

If the normal leads additionally have different temperatures there is also a coupling between the electrical current and the temperature difference. An estimate of the thermo-electric coupling is for example provided by the thermopower defined in (2.42). The calculation of the thermopower is closely related to the electrical transport since due to (2.43) we have to evaluate the same transmission coefficients. We will consider the three cases shown in figure 8.1 which Whitney and Jacquod called the symmetric (figure 8.1a) and asymmetric house (figure 8.1b) and the parallelogram (figure 8.4). We will restrict ourselves to Andreev billiards with two normal leads and two isolated superconducting leads with a phase difference ϕ. The results presented here are for the numbers of channels of the two normal leads being equal, since these numbers only enter by a prefactor $N_1N_2/(N_1+N_2)$. It is further assumed that there is no magnetic field applied. Note that we consider the superconductors to be isolated thus adjusting their chemical potential such that the net current through the superconducting leads is zero.

8.1 Symmetric house and asymmetric house

8.1.1 Symmetrtic house

We start with the setup Jacquod and Whitney called the symmetric house [51] shown in figure 8.1a. They treated the transmission coefficients perturbatively in the ratio $x = N_S/N_N$ up to second order. Within this approximation they argued that for the symmetric house with equal numbers of superconducting channels the thermopower vanishes in second order in x since B, defined in (2.37), is antisymmetric in exchanging electrons and holes which yields an exchange $\epsilon \to -\epsilon$ and in leading order in N is equivalent to reversing the superconducting phase $\phi \to -\phi$. Since additionally the electrical conductance G is symmetric as already seen in section 7.4.1 the thermopower $S = -B/G$ is antisymmetric in the phase difference. On the other hand the result has to be symmetric under exchanging the superconducting leads which is again equivalent to reversing the sign of ϕ. Thus the thermopower has to be zero. With our approach we find that this argument holds to all orders and may also be seen from the discussion in section 7.3: There we stated that as long as the superconducting leads both provide the same number of channels the transmission probability is symmetric in exchanging electrons and holes which when inserted in (2.37) gives $B = 0$.

However if the numbers of channels $N_{S_1} \neq N_{S_2}$ the symmetry towards exchanging the two superconductors is broken and the thermopower does not vanish. By using the transmission coefficients found in section 7.3, inserting in (2.41a) as already done in section 7.4 and (2.41b) and performing the integrals nu-

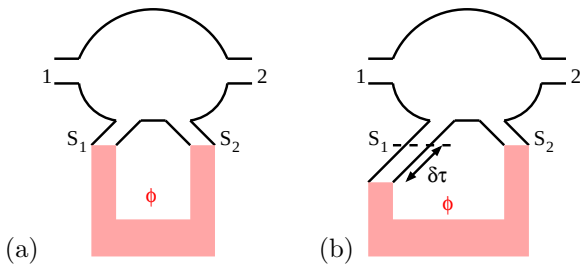

Figure 8.1: (a) The so-called symmetric house. (b) The asymmetric house where at lead 1 a neck is additionally inserted compared to (a)

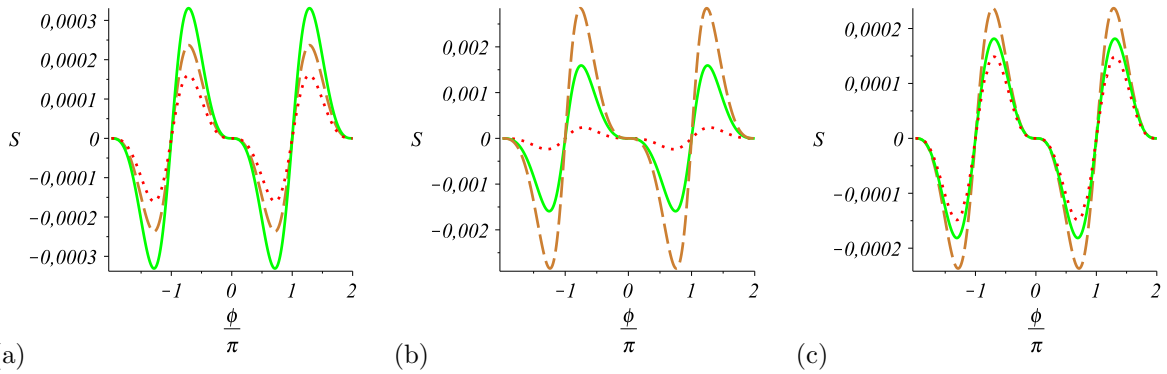

Figure 8.2: The thermopower of the symmetric house with different numbers of superconducting channels: (a) Dependence of the thermopower on the difference between the numbers of superconducting channels with $x = 0.2$, $\theta = 0.2$ and $y = 0.3$ (dashed line), $y = 0.5$ (solid line) and $y = 0.9$ (dotted line). (b) Dependence on x with $y = 0.3$, $\theta = 0.2$ and $x = 0.2$ (dotted line), $x = 0.5$ (solid line) and $x = 0.7$ (dashed line). (c) Dependence on the temperature with $x = 0.2$, $y = 0.3$ and $\theta = 0.2$ (dashed line), $\theta = 1.5$ (solid line) and $\theta = 2$ (dotted line).

merically with a total accuracy of 10^{-6} we find the results shown in figure 8.2. The thermopower is found to be antisymmetric and 2π-periodic in the phase difference ϕ. When the difference $y = (N_{S_1} - N_{S_2})/N_S$ is increased starting at zero a non-zero thermopower appears which increases up to about $y = 0.5$. If the difference is increased further the resulting thermopower decreases agian and vanishes at $y = 1$ which corresponds to the case of just one superconductor. Increasing the total number of superconducting channels $x = N_S/N_N$ results in an increase of the thermopower while an increase in the temperature $\theta = k_B T/E_T$ causes a decrease of S.

8.1.2 Asymmetric house

Moreover for $N_{S_1} = N_{S_2}$ we can also generate a non-zero thermopower by inserting a neck at one of the two superconducting leads, say at S_1 as in figure 8.1b, in which the trajectories spend an additional time $\delta\tau \cdot \tau_D$: By adding the time $\delta\tau$ to the exposure time in section 4 for each path pair hitting S_1 we find that if an e-h pair hits the superconductor S_1 apart from the phase provided by the Andreev reflection itself it picks up an additional phase $\epsilon\delta\tau$. Thus the total phase provided by the neck plus the Andreev reflection at S_1 is $(-\phi + 2\epsilon\delta\tau)/2$ if an electron is converted into a hole and $(\phi + 2\epsilon\delta\tau)/2$ if a hole is converted into an electron. Thus the electron hole symmetry is broken leading to an asymmetry in the phase difference as well as in the energy such that the symmetry argument above does not apply any more. Therefore $T_{ij}^{\alpha\beta} \neq T_{ij}^{\bar{\alpha}\bar{\beta}}$ with $\bar{\alpha}$ ($\bar{\beta}$) labelling a hole if α (β) labels an electron and vice versa. Note that we treat the neck as an ideal lead such that every quasiparticle entering the neck hits the superconductor before leaving the neck again [117]. When redoing the steps of section 7.4 and 7.2 for the calculation of the transmission coefficients again one finally finds the following changes: The variable $\beta = \cos(\phi/2)$ has to replaced by $\beta^e = \cos[(\phi - \epsilon\delta\tau)/2]$ for a side tree starting with an electron and by $\beta^h = \cos[(\phi + \epsilon\delta\tau)/2]$ for a side tree starting with a hole. Furthermore the side trees starting with an electron now have an additional factor of $e^{-i\epsilon\delta\tau/2}$ and those starting with a hole an additional factor of $e^{i\epsilon\delta\tau/2}$ compared to the case without the neck. However since in A_l^α and B_l^α each factor P^α is paired either with a factor $P^{\bar{\alpha}}$ or with a factor $(P^\alpha)^*$ this additional factor cancels. Additionally if the incident quasiparticle is an electron the phase ϕ in the second term of (7.10b) also has to replaced by $\phi - 2\epsilon\delta\tau$. Again for an incident hole the phase ϕ has to be replaced by $-\phi$.

All in all we will have to solve a 4×4 system of linear equations rather than a 2×2 system of linear equations as it was for the conductance of the symmetric version. Using $N_1 = N_2 = N_N/2$ the 4 equations

we will have to solve are

$$T_{ij}^{ee} = \frac{N_{\mathrm{N}}^2}{4N} + \sum_l^\infty A_l T_{ij}^{ee} + \sum_l^\infty B_l^e T_{ij}^{eh} \tag{8.1a}$$

$$T_{ij}^{he} = \sum_l^\infty A_l T_{ij}^{he} + \sum_l^\infty B_l^e T_{ij}^{hh} \tag{8.1b}$$

$$T_{ij}^{hh} = \frac{N_{\mathrm{N}}^2}{4N} + \sum_l^\infty A_l T_{ij}^{hh} + \sum_l^\infty B_l^h T_{ij}^{he} \tag{8.1c}$$

$$T_{ij}^{eh} = \sum_l^\infty A_l T_{ij}^{eh} + \sum_l^\infty B_l^h T_{ij}^{ee} \tag{8.1d}$$

with A_l being the same as in (7.10a) but with P^e and P^h redefined to depend on β^e and β^h, respectively, and $b = 0$. Analogously one finds

$$\begin{aligned} B_l^e = -\sum_{p=0}^{l-2} \Bigg[& \left(1 + \mathrm{i}\,(2p - l + 2)\,\epsilon\right) \left(P^e\right)^{p+1} \left(P^h\right)^p \left[\left(P^e\right)^*\right]^{l-p-1} \left[\left(P^h\right)^*\right]^{l-p-2} \\ & - \frac{x\left(-\mathrm{i}\left(P^h\right)\right)^p \left(\mathrm{i}\left(P^h\right)^*\right)^{l-p-2}}{2(1+x)} \left(\mathrm{e}^{-\mathrm{i}(2p-l+2)(\phi - 2\epsilon\delta\tau)/2} + \mathrm{e}^{\mathrm{i}(2p-l+2)\phi/2}\right) \Bigg] \end{aligned} \tag{8.2a}$$

$$\begin{aligned} B_l^h = -\sum_{p=0}^{l-2} \Bigg[& \left(1 + \mathrm{i}\,(2p - l + 2)\,\epsilon\right) \left(P^h\right)^{p+1} \left(P^e\right)^p \left[\left(P^h\right)^*\right]^{l-p-1} \left[\left(P^e\right)^*\right]^{l-p-2} \\ & - \frac{x\left(-\mathrm{i}\left(P^e\right)\right)^p \left(\mathrm{i}\left(P^e\right)^*\right)^{l-p-2}}{2(1+x)} \left(\mathrm{e}^{\mathrm{i}(2p-l+2)(\phi + 2\epsilon\delta\tau)/2} + \mathrm{e}^{-\mathrm{i}(2p-l+2)\phi/2}\right) \Bigg] \end{aligned} \tag{8.2b}$$

With this we are prepared to calculate the thermopower for the asymmetric house by inserting the transmission coefficients into (2.41a,b) and calculating the thermopower $S = -B/G$. To do this we again integrated the transmission coefficients numerically using Gaussian quadrature with a total accuracy of 10^{-10}. The results for the thermopower for different values of $\delta\tau$, x and different temperatures is shown in figure 8.3.

We find that the antisymmetry in phase found by Whitney and Jacquod in second order in x holds up to all orders in x. However this antisymmetry is in contradiction to previous experimental measurements [118, 119] where diffusive normal metal regions have been used. Moreover one can see from figure 8.3 that the thermopower is 2π-periodic in ϕ. A period of 2π has been found previously also in [120]. This periodicity may also be seen from (8.2a,b) combined with (2.41a,b): Due to the summation over p B_l^e and B_l^h are symmetric under an simultaneous exchange $\phi \leftrightarrow -\phi$ and $\epsilon \leftrightarrow -\epsilon$ and satisfy $B_l^h = B_l^e|_{\epsilon\to-\epsilon}$. Thus replacing ϕ by $-\phi$ is the same as replacing ϵ by $-\epsilon$. Now if we replace ϵ by $-\epsilon$ we get an additional minus sign in (2.41b) and therefore a minus sign in the thermopower. In contrast to the symmetric case however the symmetry due to the exchange of the leads is broken and thus the thermopower is non-zero but antisymmetric in ϕ. Moreover the arguments for the periodicity of the conductance in section 7.4.1 also apply to B and thus the thermopower is periodic in the phase difference ϕ with period 2π. Furthermore for specific combinations of x and $\delta\tau$ the thermopower as a function of the phase difference may show additional oscillations with period smaller than 2π. However these additional oscillations are smoothed out if the temperature is increased.

Over a pretty wide range of increasing the temperature the thermopower also increases before it shrinks again. This increase of the thermopower with increasing temperature is related to the decrease of the thermal resistance found in [118]. It is also clearly seen from figure 8.3c that the thermopower increases if the time a quasiparticle spends in the neck is increased. This is due to the fact that with increasing $\delta\tau$ the electron-hole symmetry becomes more and more broken.

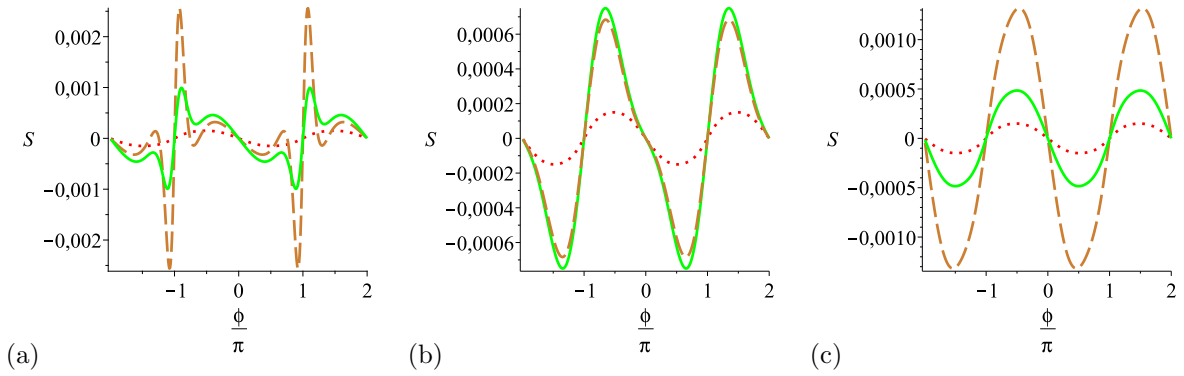

Figure 8.3: The Thermopower in units of $1/eT$ as a function of the phase difference ϕ. (a) $\delta\tau = 0.03$, $\theta = K_B T/E_T = 0.2$ and $x = 0.2$ (dotted line), $x = 2$ (solid line) and $x = 10$ (dashed line). (b) $\delta\tau = 0.03$, $x = 0.2$ and $\theta = 0.2$ (dotted line), $\theta = 4$ (solid line) and $\theta = 10$ (dashed line). (c) $\theta = 0.2$, $x = 0.2$ and $\delta\tau = 0.03$ (dotted line), $\delta\tau = 0.1$ (solid line) and $\delta\tau = 0.3$ (dashed line).

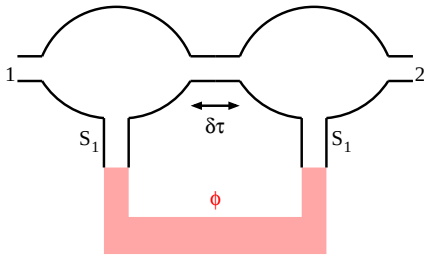

Figure 8.4: Schematic picture of the parallelogram.

It should be noted that the thermopower arises solely from the non-diagonal diagrams since for the diagonal diagrams the energy differences of the links are always zero and thus the neck does not play any role.

8.2 Parallelogram

For the double dot model shown in figure 8.4c, where the quasiparticles in average stay a time $\delta\tau \cdot \tau_D$ in the neck connecting the two dots, the necessary modifications are more substantial than in the previous case. First of all we have to find a way to calculate the transmission probabilities in all orders in x and in $n = N_n/N_N$ where N_n is the number of channels of the neck connecting the two different dots. For simplicity we additionally assume that the two dots have the same dwell time. Since we consider the neck to be represented by an ideal lead every electron in the left dot entering the neck at channel i leaves the neck at the same channel into the right dot and vice versa.

The idea of the calculation is as follows: Consider an electron entering the left dot which we will also refer to as dot 1 through lead 1. Then there are two possibilities where to put the first l-encounter of the diagonal stretch. If it is in the left dot and the number of side trees built by ζ is even we call the contribution of this encounter together with the side trees arising from it $A^e_{11,l}$. The side trees emerging from this encounter and starting with an electron, *i.e.* the odd numbered side trees, will be denoted by P^e_1 and those starting with a hole by P^h_1. The diagonal stretch, however, has the possibility to pass the neck several times before reaching the first encounter, but in order to have the encounter in the left dot this number of traversals has to be even. Moreover each traversal of the neck provides a factor N_n, since the quasiparticle has N_n possibilities through which channel to enter the neck but has to leave the neck

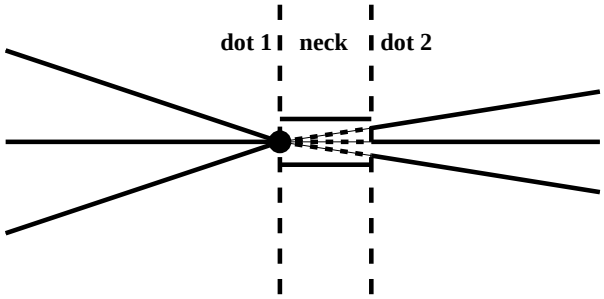

Figure 8.5: A 3-encounter touching the neck: three stretches traverse the neck building side trees starting in dot 2 while the remaining 3 stretches lie in dot 1.

through the same channel, while the stretches connecting two traversals of the neck to each other provide a factor N^{-1}. Thus

$$A^e_{11,l} = -\sum_{m=0}^{\infty}\left(\frac{N_\mathrm{n}}{N}\right)^{2m}\sum_{p=0}^{l-1}\left[1+\mathrm{i}\,(2p-l+1)\,\epsilon\right]\left(P^e_1P^h_1\right)^p\left[\left(P^e_1P^h_1\right)^*\right]^{l-p-1}. \tag{8.3}$$

If the first l-encounter however lies in the right dot we call its contribution combined with the contributions of its side trees $A_{21,l}$. The number of traversals of the neck has to be odd now and the side tree contributions P^e_2, P^h_2 are those of the side trees starting in the right dot, thus

$$A^e_{21,l} = -\sum_{m=0}^{\infty}\left(\frac{N_\mathrm{n}}{N}\right)^{2m+1}\sum_{p=0}^{l-1}\left[1+\mathrm{i}\,(2p-l+1)\,\epsilon\right]\left(P^e_2P^h_2\right)^p\left[\left(P^e_2P^h_2\right)^*\right]^{l-p-1}. \tag{8.4}$$

For the encounters with an odd number of side trees built by ζ we have to be even more careful. This is because the encounter now can also be moved into the neck or into the superconductor coupled to the dot the encounter lies in. If it happens that the encounter touches the neck again p ζ- and $l-p-2$ ζ'-side trees starting in dot 1 will remain. The remaining $p+1$ ζ- and $l-p-1$ ζ'-side trees will start after traversing the neck in dot 2 as indicated in figure 8.5 thus yielding a factor $\mathrm{e}^{\mathrm{i}\epsilon\delta\tau}P^e_2$ and $(\mathrm{e}^{\mathrm{i}\epsilon\delta\tau}P^e_2)^*$, respectively. The in total $l-2$ side trees still starting in the left dot are the originally even numbered side trees and therefore start with a hole. If again the encounter is in the left dot the contribution of the encounters with an odd number of side trees built by ζ is

$$\begin{aligned}B^e_{11,l} = -\sum_{m=0}^{\infty}\left(\frac{N_\mathrm{n}}{N}\right)^{2m}\sum_{p=0}^{l-2}\Bigg\{&\left[1+\mathrm{i}\,(2p-l+2)\,\epsilon\right](P^e_1)^{p+1}\left(P^h_1\right)^p\left[(P^e_1)^*\right]^{l-p-1}\left[\left(P^h_1\right)^*\right]^{l-p-2}\\ &-\frac{N_{\mathrm{S}_1}}{2N}\mathrm{e}^{-\mathrm{i}\phi(2p-l+2)/2}\left(-\mathrm{i}P^h_1\right)^p\left[\mathrm{i}\left(P^h_1\right)^*\right]^{l-p-2}\\ &-\frac{N_\mathrm{n}}{N}\mathrm{e}^{\mathrm{i}(2p-l+2)\epsilon\delta\tau}\left(P^h_1\right)^p\left[\left(P^h_1\right)^*\right]^{l-p-2}(P^e_2)^{p+1}\left[(P^e_2)^*\right]^{l-p-1}\Bigg\}\end{aligned} \tag{8.5}$$

If this encounter however is in the right dot, the number of traversals of the neck has to be odd again such that we have to replace of $(N_\mathrm{n}/N_\mathrm{N})^{2m} \to (N_\mathrm{n}/N_\mathrm{N})^{2m+1}$, $P^\alpha_1 \to P^\alpha_2$ as well as $\phi \to -\phi$ due to the fact that an encounter lying in the right dot can only touch the superconductor S_2 instead of S_1. Equivalently one finds the contributions to $A^h_{j1,l}$, $B^h_{j1,l}$ as well as for $A^\alpha_{j2,l}$ and $B^\alpha_{j2,l}$ ($j\in\{1,2\}$, $\alpha\in\{e,h\}$). For $i\neq j$ the relations $A^\alpha_{ij,l} = (N\mathrm{n}/N)A^\alpha_{ii,l}$ and $B^\alpha_{ij,l} = (N_\mathrm{n}/N)B^\alpha_{ii,l}$ hold.

Having all these coefficients we can start calculating the transmission coefficients in a similar way as in section 7.3. However after cutting the tree at the first encounter we again have to take care about the dot in which the encounter is. To do this we introduce a 'normalised' transmission coefficient

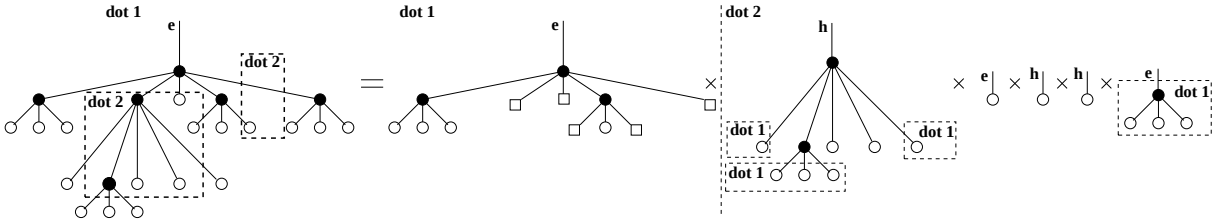

Figure 8.6: A side tree starting in dot 1 may also have parts lying in dot 2. If a quasiparticle hits the neck we will treat this as an electron being retroreflected as its counter-particle indicated by the empty boxes and include an additional factor of the side tree starting in the other dot for each traversal of the neck. 'e' and 'h' denote that the side tree starts with an electron or hole, respectively.

$\tilde{t}_{ij}^{\alpha\beta} = T_{ij}^{\alpha\beta}/N_j$. $\tilde{t}_{ij}^{\alpha\beta}$ may then be interpreted as the probability that an α-type quasiparticle in dot j but not necessarily starting at the lead enters lead i as a β-type quasiparticle. Thus if we cut the diagram after an encounter lying in dot 1 and leaving out the contributed number of channels of the incoming lead the remaining diagrams contribute to $\tilde{t}_{i1}^{\alpha\beta'}$ with $\beta' = \beta$ if the first encounter has an even number of ζ-side trees and $\beta = \bar{\beta}$ otherwise. Analogously if the first encounter lies in the right dot the remaining diagrams contribute to $\tilde{t}_{i,2}^{\alpha\beta'}$. However for the trajectories having no encounters we also have to allow for an arbitrary number of traversals of the neck. Hence the $N_i N_j/N$-term in (7.9a) has to be replaced by $N_i/N \sum_{n=0}^{\infty} (N_\mathrm{n}/N)^{2n+1-\delta_{ij}} = (N_\mathrm{n}/N)^{1-\delta_{ij}} N_i/(N - N_\mathrm{n}^2/N)$. Thus in order to find the transmission coefficients in general one has to solve a 16-dimensional system of linear equations where we only give four of them since the remaining 12 are obtained by exchanging the labels of the leads $1 \leftrightarrow 2$ as well as electrons and holes $e \leftrightarrow h$:

$$\tilde{t}_{11}^{ee} = \frac{N_\mathrm{N}}{2\left(N - N_\mathrm{n}^2/N\right)} + \sum_{l=0}^{\infty} A_{11,l}^{e} \tilde{t}_{11}^{ee} + \sum_{l=0}^{\infty} A_{21,l}^{e} \tilde{t}_{12}^{ee} + \sum_{l=0}^{\infty} B_{11,l}^{e} \tilde{t}_{11}^{eh} + \sum_{l=0}^{\infty} B_{21,l}^{e} \tilde{t}_{12}^{eh} \tag{8.6a}$$

$$\tilde{t}_{12}^{ee} = \frac{N_\mathrm{N} N_\mathrm{n}}{2\left(N^2 - N_\mathrm{n}^2\right)} + \sum_{l=0}^{\infty} A_{22,l}^{e} \tilde{t}_{12}^{ee} + \sum_{l=0}^{\infty} A_{12,l}^{e} \tilde{t}_{11}^{ee} + \sum_{l=0}^{\infty} B_{22,l}^{e} \tilde{t}_{12}^{eh} + \sum_{l=0}^{\infty} B_{12,l}^{e} \tilde{t}_{11}^{eh} \tag{8.6b}$$

$$\tilde{t}_{11}^{eh} = \sum_{l=0}^{\infty} A_{11,l}^{h} \tilde{t}_{11}^{eh} + \sum_{l=0}^{\infty} A_{21,l}^{h} \tilde{t}_{12}^{eh} + \sum_{l=0}^{\infty} B_{11,l}^{h} \tilde{t}_{11}^{ee} + \sum_{l=0}^{\infty} B_{21,l}^{h} \tilde{t}_{12}^{ee} \tag{8.6c}$$

$$\tilde{t}_{12}^{eh} = \sum_{l=0}^{\infty} A_{22,l}^{h} \tilde{t}_{12}^{eh} + \sum_{l=0}^{\infty} A_{12,l}^{h} \tilde{t}_{11}^{eh} + \sum_{l=0}^{\infty} B_{22,l}^{h} \tilde{t}_{12}^{ee} + \sum_{l=0}^{\infty} B_{12,l}^{h} \tilde{t}_{11}^{ee} \tag{8.6d}$$

where we again used that $N_1 = N_2 = N_\mathrm{N}/2$. However this system of linear equations decomposes into four independent systems of linear equations. When defining the vectors

$$\mathbf{a} = (-a_1, 0, -a_2, 0, 0, -a_1, 0, -a_2, -a_2, 0, -a_1, 0, 0, -a_2, 0, -a_1)^T$$
$$\mathbf{t} = (t_{11}^{ee}, t_{11}^{eh}, t_{12}^{ee}, t_{12}^{eh}, t_{11}^{he}, t_{11}^{hh}, t_{12}^{he}, t_{12}^{hh}, t_{21}^{ee}, t_{21}^{eh}, t_{22}^{ee}, t_{22}^{eh}, t_{21}^{he}, t_{21}^{hh}, t_{22}^{he}, t_{22}^{hh})^T$$

with $a_1 = N_\mathrm{N}/[2(N - N_\mathrm{n}^2/N)]$, $a_2 = N_\mathrm{n} N_\mathrm{N}/[2N(N - N_\mathrm{n}^2/N)]$, the normalised transmission coefficients are given by the solution of the equation $\mathbf{a} = \sum_l \mathcal{A}_l \mathbf{t}$, where $\mathcal{A}_l$ is a block diagonal matrix with each block being the 4×4 matrix

$$\begin{pmatrix} A_{11,l}^{e} - 1 & B_{11,l}^{e} & A_{21,l}^{e} & B_{21,l}^{e} \\ B_{11,l}^{h} & A_{11,l}^{h} - 1 & B_{21,l}^{h} & A_{21,l}^{h} \\ A_{12,l}^{e} & B_{12,l}^{e} & A_{22,l}^{e} - 1 & B_{22,l}^{e} \\ B_{12,l}^{h} & A_{12,l}^{h} & B_{22,l}^{h} & A_{22,l}^{h} - 1 \end{pmatrix}.$$

What is left now is to calculate the side tree contribution. This may be done following the steps in section 7.2 with slight changes. First of all it is no longer enough just to consider the generating

functions F and $\hat{F}$ for side trees starting with an electron or a hole, respectively, but we have to consider the generating functions F_1, $\hat{F}_1$, F_2 and $\hat{F}_2$ for side trees starting with an electron (without the hat) or a hole (with the hat) in the left (subscript '1') or in the right dot (subscript '2'). Here we will only consider F_1 for the side trees starting with an electron in the left dot explicitly since the derivation of the remaining 3 is similar and needs only simple replacements.

First of all we have to slightly modify the way we look to the side trees. In general they may consist of parts lying in dot 1 and parts lying in dot 2 as indicated in figure 8.6. Since each tree - and therefore also each subtree - provides an odd number of Andreev reflections a quasiparticle traversing the neck in order to enter the right dot will come back into dot 1 following the stretch hitting the neck as the opposite quasiparticle in opposite direction. Thus every time a link of a tree hits the neck we cut the tree at the corresponding channel and insert a retro-reflection there. The remaining part we cut off is then a side tree starting with the quasiparticle that hit the neck in dot 2. Thus the contribution of the part cut off is equal to F_2 if an electron traversed the neck and equal to $\hat{F}_2$ if a hole hits the neck. Moreover we have to include the additional phase $\epsilon\delta\tau$ due to the time a quasiparticle spends in the neck. Therefore we may write a diagonal rule for a path pair hitting the neck:

An electron hitting the neck contributes a factor $N_{\mathrm{n}}\mathrm{e}^{\mathrm{i}\epsilon\delta\tau}F_2$.

A hole hitting the neck contributes a factor $N_{\mathrm{n}}\mathrm{e}^{\mathrm{i}\epsilon\delta\tau}\hat{F}_2$.

We may then start with (7.4c) and adapting it to our new problem since the steps leading to this can be used here in exactly the same way. The second term which previously corresponded to a tree consisting of a link and an Andreev reflection at S_2 is now given by a link hitting the neck and therefore building a side tree in dot 2 yielding a contribution F_2. Moreover we replace the contribution $z_{o,l}^{(2)}$ of a node of degree $2l$ touching S_2 by the contribution $z_{o,l}^{(\mathrm{n})}$ of a node of degree $2l$ touching the neck. Thus

$$F = -\mathrm{i}\frac{N_{\mathrm{S}_1}}{N}\mathrm{e}^{-\mathrm{i}\phi/2} + \frac{N_{\mathrm{n}}}{N}\mathrm{e}^{\mathrm{i}\epsilon\delta\tau}F_2 + \sum_{l=2}^{\infty}\left[x_l F^l \hat{F}^{l-1} + \left(z_{o,l}^{(1)} + z_{o,l}^{(\mathrm{n})}\right)\hat{F}^{l-1}\right] \tag{8.7}$$

Due to the assumption that the neck may be represented by an ideal lead an l-encounter may touch the neck even if the odd numbered side trees do not have zero characteristic. The only restriction to them is that they traverse the neck before having an encounter or hitting a superconductor. Thus when sliding an l-encounter into the neck we get the situation depicted in figure 8.5: The odd numbered side trees, which start with an electron, now start in dot 2 instead of dot 1. Moreover there are l path pairs traversing the neck each giving a phase $\epsilon\delta\tau$. Therefore we get $z_{o,l}^{(\mathrm{n})} = N_{\mathrm{n}}\mathrm{e}^{\mathrm{i}l\epsilon\delta\tau}F_2^l/N$.

The remaining steps then are again the same as in section 7.2. For a side trees starting with an electron in dot 2 we have to exchange the labels '1' and '2' as well as the phase ϕ by $-\phi$ with respect to F_1. If we consider side trees starting with a hole in dot i instead of electrons we have also to reverse the phase with respect to F_i and exchange $F_j \leftrightarrow \hat{F}_j$, $j \in \{1,2\}$. All in all after performing the sums using geometric series we obtain

$$\frac{\left(-P_1^e P_1^h - \mathrm{i}\epsilon\left(P_1^e P_1^h\right)^2 + 2\mathrm{i}\epsilon P_1^e P_1^h - 1\right)P_1^e P_1^h}{\left(1 - P_1^e P_1^h\right)^2} + \frac{1}{1+x+n}\left[\frac{\mathrm{i}x\,(1+y)\,P_1^h}{2\left(\mathrm{i}P_1^h + \mathrm{e}^{\mathrm{i}\phi/2}\right)} + \frac{nP_1^h P_2^e}{\left(P_1^h P_2^e - \mathrm{e}^{-\mathrm{i}\epsilon\delta\tau}\right)}\right] = 0 \tag{8.8}$$

and similar equations for P_1^h, P_2^e and P_2^h where again $y = \left(N_{\mathrm{S}_1} - N_{\mathrm{S}_1}\right)/N_{\mathrm{S}}$ is the difference between the numbers of channels of the two superconductors.

If the two dots not only have the same dwell time but also the two superconductors have the same numbers of channels one finds that $P_2^\alpha = P_1^{\bar{\alpha}}$ where $\bar{\alpha}$ labels a hole if α labels an electron and vice versa. If $y = 0$ meaning that the two superconductors provide the same numbers of channels exchanging electrons and holes is the same as exchanging dot 1 and dot 2 and is related to the fact that when exchanging electrons and holes this is essentially an exchange $\phi \leftrightarrow -\phi$. This also reduces the number of

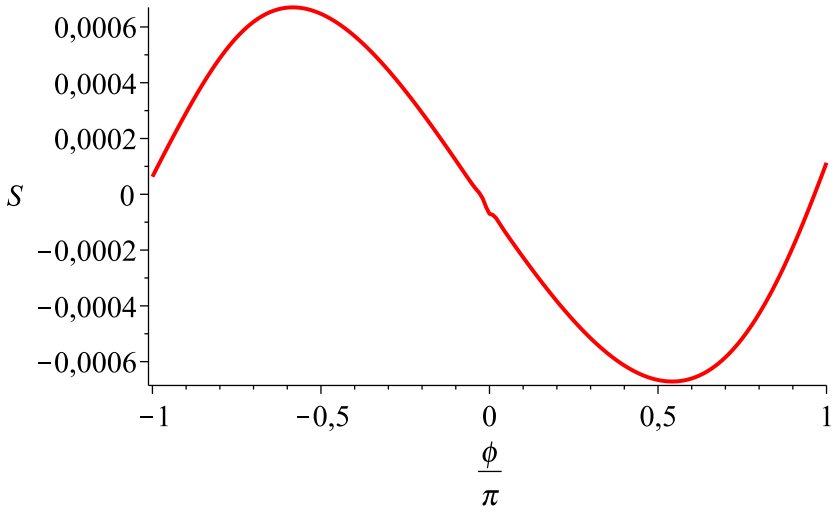

Figure 8.7: The thermopower of the parallelogram as a function of the phase difference between the two superconductors for $N_1 = N_2$, $x = 0.2$, $y = 0.3$, $N_\mathrm{n}/N_\mathrm{N} = 0.1$, $\delta\tau = 0.03$ and $\theta = 0.2$.

linear equations for the normalised transmission coefficients by a factor of 2 since it yields $A^e_{ij} = A^h_{\bar{i}\bar{j}}$ and $B^e_{ij} = B^h_{\bar{i}\bar{j}}$ where $\bar{i} = 2$ if $i = 1$ and vice versa. Therefore we have $\tilde{t}^{ee}_{11} = \tilde{t}^{hh}_{22}$ etc. The set of 4 nonlinear equations (8.8-d) decomposes into two distinct sets of two nonlinear equations where the second set is the same as the first one.

We expect the thermopower to be an odd function of the phase difference as indicated by previous experiments [119, 118] and theoretical predictions [121], since replacing ϕ by $-\phi$ is equal to exchanging electrons and holes. This is due to the fact that the coefficients $A^\alpha_{ij,l}$ and $B^\alpha_{ij,l}$ are symmetric in ϵ due to the summation over p and therefore the transmission coefficients themselves are symmetric in ϵ and thus symmetric under an exchange of electrons and holes. However the $\bar{T}^{\alpha\beta}_{ij}$'s are antisymmetric in an exchange $\epsilon \leftrightarrow -\epsilon$. The expected antisymmetry of the thermopower also includes the expectation that if the two superconducting leads carry the same number of channels the thermopower will vanish again since it has to be symmetric in exchanging the leads which is an exchange $\phi \leftrightarrow -\phi$.

Moreover if we replace $\phi \to \phi + 2\pi$ the side tree contributions change their sign. However in $A^\alpha_{ij,l}$ and the first and the last term of $B^\alpha_{ij,l}$ in (8.5) this sign cancels since the total number of side tree contributions entering them is always even. The additional '$-$' sign enters the second term of $B^\alpha_{ij,l}$ if l is odd. On the other hand if l is odd the phase factor of this term also contributes an additional '$-$' sign and thus they cancel again. If l is even the total number of side trees entering this term is again even and the phase factor does not contribute an additional '$-$' sign on increasing the phase difference by 2π. Thus the transmission coefficients are symmetric under replacing ϕ by $\phi + 2\pi$ and the thermopower is expected to oscillate as a function of the phase difference again with a period of 2π as already found experimentally [119, 118].

When comparing the equations for P^α_1 with the one for $P^{\bar{\alpha}}_2$, we find that

$$P^e_2 = \frac{(1+y)P^h_1}{1 - y - 2\mathrm{i}yP^h_1 \mathrm{e}^{\mathrm{i}(\epsilon\delta\tau+\phi)/2}} \tag{8.9a}$$

$$P^h_2 = \frac{(1+y)P^e_1}{1 - y - 2\mathrm{i}yP^e_1 \mathrm{e}^{\mathrm{i}(\epsilon\delta\tau-\phi)/2}} \tag{8.9b}$$

Moreover if $\phi = 2n\pi$, with n being even, from (8.8) follows that $P^h_1|_{\phi=2n\pi} = P^e_1|_{\phi=2n\pi} = P^h_1|_{\phi=0}$. This is the starting point for solving (8.8) and integrating the resulting transmission coefficients numerically with a total accuracy of 10^{-6}. The resulting thermopower is shown in figure 8.7.

The thermopower is indeed periodic in the phase difference with a period of 2π. However figure 8.7 does not show the expected antisymmetry which may be due to numerical errors. We used a total accuracy of just 10^{-10} for solving (8.8) and performing the integral numerically.

9 Conclusion and Outlook

The proximity of superconductors modifies many properties of a normal region, among them the appearance of a gap in the density of states of an chaotically shaped Andreev billiard and changes in the conductance which are of the order of the numbers of channels as well as odd oscillations of the thermopower in the phase difference of the superconductors. These effects are mainly due to Andreev scattering of electrons or holes at the normal metal-superconductor interface.

We have shown how different properties of chaotic Andreev billiards may be described using a trajectory based semiclassical approach. Our calculations show that as long as the Ehrenfest time does not tend to ∞ it is necessary for these superconductor-normal metal hybrid structures to go beyond the diagonal approximation. Our treatment (*c.f.* the reservations in [44]) builds on the recent advances in identifying [122], codifying [83, 82] and generating [88] the semiclassical contributions, and, because of the slow convergence of the expansion for the density of states in (2.14) or because of the necessity to include all orders in $N_{\mathrm{S}}/N_{\mathrm{N}}$, where N_{S} is the total number of superconducting channels and N_{N} the total number of channels of the normal leads, for the transmission, relies on the ability to treat correlations between n trajectories for essentially all n. The correlations between these trajectories, encoded in encounter regions where they differ slightly, are represented by simple diagrams. These diagrams are related to those that appear for the conductance [83] say where for increasing n they cause ever decreasing (in inverse channel number) corrections; here though they all may contribute with roughly the same (slowly decreasing) importance. Equally it is because we need to treat all orders that makes Andreev billiards so interesting and the resultant effects so large.

Based on the calculation of the density of states for an Andreev billiard with a single lead [48] we obtained the full result for a billiard with two superconducting leads at phase difference ϕ, treated using RMT [41]. The shrinking of the gap with increasing phase difference and its vanishing in the limit $\phi \to \pi$ has been found to be due to the accumulation of a phase $\mathrm{e}^{\pm \mathrm{i}\phi}$ of paths connecting the two different leads thus causing decoherence of the electrons and holes. The effect of a symmetry breaking magnetic field applied to the Andreev billiard with two leads as treated in [41] has also been taken into account and the dependence of the critical magnetic field at which the gap closes as predicted by RMT has been confirmed. In the limits $\phi \to \pi$ and $b \to \infty$ the density of states of the isolated billiard has been found. All this is in agreement with RMT [41] and the statement that the density of states could not be calculated semiclassically [44] has been shown to hold only for semiclassics based on the diagonal approximation.

Besides we could apply our method to Andreev billiards with two superconducting leads carrying different numbers of channels. For this to our best knowledge no RMT-prediction exists. When screening the difference in the numbers of superconducting channels $N_{\mathrm{S}_1} - N_{\mathrm{S}_2}$ from 0 to $\pm N_{\mathrm{S}} = \pm(N_{\mathrm{S}_1} + N_{\mathrm{S}_2})$ we get a continuous crossover from the density of states of an Andreev billiards with two superconducting leads and a phase difference ϕ to the single lead result. Moreover if the phase difference is large enough increasing the difference between the numbers of channels causes the formation of a second gap in the density of states. This is that the states shifted to smaller energies by the phase difference leading to an enhancement of the density of states right above the gap retain from vanishing.

It is worth noting that the semiclassical techniques we used here are only valid up to the Heisenberg time, meaning that we have no access to the density of states on energy scales of the order of the mean level spacing. Though for ballistic transport the Heisenberg time is much longer than the average dwell time (so the mean level spacing is much smaller than the Thouless energy) importantly the RMT treatment [123] shows that a microscopic gap persists in this regime even when the time reversal symmetry is completely broken (by the magnetic field say). It may be possible that applying the semiclassical treatment of times longer than the Heisenberg time for closed systems [124, 125] to transport would allow for accessing this regime as well.

In the opposite regime however, that of the Ehrenfest time, semiclassics provides a surprisingly simple result [95] allowing complete access to the crossover from the universal RMT regime to the more classical Bohr-Sommerfeld regime. The modifications to this result in order to be able to include a phase difference are just marginal. We then found that with increasing the phase difference not only the first gap shrinks but also the second intermediate gap predicted in [48] at intermediate Ehrenfest times shrinks and closes at rather small phase differences. Note that here we have considered hard chaotic systems with just one well defined Lyapunov coefficient thus neglecting fluctuations in the Lyapunov coefficients which may additionally affect the gap [126]. Moreover in general there may be further mechanisms like scarring [127] and disorder [128] affecting the gap.

Furthermore our calculation of the electrical transport extends the work of [49] to all orders in the ratio $N_\mathrm{S}/N_\mathrm{N}$. We could reproduce the large-N limit of the random matrix theory [50] for two isolated superconductors which shows in the limit $N_\mathrm{S}/N_\mathrm{N} \to \infty$ the conductance doubling of the N-S interface consisting of one normal conducting and one superconducting lead [28]. Our result shows a 2π-periodicity and symmetry with respect to the phase difference of the superconductors which have already been found by other approaches [107, 129]. If a magnetic field is applied or the temperature is increased the conductance correction will decrease.

An Andreev billiard with two normal leads and two superconducting leads having the same chemical potential as one of the two normal leads shows more interesting features than the setup with superconducting islands which depend on the ratio of the numbers of channels of the two normal conducting leads as well as on the ratio of the number of superconducting channels and the number of normal channels. The results found here are partly similar to those already found previously in the conductance of N-S junctions. Again the conductance is doubled in the limit $N_\mathrm{S}/N_\mathrm{N} \to \infty$. Moreover the conductance is again 2π-periodic and symmetric with respect to the phase difference ϕ which has been observed for N-S junctions with two superconducting leads in several approaches [110, 130, 131, 49]. It also shows a nonmonotonic behaviour similar to the conductance through quantum dots with one normal and two superconducting leads [110]. The phase difference may even cause a change of the sign of the conductance correction. Furthermore the magnetic field dependence also inherits a nonmonotonic behaviour from the N-S junction [109, 112] and again the sign of the conductance correction may be changed by increasing the magnetic field. This has already been found by Whitney and Jacquod [49] in their consideration of the contribution in leading order in $N_\mathrm{S}/N_\mathrm{N}$. Further a non zero temperature may even cause an increase of the conductance correction similar to the reentrance in the case of the N-S junction [115, 116].

The investigations of the thermopower in [51] have also been extended to all orders in the number of superconducting channels for the symmetric house, the asymmetric house and the parallelogram though we have not been able to solve the equations found for the parallelogram. For the former two setups we could show that the antisymmetry of the thermopower towards the phase difference ϕ holds in all orders in x and that the thermopower of the symmetric house is identically 0. In the case of the asymmetric house this antisymmetry however is in contradiction with some previous experimental results [118, 119], which found a symmetric thermopower for diffusive normal regions. Moreover the thermopower oscillates in both cases with a period 2π in agreement with experimental results [119, 118]. Additionally the thermopower increases with increasing temperature over a pretty wide range. Although we could not evaluate the thermopower for the parallelogram, our approach indicates that for this setup the antisymmetry towards replacing ϕ by $-\phi$ found in leading order in $N_\mathrm{S}/N_\mathrm{N}$ and $N_\mathrm{n}/N_\mathrm{N}$ where N_n is the number of channels of the neck connecting the two dots holds up to all orders in $N_\mathrm{S}/N_\mathrm{N}$ in agreement with [118, 119, 121]. We also found that it oscillates as a function of the phase difference with a period of 2π as found in [118, 119].

All these results (and for the density of states the RMT ones [33, 41]) are only valid to leading order in inverse channel number. With the formalism shown in this diploma thesis, to go to subleading order only requires a way of systematically finding the possible semiclassical diagrams. The contribution of each [83, 82] is in principle known, but the key problem is that the structure we used here breaks down, namely that in the tree recursions when we cut a rooted plane tree at a node we created further rooted plane trees [88]. How to treat the possible diagrams which include closed loops etc, though generated for $n = 1$ [83] and $n = 2$ [82] by cutting open closed periodic orbits, remains unclear. However the treatment for $n = 1$ and $n = 2$ makes clear that the diagrams that contribute at order $(1/N^m, n)$ are

related to those that contribute at order $(1/N^{m-1}, n+1)$ raising the possibility of a recursive treatment starting from the leading order diagrams described here. The idea of appending side trees as introduced for the calculation of the conductance also does not affect the order in $1/N$. Therefore for the next to leading order terms one would have to append side trees with one closed loop which contribution is again unknown. Moreover the diagrams which have to be considered for the conductance may no longer have backbones but can also contain loops which may consist of two ζ-ζ' path pairs or one ζ-ζ and one ζ'-ζ' path pair, respectively. Furthermore a next to leading order diagram can be generated by including a path pair connecting two side trees. However at least for the conductance of an Andreev billiard with two normal leads and two isolated superconductors RMT-predictions for all N exist [50].

Up to now we haven't taken into account the effect of non-zero Ehrenfest time on the conductance. The effect on the side trees of course is known via the investigations of the Ehrenfest time dependence of the density of states since the side trees give, apart from a factor of the number of the superconducting channels, the same contribution as the sum of the correlation functions. However our approach does not allow for sliding two diagonal encounters together such that a simple replacement as for the correlation functions may not necessarily hold.

For the thermopower Whitney and Jacquod considered a third geometry consisting of a series of three dots. For this a method allowing to calculate the thermopower or the conductance to all orders in the ratios of the channel numbers is still missing but is expected to be similar to the one with two dots.

However there is still a lack of experiments the calculations here refer to. Especially the density of states of ballistic chaotically shaped Andreev billiards has not been measured yet thus there is no experimental evidence for the existence of the gap predicted here. Since we used semiclassical methods the system should be large compared to the Fermi wavelength. Thus for the typical semiconductors used to mimic ballistic systems the size should be about several hundred nanometers up to a few microns. Measuring the second intermediate gap which appears for Ehrenfest times of the order of the mean dwell time would then be a further step. An estimate for the Ehrenfest time has been made in [132]: For a system length of 5μm, a Fermi wavelength of 30nm and a Lyapunov exponent on the order of the inverse time of flight through the cavity of approximately $5 \cdot 10^9$/s the Ehrenfest time is on the order of nanoseconds. Thus one needs a very high Lyapunov exponent in order to be able to see this intermediate gap. This is also the reason, why numerical calculations as *e.g.* in [133, 134] up to now did not show this second gap.

Also for the conductance as we have investigated it here up to now no experiments exist although measuring the conductance is easier than measuring the density of states and recently electronic properties of ballistic superconducting-normal metal hybrid structures have been considered experimentally [135]. The two superconductors having the same chemical potential but a phase difference ϕ may be obtained by using one single superconductor touching the normal region at two distinct points and applying a magnetic field to the superconductor away from the dot. The phase difference is then related to the magnetic flux Φ by $\phi = 2\pi\Phi/\Phi_0$, where $\Phi_0 = \pi\hbar/e$ [136].

Acknowledgements

I thank Prof. Dr. Klaus Richter for supervising this Diploma thesis and introducing me to the interesting topic of Andreev billiards. He was always interested in the process of my work and dedicated a great amount of his time for discussions. Prof. Richter also contributed largely to the familiar, pleasant and productive atmosphere at his chair. I'm further thankful for supporting me in extending my own physical horizon by offering me the participation in external educational events.

Furthermore I would like to thank Dr. Jack Kuipers for the exceeding discussions about this work and always providing further comments and information giving me a further insight in this topic. He always saved some time for discussing results or searching for mistakes. I always enjoyed working together with him. I also want to thank him for proof reading this work.

Next I want to thank Dipl. Phys. Daniel Waltner for supporting me in understanding the calculation about the Ehrenfest time dependence of the density of states and further discussing about it.

Finally I thank my parents for always supporting my studies and therefore making this work possible, encouraging me in my interests and providing friendship.

Appendix A: Generating functions and side tree contributions

Generating functions

The intermediate generating function $I(\epsilon, r)$ for the billiard with a single lead and no magnetic field in section 5.2 is given by

$$\begin{aligned} 1 - \left[(1-a)^2 + 6r + (1+a)^2 r^2\right] I \\ + \left[4(1-a)^3 - \left(8 + 20a^2 - a^4\right) r + 4(1+a)^3 r^2\right] r I^2 \\ + \Big[4(1-a)^3 - \left(16 - 24a + 44a^2 - 8a^3 - a^4\right) r + 2\left(12 + 32a^2 - a^4\right) r^2 \\ - \left(16 + 24a + 44a^2 + 8a^3 - a^4\right) r^3 + 4(1+a)^3 r^4\Big] r I^3 = 0, \end{aligned} \tag{A.1}$$

where we set $a = \mathrm{i}\epsilon$.

The generating function $H(\epsilon, \phi, b, r)$ for the billiard with equal leads at phase difference ϕ and magnetic field b in section 6.2 is given by

$$\begin{aligned} \beta^2 - \left((1-a+b)^2 + r^2 - 2r(1-a+b)\left(2\beta^2 - 1\right)\right) H \\ - r\left[(1-a+b)(1-3a+7b) - 2r\left(1 + 5b + b^2 - (3+2b)a + a^2\right)\left(2\beta^2 - 1\right)\right. \\ \left. + r^2(1 - 2a + 2b)\right] H^2 \\ + r^2\left[-b(19b+10) + 2a(9b+1) - 3a^2\right. \\ \left. + 2r\left(2b(3b+4) - 2a(4b+1) + 2a^2\right)\left(2\beta^2 - 1\right)\right. \\ \left. + r^2\left(-b(b+6) + 2a(b+1) - a^2\right)\right] H^3 \\ - r^3\left[b(25b+4) - 14ab + a^2 - 2r\left(b(13b+4) - 10ab + a^2\right)\left(2\beta^2 - 1\right)\right. \\ \left. + r^2\left(b(5b+4) - 6ab + a^2\right)\right] H^4 \\ - 4r^4 b\left[4b - a - 2r(3b-a)\left(2\beta^2 - 1\right) + r^2(2b-a)\right] H^5 \\ - 4r^5 b^2\left[1 + r^2 - 2r\left(2\beta^2 - 1\right)\right] H^6 = 0, \end{aligned} \tag{A.2}$$

where we also used $a = \mathrm{i}\epsilon$. For the billiard with unequal leads and no magnetic field in section 6.3, the

generating function $H(\epsilon,\phi,y,r)$ is given by

$$\begin{aligned}
&\beta\beta^*(1-a)^2+\beta\beta^* r^2-\left(\beta^2+\beta^{*2}\right)(1-a)\,r\\
&+\Big[-(1-a)^4+r\left((\beta+\beta^*)^2\left(1-a^3\right)+\left(3(\beta+\beta^*)^2+2\beta\beta^*\right)a(a-1)\right)\\
&+r^2\left(\left(3(\beta+\beta^*)^2-2\beta\beta^*-2\right)a(2-a)+2(1+\beta+\beta^*)(1-\beta-\beta^*)\right)\\
&+r^3\left((\beta+\beta^*)^2-a\left((\beta+\beta^*)^2+2\beta\beta^*\right)\right)-r^4\Big]H\\
&+r\Big[(1-a)^3(5a-1)\\
&+\left((\beta+\beta^*)^2\left(1-7a-7a^3+a^4\right)+(3\beta+4\beta^*)(4\beta+3\beta^*)a^2\right)r\\
&+2(1+\beta+\beta^*)(1-\beta-\beta^*)\left(1-6a-2a^3\right)r^2\\
&-\left(15\beta^2+15\beta^{*2}-14+28\beta\beta^*\right)a^2r^2\\
&+\left((\beta+\beta^*)^2(1-5a)+\left(3\beta^2+3\beta^{*2}+7\beta\beta^*\right)a^2\right)r^3+(4a-1)\,r^4\Big]H^2\\
&+ar^2\Big[2(1-a)^2(2-5a)+(\beta+\beta^*)^2\left(4a^3-15a^2+15a-4\right)r\\
&+2(1+\beta+\beta^*)(1-\beta-\beta^*)\left(a^3-8a^2+12a-4\right)r^2\\
&+(\beta+\beta^*)^2\left(-3a^2+9a-4\right)r^3+(4-6a)\,r^4\Big]H^3\\
&+a^2r^3\Big[16a-10a^2-6+(\beta+\beta^*)^2\left(6-13a+6a^2\right)r\\
&+2(1+\beta+\beta^*)(1-\beta-\beta^*)\left(6-10a+3a^2\right)r^2\\
&+(\beta+\beta^*)^2\left(6-7a+a^2\right)r^3+(4a-6)\,r^4\Big]H^4\\
&+a^3r^4\Big[4-5a+4(\beta+\beta^*)^2(a-1)\,r+2(1+\beta+\beta^*)(1-\beta-\beta^*)(3a-4)\,r^2\\
&+(\beta+\beta^*)^2(2a-4)\,r^3+(4-a)\,r^4\Big]H^5\\
&+a^4r^5\left(-1-r^4+r\left(1+r^2\right)(\beta+\beta^*)^2+2r^2\left[1+\beta+\beta^*\right)(1-\beta-\beta^*)\right]H^6=0,
\end{aligned}\tag{A.3}$$

likewise with $a=\mathrm{i}\epsilon$.

Side tree contributions

If the numbers of channels of the superconductors are zero the contributions of the side trees starting with an electron P is given by

$$\begin{aligned}
&-P^7+(2\mathrm{i}\beta+\mathrm{i}\beta x)\,P^6+\left(-b^2x+3+\mathrm{i}\epsilon\,x-b^2+\mathrm{i}\epsilon\right)P^5\\
&+\left(-\mathrm{i}\beta x+2\mathrm{i}b^2\beta+2\epsilon\beta+2\mathrm{i}b^2\beta x+2\epsilon\beta x-4\mathrm{i}\beta\right)P^4\\
&+(-2\mathrm{i}\epsilon-3-2\mathrm{i}\epsilon x)\,P^3+\left(2\mathrm{i}b^2\beta+2\mathrm{i}b^2\beta x-2\epsilon\beta x-2\epsilon\beta+2\mathrm{i}\beta-\mathrm{i}\beta x\right)P^2\\
&+\left(\mathrm{i}\epsilon x+b^2+b^2x+1+\mathrm{i}\epsilon\right)P+\mathrm{i}\beta x=0
\end{aligned}\tag{A.4}$$

with $\beta=\cos(\phi/2)$.

If the two superconductors provide different numbers of channels with $(N_{\mathrm{S}_1}-(N_{\mathrm{S}_2})/N_{\mathrm{S}}=y$ at $T=0$,

i.e. with $\epsilon = 0$, and $b = 0$ one has to solve

$$\begin{aligned}
&-P^5 + (2\mathrm{i}b_2 + \mathrm{i}b_1 x + 2\mathrm{i}b_1 + 2\mathrm{i}xb_2)\,P^4 \\
&+ \left({b_2}^2x^2 + 2b_1b_2 + 3b_1xb_2 + 2 + {b_2}^2x + {b_1}^2 + b_1b_2x^2 + 2{b_1}^2x + {b_2}^2 + 2x\right)P^3 \\
&+ \left(-3\mathrm{i}xb_2 + \mathrm{i}{b_2}^3x^2 - \mathrm{i}{b_1}^2b_2x - 2\mathrm{i}b_2 + \mathrm{i}{b_2}^3x - \mathrm{i}b_2x^2 - \mathrm{i}{b_1}^3x + \mathrm{i}b_1x{b_2}^2\right. \\
&\qquad \left. -\mathrm{i}b_1x^2 - 3\mathrm{i}b_1x - 2\mathrm{i}b_1 - \mathrm{i}{b_1}^2b_2x^2\right)P^2 \\
&+ \left(b_1b_2x^2 + 2{b_2}^2x^2 - 2x - {b_1}^2x^2 - {b_1}^2x - 1 + 2{b_2}^2x + b_1xb_2\right)P \\
&\qquad -\mathrm{i}xb_2 - \mathrm{i}b_1x^2 - \mathrm{i}b_2x^2 = 0. \qquad \text{(A.5)}
\end{aligned}$$

Appendix B: Step function

Consider a function f depending on $E \in \mathbb{R}$ that may have only real valued zeroes E_n, $n \in \{1, \ldots, N\}$ where N is the number of different zeroes. Then it may be decomposed into

$$f(E) = a \prod_{n=1}^{N} (E_n - E)^{k_n}. \tag{B.1}$$

Here k_n is the multiplicity of the zero E_n and a is some normalisation constant which we will set to 1. (If $a \neq 1$ we would consider $f(E)/a$.). Including the iϵ and building the logarithm yields

$$\ln f(E + \mathrm{i}\varepsilon) = \sum_{n=1}^{N} k_n \ln(E_n - E - \mathrm{i}\varepsilon) \tag{B.2}$$

After replacing the complex number $(E_n - E - \mathrm{i}\varepsilon) = r_n \mathrm{e}^{\mathrm{i}\varphi_n}$ then gives

$$f(E + \mathrm{i}\varepsilon) = \sum_{n=1}^{N} k_n \left(\ln r_n + \mathrm{i}\varphi_n\right). \tag{B.3}$$

Since we consider the zeroes of f to be real and only allow real values for E, the phase φ_n is given by $\varphi_n = \arctan\left[-\varepsilon/\left(E - E_n\right)\right]$ and the imaginary part of $\ln f(E + \mathrm{i}\varepsilon)$ is given by

$$\mathrm{Im} \ln f(E + \mathrm{i}\varepsilon) = \sum_{n=1}^{N} k_n \varphi_n \tag{B.4}$$

Now if $E < E_n$ the complex number $(E_n - E_n - \mathrm{i}\varepsilon)$ lies in the fourth quadrant of the complex plain and the limit $\varepsilon \to 0$ pushes it onto the positive real axis such that the phase becomes $\varphi_n = 0$. If however $E > E_n$ it lies in the third quadrant of the complex plain and performing the limit causes $\varphi_n = -\pi$.

Thus if the energy E is smaller than the lowest zero $\lim_{\varepsilon \to 0} \mathrm{Im} \ln f(E + \mathrm{i}\varepsilon) = 0$ and every time the Energy reaches a zero it is decreased by $-\pi$. Thus the number of zeroes smaller than E are given by

$$N(E) = -\frac{1}{\pi} \lim_{\varepsilon \to 0} \mathrm{Im} \ln f(E + \mathrm{i}\varepsilon). \tag{B.5}$$

Note that the additional term iε is needed in order to ensure that the logarithm is well defined and its argument do not lie on the negative real axis.

Bibliography

[1] H. K. Onnes, *Commun. Phys. Lab. Univ. Leiden* , 120 (1911).

[2] J. Bardeen, L. N. Cooper, and J. R. Schrieffer, *Phys. Rev.* **108**, 1175 (1957).

[3] V. L. Ginzburg and L. D. Landau, *Zh. Eksp. Teor. Fiz.* **20**, 1064 (1950).

[4] F. London and H. London, *Proc. R. Soc. London* **A149**, 71 (1935).

[5] B. D. Josephson, *Phys. Lett.* **1**, 251 (1962).

[6] W. Meissner and R. Ochsenfeld, *Naturwissenschaften* **21**, 787 (1933).

[7] R. Doll and M. Näbauer, *Phys. Rev. Lett.* **7**, 51 (1961).

[8] B. S. Deaver and W. M. Fairbank, *Phys. Rev. Lett.* **7**, 43 (1961).

[9] D. Cribier, B. Jacrot, L. M. Rao, and B. Farnoux, *Phys. Lett.* **9**, 106 (1964).

[10] U. Essmann and H. Träuble, *Phys. Lett. A* **24**, 526 (1967).

[11] J. Schelten, H. Ullmaier, and W. Schmatz, *Physica Status Solidi (B)* **48**, 619 (1971).

[12] H. Meissner, *Phys. Rev.* **117**, 672 (1960).

[13] S. Guéron, H. Pothier, N. O. Birge, D. Esteve, and M. H. Devoret, *Phys. Rev. Lett.* **77**, 3025 (1996).

[14] A. F. Morpurgo, S. Holl, B. J. van Wees, T. M. Klapwijk, and G. Borghs, *Phys. Rev. Lett.* **78**, 2636 (1997).

[15] S. G. den Hartog, B. J. van Wees, Y. V. Nazarov, T. M. Klapwijk, and G. Borghs, *Phys. Rev. Lett.* **79**, 3250 (1997).

[16] M. Jakob, H. Stahl, J. Knoch, J. Appenzeller, B. Lengeler, H. Hardtdegen, and H. Luth, *Appl. Phys. Lett.* **76**, 1152 (2000).

[17] N. Moussy, H. Courtois, and B. Pannetier, *Europhys. Lett.)* **55**, 861 (2001).

[18] M. Vinet, C. Chapelier, and F. Lefloch, *Phys. Rev. B* **63**, 165420 (2001).

[19] J. Eroms, M. Tolkiehn, D. Weiss, U. Rössler, J. D. Boeck, and G. Borghs, *Europhys. Lett.)* **58**, 569 (2002).

[20] W. Escoffier, C. Chapelier, N. Hadacek, and J.-C. Villégier, *Phys. Rev. Lett.* **93**, 217005 (2004).

[21] W. Escoffier, C. Chapelier, and F. Lefloch, *Phys. Rev. B* **72**, 140502 (2005).

[22] C. J. Lambert and R. Raimondi, *J. Phys.: Cond. Mat.* **10**, 901 (1998).

[23] A. Altland, B. D. Simons, and D. T. Semchuk, *Adv. Phys.* **49**, 321 (2000).

[24] D. Taras-Semchuk and A. Altland, *Phys. Rev. B* **64**, 014512 (2001).

[25] C. W. J. Beenakker, *Lect. Notes. Phys.* **667**, 131 (2005).

[26] P. G. de Gennes, *Superconductivity of Metals and Alloys*, Benjamin, New York, 1966.

[27] A. F. Andreev, *Sov. Phys. JETP* **19**, 1228 (1964).

[28] G. E. Blonder, M. Tinkham, and T. M. Klapwijk, *Phys. Rev. B* **25**, 4515 (1982).

[29] M. Büttiker, Y. Imry, R. Landauer, and S. Pinhas, *Phys. Rev. B* **31**, 6207 (1985).

[30] A. Kastalsky, A. W. Kleinsasser, L. H. Greene, R. Bhat, F. P. Milliken, and J. P. Harbison, *Phys. Rev. Lett.* **67**, 3026 (1991).

[31] C. Nguyen, H. Kroemer, and E. L. Hu, *Phys. Rev. Lett.* **69**, 2847 (1992).

[32] I. Kosztin, D. L. Maslov, and P. M. Goldbart, *Phys. Rev. Lett.* **75**, 1735 (1995).

[33] J. A. Melsen, P. W. Brouwer, K. M. Frahm, and C. W. J. Beenakker, *Europhys. Lett.* **35**, 7 (1996).

[34] A. Lodder and Y. V. Nazarov, *Phys. Rev. B* **58**, 5783 (1998).

[35] H. Schomerus and C. W. J. Beenakker, *Phys. Rev. Lett.* **82**, 2951 (1999).

[36] W. Ihra, M. Leadbeater, J. Vega, and K. Richter, *Eur. Phys. J. B* **21**, 425 (2001).

[37] W. Ihra and K. Richter, *Physica E* **9**, 362 (2001).

[38] J. Cserti, A. Kormányos, Z. Kaufmann, J. Koltai, and C. J. Lambert, *Phys. Rev. Lett.* **89**, 057001 (2002).

[39] I. Adagideli and P. M. Goldbart, *International Journal of Modern Physics B* **16**, 1381 (2002).

[40] O. Zaitsev, *J. Phys. A* **39**, L467 (2006).

[41] J. A., P. W. Brouwer, K. M. Frahm, and C. W. J. Beenakker, *Physica Scripta* **T69**, 223 (1997).

[42] I. Adagideli and C. W. J. Beenakker, *Phys. Rev. Lett.* **89**, 237002 (2002).

[43] P. G. Silvestrov, M. C. Goorden, and C. W. J. Beenakker, *Phys. Rev. Lett.* **90**, 116801 (2003).

[44] M. G. Vavilov and A. I. Larkin, *Phys. Rev. B* **67**, 115335 (2003).

[45] P. W. Brouwer and S. Rahav, *Phys. Rev. B* **74**, 085313 (2006).

[46] M. C. Goorden, P. Jacquod, and J. Weiss, *Phys. Rev. Lett.* **100**, 067001 (2008).

[47] T. Micklitz and A. Altland, *Phys. Rev. Lett.* **103**, 080403 (2009).

[48] J. Kuipers, D. Waltner, C. Petitjean, G. Berkolaiko, and K. Richter, *Phys. Rev. Lett.* **104**, 027001 (2010).

[49] R. S. Whitney and P. Jacquod, *Phys. Rev. Lett.* **103**, 247002 (2009).

[50] C. W. J. Beenakker, J. A. Melsen, and P. W. Brouwer, *Phys. Rev. B* **51**, 13883 (1995).

[51] P. Jacquod and R. S. Whitney, arXiv:0910.2943, 2009.

[52] J. Kuipers, T. Engl, G. Berkolaiko, C. Petitjean, D. Waltner, and K. Richter, arXiv:1004.1327, 2010.

[53] K. K. LIKHAREV, *Rev. Mod. Phys.* **51**, 101 (1979).

[54] C. W. J. BEENAKKER, *Phys. Rev. Lett.* **67**, 3836 (1991).

[55] E. DORON and U. SMILANSKY, *Phys. Rev. Lett.* **68**, 1255 (1992).

[56] O. BOHIGAS, M. J. GIANNONI, and C. SCHMIT, *Phys. Rev. Lett.* **52**, 1 (1984).

[57] C. W. J. BEENAKKER, *Rev. Mod. Phys.* **69**, 731 (1997).

[58] P. W. BROUWER and C. W. J. BEENAKKER, *J. Math. Phys.* **37**, 4904 (1996).

[59] C. J. LAMBERT and R. RAIMONDI, *J. Phys.: Cond. Mat.* **10**, 901 (1998).

[60] C. J. LAMBERT, *J. Phys.: Cond. Mat.* **3**, 6579 (1991).

[61] V. C. HUI and C. J. LAMBERT, *J. Phys.: Cond. Mat.* **5**, 697 (1993).

[62] C. J. LAMBERT, V. C. HUI, and S. J. ROBINSON, *J. Phys.: Cond. Mat.* **5**, 4187 (1993).

[63] N. R. CLAUGHTON and C. J. LAMBERT, *Phys. Rev. B* **53**, 6605 (1996).

[64] C. STRUNK, Moderne Thermodynamik.

[65] R. P. FEYNMAN, *Rev. Mod. Phys.* **20**, 367 (1948).

[66] R. P. FEYNMAN and A. R. HIBBS, *Quantum Mechanics and Path Integrals*, McGraw-Hill Companies, 1965.

[67] L. S. SCHULMAN, *Techniques and Applications of Path Integration*, Dover Publications, 2005.

[68] W. MAGNUS, *Communications on Pure and Applied Mathematics* **7**, 649 (1954).

[69] E. NELSON, *J. Math. Phys.* **5**, 332 (1964).

[70] H. F. TROTTER, *Proceedings of the American Mathematical Society* **10**, 545 (1959).

[71] H.-J. STÖCKMANN, *Quantum Chaos: An Introduction*, Cambridge University Press, 2007.

[72] D. S. FISHER and P. A. LEE, *Phys. Rev. B* **23**, 6851 (1981).

[73] K. RICHTER, *Semiclassical Theory of Mesoscopic Quantum Systems (Springer Tracts in Modern Physics)*, Springer, Berlin, 2000.

[74] R. A. JALABERT, H. U. BARANGER, and A. D. STONE, *Phys. Rev. Lett.* **65**, 2442 (1990).

[75] H. U. BARANGER, R. A. JALABERT, and A. D. STONE, *Chaos* **3**, 665 (1993).

[76] W. H. MILLER, *Adv. Chem. Phys* **30**, 77 (1975).

[77] H. U. BARANGER, R. A. JALABERT, and A. D. STONE, *Phys. Rev. Lett.* **70**, 3876 (1993).

[78] M. V. BERRY, *Proc. R. Soc. Lond. A* **400**, 229 (1985).

[79] M. SIEBER and K. RICHTER, *Physica Scripta* **T90**, 128 (2001).

[80] K. RICHTER and M. SIEBER, *Phys. Rev. Lett.* **89**, 206801 (2002).

[81] M. TUREK and K. RICHTER, *J. Phys. A* **36**, L455 (2003).

[82] S. MÜLLER, S. HEUSLER, P. BRAUN, and F. HAAKE, *New J. Phys.* **9**, 12 (2007).

[83] S. HEUSLER, S. MÜLLER, P. BRAUN, and F. HAAKE, *Phys. Rev. Lett.* **96**, 066804 (2006).

[84] S. Müller, S. Heusler, P. Braun, F. Haake, and A. Altland, *Phys. Rev. Lett.* **93**, 014103 (2004).

[85] M. Turek, D. Spehner, S. Müller, and K. Richter, *Phys. Rev. E* **71**, 016210 (2005).

[86] D. Spehner, *J. Phys. A* **36**, 7269 (2003).

[87] A. M. O. de Almeida, *Hamiltonian Systems: Chaos and Quantization (Cambridge Monographs on Mathematical Physics)*, Cambridge University Press, 1990.

[88] G. Berkolaiko, J. M. Harrison, and M. Novaes, *J. Phys. A* **41**, 365102 (2008).

[89] T. Nagao and K. Saito, *Phys. Lett. A* **311**, 353 (2003).

[90] K. Saito and T. Nagao, *Phys. Lett. A* **352**, 380 (2006).

[91] J. Kuipers and M. Sieber, *J. Phys. A* **40**, 935 (2007).

[92] T. Nagao, P. Braun, S. Müller, K. Saito, S. Heusler, and F. Haake, *J. Phys. A* **40**, 47 (2007).

[93] W. T. Tutte, *The American Mathematical Monthly* **71**, 272 (1964).

[94] R. P. Stanley, *Enumerative Combinatorics*, Cambridge University Press, 2001.

[95] D. Waltner and et al., in preperation, 2010.

[96] R. S. Whitney. and P. Jacquod, *Phys. Rev. Lett.* **96**, 206804 (2006).

[97] R. S. Whitney and P. Jacquod, *Phys. Rev. Lett.* **94**, 116801 (2005).

[98] P. Jacquod and R. S. Whitney, *Phys. Rev. B* **73**, 195115 (2006).

[99] P. W. Brouwer and C. W. J. Beenakker, *Chaos Solitons and Fractals* **8**, 1249 (1997).

[100] A. Andreev, *Sov. Phys. JETP* **22**, 455 (1966).

[101] I. O. Kulik, *Sov. Phys. JETP* **30**, 944 (1970).

[102] C. Ishii, *Prog. Theor. Phys.* **44**, 1525 (1970).

[103] C. W. J. Beenakker and H. van Houten, *Phys. Rev. Lett.* **66**, 3056 (1991).

[104] J. Sköldberg, T. Löfwander, V. S. Shumeiko, and M. Fogelström, *Phys. Rev. Lett.* **101**, 087002 (2008).

[105] M. C. Goorden, P. Jacquod, and C. W. J. Beenakker, *Phys. Rev. B* **72**, 064526 (2005).

[106] G. Berkolaiko and J. Kuipers, *J. Phys. A* **43**, 035101 (2010).

[107] C. J. Lambert, *J. Phys.: Cond. Mat.* **5**, 707 (1993).

[108] C. J. Lambert, *J. Phys.: Cond. Mat.* **3**, 6579 (1991).

[109] A. A. Clerk, P. W. Brouwer, and V. Ambegaokar, *Phys. Rev. B* **62**, 10226 (2000).

[110] Y. V. Nazarov, *Phys. Rev. Lett.* **73**, 1420 (1994).

[111] A. F. Volkov and A. V. Zaitsev, *Phys. Rev. B* **53**, 9267 (1996).

[112] N. G. Fytas, F. K. Diakonos, P. Schmelcher, M. Scheid, A. Lassl, K. Richter, and G. Fagas, *Phys. Rev. B* **72**, 085336 (2005).

[113] L. ONSAGER, *Phys. Rev.* **37**, 405 (1931).

[114] L. ONSAGER, *Phys. Rev.* **38**, 2265 (1931).

[115] P. CHARLAT, H. COURTOIS, P. GANDIT, D. MAILLY, A. VOLKOV, and B. PANNETIER, *Phys. Rev. Lett.* **77**, 4950 (1996).

[116] P. CHARLAT, H. COURTOIS, P. GANDIT, D. MAILLY, A. VOLKOV, and B. PANNETIER, *Czech. J. Phys.* **46**, 3107 (1996).

[117] P. W. BROUWER and A. ALTLAND, *Phys. Rev. B* **78**, 075304 (2008).

[118] Z. JIANG and V. CHANDRASEKHAR, *Phys. Rev. B* **72**, 020502 (2005).

[119] J. EOM, C.-J. CHIEN, and V. CHANDRASEKHAR, *Phys. Rev. Lett.* **81**, 437 (1998).

[120] M. TITOV, *Phys. Rev. B* **78**, 224521 (2008).

[121] V. P. and H. T., *Appl. Phys. A* **89**, 625 (2007).

[122] K. RICHTER and M. SIEBER, *Phys. Rev. Lett.* **89**, 206801 (2002).

[123] K. M. FRAHM, P. W. BROUWER, J. A. MELSEN, and C. W. J. BEENAKKER, *Phys. Rev. Lett.* **76**, 2981 (1996).

[124] S. HEUSLER, S. MÜLLER, A. ALTLAND, P. BRAUN, and F. HAAKE, *Phys. Rev. Lett.* **98**, 044103 (2007).

[125] S. MÜLLER, S. HEUSLER, A. ALTLAND, P. BRAUN, and F. HAAKE, *New J. Phys.* **11**, 103025 (2009).

[126] P. G. SILVESTROV, *Phys. Rev. Lett.* **97**, 067004 (2006).

[127] A. KORMÁNYOS and H. SCHOMERUS, *Phys. Rev. Lett.* **97**, 124102 (2006).

[128] F. LIBISCH, J. MÖLLER, S. ROTTER, M. G. VAVILOV, and J. BURGDÖRFER, *Europhys. Lett.)* **82**, 47006 (2008).

[129] M. C. GOORDEN, P. JACQUOD, and J. WEISS, *Nanotechnology* **19**, 135401 (2008).

[130] H. NAKANO and H. TAKAYANAGI, *Solid State Communications* **80**, 997 (1991).

[131] S. TAKAGI, *Solid State Communications* **81**, 579 (1992).

[132] C. PETITJEAN, D. WALTNER, J. KUIPERS, I. D. I. M. C. ADAGIDELI, and K. RICHTER, *Phys. Rev. B* **80**, 115310 (2009).

[133] P. JACQUOD, H. SCHOMERUS, and C. W. J. BEENAKKER, *Phys. Rev. Lett.* **90**, 207004 (2003).

[134] A. KORMÁNYOS, Z. KAUFMANN, C. J. LAMBERT, and J. CSERTI, *Phys. Rev. B* **70**, 052512 (2004).

[135] F. ROHLFING, G. TKACHOV, F. OTTO, K. RICHTER, D. WEISS, G. BORGHS, and C. STRUNK, *Phys. Rev. B* **80**, 220507 (2009).

[136] W. BUCKEL and R. KLEINER, *Superconductivity: Fundamentals and Applications*, Wiley-VCH, 2004.